

NORTRIP model development and documentation

NO_n-exhaust Road TRaffic Induced Particle emission modelling

Bruce Rolstad Denby¹ and Ingrid Sundvor¹

in collaboration with

Christer Johansson², Mari Kauhaniemi³, Jari Härkönen³, Jaako Kukkonen³, Ari Karppinen³, Leena Kangas³,
Gunnar Omstedt⁴, Matthias Ketzel⁵, Liisa Pirjola⁶, Michael Norman⁷,
Mats Gustafsson⁸, Göran Blomqvist⁸, Cecilia Bennet⁸, Kaarle Kupiainen⁹, Niko Karvosenoja¹⁰

¹Norwegian Institute for Air Research (NILU), Kjeller, Norway.

²Department of Applied Environmental Science (ITM), Stockholm University

³Finish Meteorological Institute (FMI), Helsinki, Finland.

⁴Swedish Meteorological and Hydrological Institute (SMHI), Norrköping, Sweden.

⁵National Environmental Research Institute (DMU), Aarhus University, Denmark.

⁶Helsinki Metropolia University of Applied Sciences, Finland.

⁷Environment and Health Administration, Stockholm, Sweden.

⁸Swedish National Road and Transport Research Institute (VTI), Sweden.

⁹Nordic Envicon Oy, Helsinki, Finland.

¹⁰Finnish Environment Institute (YMPARISTO), Helsinki, Finland.

Scientific report

Preface

The NORTRIP model is the result of research efforts carried out by a number of Nordic institutes to improve our understanding and ability to model non-exhaust traffic emissions. The model has been developed through the Nordic Council of Ministers project NORTRIP (NON-exhaust Road Traffic Induced Particle emissions) with substantial support for NILU from the Norwegian Climate and Pollution Agency (KLIF). The aim of the NORTRIP project was:

*“to develop a **process based non-exhaust emission model** that can be applied in any city without site specific empirical factors, for management and evaluation of abatement strategies, and which is able to describe the (non-exhaust) traffic emissions on an hourly, or at least daily basis, with satisfactory accuracy.”*

This aim requires that the model is capable of describing the direct emissions of non-exhaust wear sources (road, brake and tyre), their accumulation on the road surface and their subsequent suspension into ambient air. It also requires that other sources of accumulated road mass, such as salting and traction sanding, be described. Apart from the wear and accumulation of mass on the road the surface moisture of the road, along with the impact of dust binding activities, strongly affects the emissions of these sources. The model must include all these aspects if it is to successfully reproduce and predict the impacts of the various processes.

The model development, and its application to a number of Nordic datasets, is described here in detail, as this report is intended as a detailed documentation of the model and its application. The model has been found to successfully reproduce measured concentrations for most of the datasets assessed. Indeed, in some cases, the model exceeds expectations. However, the complexity of the processes involved means that there are a number of problems in modelling the non-exhaust emissions, not just in the process descriptions but also in the availability of data to carry out the modelling. There still remains a number of uncertainties that further observational data will hopefully help to reduce.

The NORTRIP model is currently the most comprehensive process based non-exhaust emission model available. It provides not just a means for predicting non-exhaust contributions to PM concentrations but also a platform for understanding and controlling these emissions. It is expected that the model will be further developed as more information is gathered over time and that its application to a wider range of datasets will only help improve the robustness of the model.

Contents

| | Page |
|---|-----------|
| Preface | 1 |
| Summary | 7 |
| 1 Introduction | 9 |
| 1.1 Aim of the modelling | 9 |
| 1.2 Conceptual outline of the modelling elements | 9 |
| 1.2.1 Direct emissions through road and other wear sources | 10 |
| 1.2.2 Suspended emissions induced by road traffic | 11 |
| 1.2.3 Road dust and salt loading | 12 |
| 1.2.4 Surface retention | 12 |
| 1.3 Implementation of the processes in the model | 12 |
| 2 Road dust model formulation | 14 |
| 2.1 Formula conventions | 14 |
| 2.2 Mass balance for dust and salt | 14 |
| 2.3 Road dust and salt production | 15 |
| 2.3.1 Road dust production through direct wear | 16 |
| 2.3.2 Road dust production through deposition | 17 |
| 2.3.3 Road dust production through sanding | 18 |
| 2.3.4 Road dust production through abrasion with sand (sandpaper effect) | 18 |
| 2.3.5 Road dust production through crushing of sand | 19 |
| 2.3.6 Road salt production | 19 |
| 2.4 Road dust and salt sinks | 19 |
| 2.4.1 Road dust and salt reduction through traffic induced suspension | 20 |
| 2.4.2 Road dust reduction through windblown suspension | 21 |
| 2.4.3 Road dust reduction through drainage | 21 |
| 2.4.4 Road dust reduction through cleaning and ploughing | 23 |
| 2.4.5 Road dust reduction through spray and splash | 23 |
| 2.4.6 Non-suspendable dust reduction through crushing | 23 |
| 2.5 Emissions | 24 |
| 2.5.1 Total emissions | 24 |
| 2.5.2 Direct emissions through road, brake and tyre wear sources | 24 |
| 2.5.3 Suspension from the road | 24 |
| 2.5.4 Dependency of road wear PM size fraction on wear and speed | 24 |
| 2.6 Conversion of emissions to concentrations | 25 |
| 2.7 Salting and sanding by rule | 25 |
| 3 Road moisture model formulation | 26 |
| 3.1 Mass balance for road water and snow/ice | 26 |
| 3.2 Precipitation | 27 |
| 3.3 Wetting | 27 |
| 3.4 Drainage | 28 |
| 3.5 Spray and splash | 28 |
| 3.6 Snow ploughing | 29 |

| | | |
|----------|--|-----------|
| 3.7 | Evaporation, condensation and energy balance modelling | 29 |
| 3.7.1 | Net radiation | 30 |
| 3.7.2 | Latent and sensible heat fluxes | 32 |
| 3.7.3 | Vehicle induced heat flux | 34 |
| 3.7.4 | Surface heat flux and temperature | 35 |
| 3.7.5 | Implementation of evaporation and condensation | 36 |
| 3.8 | Melting and freezing | 37 |
| 3.9 | Vapour pressure and melt temperature dependence on salt concentration | 37 |
| 3.10 | Surface moisture retention parameters | 40 |
| 4 | Analytical and numerical solutions to the road dust model | 41 |
| 4.1 | Time integrated mass balance solution | 41 |
| 4.2 | Implicit surface temperature solution | 41 |
| 4.3 | Numerical limitations when calculating surface moisture | 42 |
| 5 | Parameter estimation and sensitivity analysis | 43 |
| 5.1 | Road wear, PM fractions and their functional dependencies | 43 |
| 5.1.1 | Basic road wear for studded tyres | 43 |
| 5.1.2 | PM ₁₀ fraction of studded tyre road wear | 44 |
| 5.1.3 | PM ₁₀ wear rate fraction for studded tyre road wear based on model calibration | 46 |
| 5.1.4 | Non-studded road wear and PM ₁₀ fraction | 48 |
| 5.1.5 | PM _{2.5} size distribution of road wear particles | 48 |
| 5.2 | Tyre and brake wear | 50 |
| 5.3 | Suspension rates and dependencies | 50 |
| 5.4 | Sanding parameters: suspension, size distribution, abrasion and crushing | 52 |
| 5.5 | Salting: drainage and spray efficiencies | 54 |
| 5.6 | Drainage parameters | 55 |
| 5.7 | Spray parameters | 56 |
| 5.8 | Surface retention parameters | 57 |
| 5.9 | Energy balance parameters | 57 |
| 5.9.1 | Sensitivity to surface roughness and traffic induced turbulence | 58 |
| 5.10 | Impact of salt on surface moisture | 58 |
| 5.11 | Conversion of emissions to concentrations | 60 |
| 6 | Steady state solution to the road dust model under dry conditions | 60 |
| 6.1 | Simplified steady state equation for road dust loading | 60 |
| 6.2 | Ratio of direct to suspended emissions | 61 |
| 7 | Datasets and NORTRIP model results | 62 |
| 7.1 | Hornsgatan, Stockholm | 70 |
| 7.2 | Essingeleden, Stockholm | 70 |
| 7.3 | Riksvei 4 (RV4), Oslo | 70 |
| 7.4 | H. C. Andersen Boulevard (HCAB), Copenhagen | 71 |
| 7.5 | Mannerheimintie, Helsinki | 71 |
| 7.6 | Nordby Sletta (NB), Oslo | 71 |
| 7.7 | Runeberg, Helsinki | 71 |
| 8 | Conclusions and future development | 72 |

| | |
|---|------------|
| 9 Acknowledgments..... | 74 |
| 10 References | 74 |
| Appendix A Physical constants and equations used in the NORTRIP model | 77 |
| A.1 Physical constants..... | 79 |
| A.2 Physical equations | 79 |
| Appendix B NORTRIP model variables | 81 |
| Appendix C NORTRIP model parameters and input data requirements | 91 |
| C.1 Default set of model parameters | 93 |
| C.2 Control flags for model processes | 96 |
| C.3 Input data for the sand and salt model | 97 |
| C.4 Dataset input | 98 |
| C.4.1 Metadata | 98 |
| C.4.2 Initial conditions | 99 |
| C.4.3 Traffic data | 100 |
| C.4.4 Meteorological data | 100 |
| C.4.5 Activity data | 101 |
| C.4.6 Air quality data | 101 |
| Appendix D Graphical summary presentation of model results | 103 |
| D.1 Hornsgatan, Stockholm | 105 |
| D.2 Essingeleden, Stockholm..... | 111 |
| D.3 Riksvei 4 (RV4), Oslo | 112 |
| D.4 H. C. Andersen Boulevard (HCAB), Copenhagen..... | 113 |
| D.5 Mannerheimintie, Helsinki | 115 |
| D.6 Nordby Sletta (NB), Oslo | 116 |
| D.7 Runeberg, Helsinki | 117 |
| Appendix E Example of a complete set of model output plots, Hornsgatan 2010-2011 | 119 |

Summary

PM₁₀ concentrations exceed the EU limit values in almost all countries in Europe. Up to 49% of the European urban population is exposed to PM₁₀ concentrations in excess of the EU daily air quality limit value, and there is little or no downward trend in most cities (EEA, 2010). Non-exhaust particle emissions make an important and increasing contribution to PM₁₀ concentrations in cities. In many Nordic cities non-exhaust particle emissions are the main reason for high PM₁₀ levels along densely trafficked roads. This is connected to the use of studded tyres and winter time road traction maintenance, e.g. salting and sanding. In order to better understand and control these emissions both measurement and modelling is required. This document describes the model development undertaken to address this issue.

The NORTRIP model is the result of research efforts carried out by a number of Nordic institutes to improve our understanding and ability to model the non-exhaust traffic emissions. The model has been developed through the Nordic Council of Ministers project NORTRIP (NON-exhaust Road Traffic Induced Particle emissions) with substantial additional support from the Norwegian Climate and Pollution Agency (KLIF). The aim of the project is to develop a **process based emission model** that can be applied in any city without site specific empirical factors, for management and evaluation of abatement strategies, and which is able to describe the (non-exhaust) traffic emissions on an hourly or at least daily basis with satisfactory accuracy. This aim requires that the model is capable of describing the direct emissions of non-exhaust wear sources (road, brake and tyre), their accumulation on the road surface and their subsequent suspension into ambient air. It also requires that other sources of accumulated road mass, such as salting and traction sanding, be described. Apart from the wear and accumulation of mass on the road the surface moisture of the road, along with the impact of dust binding activities, strongly effects the emissions of these sources. The model must include all these aspects if it is to successfully reproduce and predict the impacts of the various processes.

The model consists of two parts: The **road dust sub-model** that predicts the road dust, sand and salt loading through a mass balance approach and determines the emissions through suspension of these loadings as well as through direct wear of road, tyre and brake sources. In addition the **road surface moisture sub-model** determines road surface moisture essential for the prediction of suspension and the retention of dust from the road surface. A surface mass balance approach is also applied, coupled to an energy balance model to predict evaporation/condensation. The model has been developed and assessed using observational data from seven different sites in Oslo, Stockholm, Helsinki and Copenhagen. Experimental data from the road simulator from the Swedish National Road and Transport Research Institute (VTI) has also been included along with extensive assessment of the available literature.

The resulting model successfully reproduces measured concentrations, with satisfactory accuracy, for most of the datasets assessed. Indeed, in some cases, the model exceeds expectations. This is particularly true for simulations of

Hornsgatan in Stockholm which provides the best set of data for model development and assessment. A studded tyre ban has been implemented in 2010 in Hornsgatan and the model successfully reproduced the changes from year to year as a result of this ban. The Hornsgatan site also provides clear proof of the importance of accurate moisture modelling if an understanding of the underlying wear and suspension processes is to be achieved. The results of the model for a site in Copenhagen are less satisfactory and in that case more effort is needed to understand the processes affecting PM concentrations. In Oslo, where speed reduction has been implemented as a mitigation strategy, the model successfully reproduces the observed change in concentrations during this reduction period and also reproduces the effect of meteorological conditions, particularly precipitation, on the observed concentrations. Data from Helsinki, Mannerheimintie, has also been successfully modelled even though this road is made of cobbled stone, different to paved roads. Importantly all these datasets are modelled with a consistent set of model parameters.

There still remain large uncertainties concerning a number of the processes and their description within the model. One large part of the uncertainties regards the availability of information required by the model. For example it is shown that salting will affect the surface moisture due to its impact on the surface vapour pressure. However, if no information concerning salting activities is available then this is difficult to reproduce with the model. Road pavement types and their rate of wear has also been shown in the laboratory to vary significantly but little information is available on real road surfaces. Various processes such as crushing and abrasion of sand particles can only be assessed in the model through sensitivity analysis since there is no experimental data to provide reliable input parameters.

One of the ambitious aims of the model is that it can be used to predict the contribution of salt and traction sand to the PM concentrations. The model is capable of achieving this, and comparisons with salting data in Oslo provide some confidence in the results. For Hornsgatan where some sanding data is available, the model indicates that sanding does not contribute more than around 10% of the annual mean concentrations but may contribute to the number of exceedance days. The contribution from these sources is still quite uncertain and further development is required to refine and build confidence in the modelling results.

The NORTRIP model is currently the most comprehensive process based non-exhaust emission model available. It provides not just a means for predicting non-exhaust contributions to PM concentrations but also a platform for understanding and controlling these emissions. It is expected that the model will be further developed as more information is gathered over time and that its application to a wider range of datasets will only help improve the robustness and performance of the model.

NORTRIP model development and documentation

1 Introduction

This document describes the NORTRIP emission model developed at NILU in conjunction with the Nordic Council of Ministers project NORTRIP (Johansson et al., 2012). The model is based on the work previously carried out by Berger and Denby (2011) but has undergone a large number of changes as a result of activities in NORTRIP, both in terms of model development and improvements in the definition of model parameters. The model concept also has a strong basis in the model from Omstedt et al. (2005), where the concept of surface mass balance for dust and moisture was first developed.

1.1 Aim of the modelling

There are five aims of the model and its development:

1. To predict, as well as possible, the vehicle induced road dust, and other non-exhaust, emissions for a range of road types in the urban environment
2. To have a modelling tool that can be used for air quality management purposes (to assess measures)
3. To have a modelling tool that is sufficiently universal for it to be applied in a variety of environments
4. To have a conceptual tool, that describes the range of processes involved in road dust emissions, providing an overview of these processes and their likely dependencies.
5. To improve the understanding and identify knowledge gaps in processes affecting non-exhaust emissions through application of the model

These five aims have consequences for the model development:

1. The model should function as well as possible for a variety of roads, and should avoid site specific empirical corrections.
2. The model must describe processes that are relevant for any mitigation strategy that may influence the emissions. E.g. speed, road salting, vehicle types, tyre types, road surface types, cleaning activities.
3. The model must describe processes in a universal way, so that it can be applied in all areas, e.g. with other road surface types, other vehicle make ups, other tyre types.

1.2 Conceptual outline of the modelling elements

One of the most fundamental problems with road dust emission modelling is the complexity and variety of processes. These may be very different in different environments. This problem is enhanced by a general lack of monitoring data to support process descriptions and a lack of input data suitable for describing the processes.

There are some basic elements of the model that are required. These are:

1. Direct emissions due to road and other wear sources
2. Indirect emissions (suspension) of road dust, sand and salt loading
3. Road dust and salt loading, dependent on the road dust and salt mass balance
4. Retention of the direct and indirect emissions based on road surface conditions, requiring a description of surface wetness

The key elements of the modelling system are presented schematically in Figure 1.1

Model concept and processes

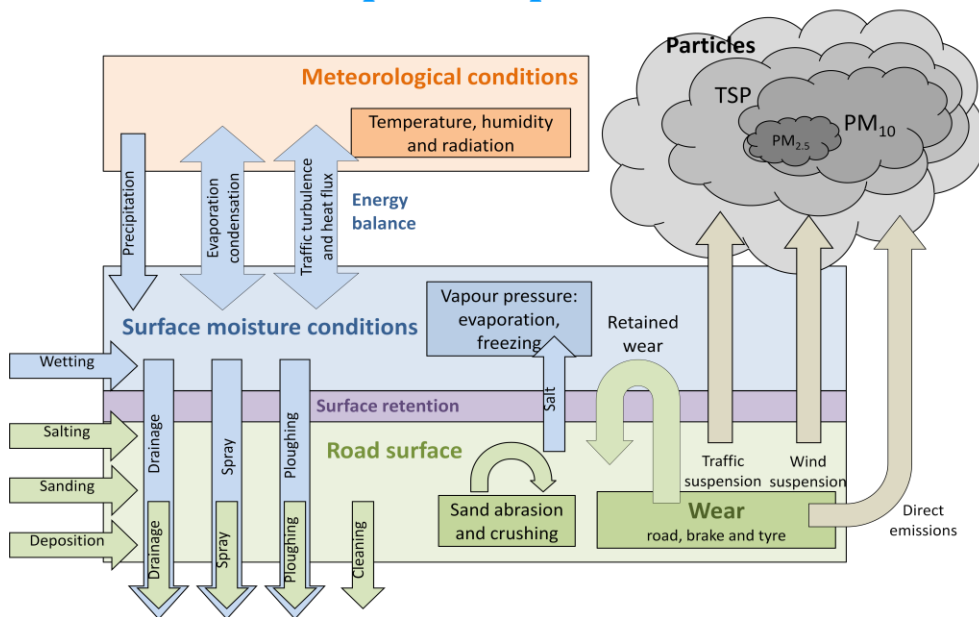


Figure 1.1. Schematic outline of the NORTRIP emission model.

The rest of this section conceptually outlines the model processes before implementing these mathematically and numerically in Sections 2 - 4. Derivation of model parameters is described further in Section 5. In Section 6 a simplified steady state solution to the road dust equations is presented and in Section 7, and Appendix D, the datasets are described and the results presented.

1.2.1 Direct emissions through road and other wear sources

Tyres, especially studded tyres, scrape the surface of the road, releasing a range of particle sizes through wear of the road surface. The process is likely dependent on a range of inputs including:

- the stud type and number (tyre type)
- the weight of the vehicles (vehicle type)
- the speed of the vehicles (speed limits)
- the pavement type
- the driving cycle
- the road surface conditions (temperature, retention through wetness, freezing, snow/ice cover)

In addition to road wear other wear sources of direct emissions will occur. These sources include brake wear and tyre wear. There exists a range of non-exhaust emission factors, dependent on vehicle type and speed, in the literature. These sources can be dealt with, and are dealt with, by vehicle type specific emissions factors with speed dependence. For the case of tyre wear this is also likely to be dependent on surface temperature.

A proportion of the road wear particles are emitted instantaneously to the air and the remaining fraction accumulates on the road, depending on the surface conditions. Tyre and brake wear may also be retained on the surface when the surface is moist. Brake wear is likely only to be retained under very wet conditions when brakes may become wet.

Under dry conditions the accumulated wear will be quickly suspended again, on very short time scales. Such particles may be effectively described as direct emissions but they may be crushed by the passage of tyres(studded and non-studded) and as a result alter their size distribution. Road wear will also occur due to the abrasion of existing road dust or sand between the tyre and road surface, also called the 'sandpaper' effect. This is most likely to occur due to the addition of traction sanding or gravel but may also occur with the road wear particles themselves.

The NORTRIP model bases its emissions firstly on total wear and then secondly on the size distribution of that wear. As a result the different size distributions of the different wear sources need to be taken into account.

1.2.2 Suspended emissions induced by road traffic

Particles may arrive on the road surface through a variety of means. These include road wear, deposition from external ambient air sources, deposition from traffic sources (e.g. exhaust, non-exhaust wear), sanding or gravel, migration from kerbs and salting. The road surface particles may be emitted by direct contact with the tyre or by the induced turbulence of the vehicle. The suspension process becomes more complicated when one considers that road dust accumulated on the shoulder of the road may also migrate onto the road due to vehicle turbulence, runoff or meandering of cars from the normal traffic lanes, including parking activities. Road dust is likely to accumulate within pores in the road surface and the rate of suspension will likely depend on the road surface macro-structure. In this regard it is also important to note that the suspension rate of freshly distributed dry dust, and also by inference road wear particles under dry conditions, may show significantly different suspension rates to dust that has been wet and is bonded within the road surface macro-structure.

The suspension process will likely be dependent on:

- The mass, the characteristics and the size distribution of the road dust on the surface (road dust loading). This means the amount of salting and sanding and the amount of external deposition as well as cleaning and ploughing activities need to be known.

- The suspension rate, which may depend on a range of processes, e.g. tyre contact, vehicle turbulence, migration, road surface macro-structure, etc.
- The surface conditions. The wetness or retentiveness of the road surface is an essential element for the process of suspension. In addition, wet surfaces retain the particles and this may increase road wear, building up the dust reservoir on the road surface.

As in direct wear, the suspension rates for different size distributions, or the size distribution of the dust loading, is required if the emissions are to be described.

1.2.3 Road dust and salt loading

Road wear and other sources will contribute to a build up of road dust, something that is quite obvious in the studded tyre season. At the same time suspension and other removal processes such as drainage, spray, cleaning or snow ploughing will reduce the amount of road dust and salt. This process is described in terms of the surface mass balance of the road, where 'the road surface' is loosely defined as the surface area that stores the road dust/salt that is still available in some way for suspension. This may partially include the shoulder of the road. In Berger and Denby (2011) the shoulder was included as a separate road dust reservoir but in the current modelling this concept has been removed.

For road dust an equilibrium loading will be achieved when the production of dust is equivalent to the removal of dust. In Berger and Denby (2011) a time scale was defined indicative of the time required to reach equilibrium under dry conditions. In addition it was shown that under dry conditions the equilibrium dust loading was independent of the number of vehicles and as such should be fairly constant irrespective of the traffic volume in dry periods, see Section 6. However, the rates of suspension and subsequent time scales, as described above, may be much longer than the length of the dry periods and so equilibrium may never be reached.

1.2.4 Surface retention

This is perhaps the most important short term parameter that impacts on the road dust emissions. When the surface is wet then particles will be in suspension with droplets of water. These droplets are too heavy to be suspended and are only temporarily lifted from the surface with the passage of a vehicle (vehicle spray). This is also true when the surface is snow covered. In the case of frozen surfaces (dry) suspension through turbulence is inhibited as particles are frozen to the surface in the pores of the road surface. A similar retentive process occurs when hygroscopic salt inhibiting solution ($MgCl_2$ or CMA) is sprayed on the surface. This keeps a layer of water on the surface, attaching the particles. Knowing when the surface is wet, when it is frozen and when the surface is covered in prohibitive solutions is necessary in order to assess the retentive ability of the surface.

1.3 Implementation of the processes in the model

The model developed consists of two main sub-models. These two sub-models are:

1. Road dust sub-model:

This predicts the road dust, sand and salt loading through a mass balance approach and determines the emissions through suspension of these loadings as well as through direct wear of road, tyre and brake sources.

2. Road surface moisture sub-model:

This determines road surface moisture essential for the prediction of suspension and the retention of dust from the road surface. A surface mass balance approach is also applied coupled to an energy balance model to predict evaporation/condensation.

Within the **road dust sub-model** the following parameterised forms of the processes, outlined in Section 1.2, are described.

1. Mass balance for accumulated dust and salt loadings
2. Road wear, based on the Swedish road wear model
3. Tyre and brake wear, based on literature
4. Addition of salt and sand through road maintenance activities
5. PM size fractions, based on literature and experimental data
6. Retention of wear particles (dust loading) on the road surface due to surface moisture
7. Removal of the dust loading through traffic induced suspension
8. Direct emissions from wear sources
9. Suspended emissions from dust and salt loading
10. Drainage of the dust and salt load
11. Spraying of the dust and salt load
12. Removal of the dust and salt loading through cleaning and snow ploughing
13. Abrasion of the road surface through sand (sand paper effect)
14. Crushing of sand into suspendable particles
15. Windblown suspension
16. Accumulation of dust through atmospheric deposition
17. Salting and sanding maintenance activity modelling

Within the **road surface moisture sub-model** the following parameterised forms of the processes, outlined in Section 1.2, are described.

1. Mass balance for surface moisture (water and ice/snow)
2. Production through precipitation
3. Production through road maintenance wetting activities
4. Removal through drainage
5. Removal through spray processes
6. Removal of snow through snow ploughing activities
7. Evaporation and condensation using an energy balance model
8. Melting and freezing processes
9. Impact of salt solution on vapour pressure and freezing temperatures

The model has been programmed in the MATLAB scripting environment and makes use of Excel files as input formats for data and model parameters. The model is also available as an executable. See the '*NORTRIP emission model user guide*' (Denby, 2012) for more information concerning implementation of the model.

2 Road dust model formulation

In this section the model formulation of the road dust sub- model is described. In Section 3 the surface moisture model is described. In Section 4 some numerical aspects of the modelling are described.

2.1 Formula conventions

For clarity the following conventions are used in the equation formulation. For any model parameter (Y) we use the following sub- and postscript conventions:

$$Y_{\text{discriptive subscript}}^{\text{table dependence}}(\text{functional dependence})$$

For emission variables this is given by:

$$E_{\text{discriptive subscript}}^{PM \text{ size fraction}(x)}$$

In general factors that represent non-dimensional ratios or ratios veh^{-1} are indicated by the letters f and h , mass loading terms by the letter M (g.km^{-1}), production terms by the letter P ($\text{g.km}^{-1}.\text{hr}^{-1}$), sink terms by the letter S ($\text{g.km}^{-1}.\text{hr}^{-1}$), emissions by the letter E ($\text{g.km}^{-1}.\text{hr}^{-1}$) and rate terms by the letter R (hr^{-1}). In regard to the surface wetness and retention parameters we use the same naming convention as Omstedt et al. (2005). The conventions are similar to but differ somewhat to the original description of the model described by Berger and Denby (2011). These changes are intended to aid clarity to the model.

The terms used here in the model description are directly reflected in the model coding so that there is no confusion concerning the variables and parameters.

2.2 Mass balance for dust and salt

The *dust* mass, or dust loading, may be separated into different size fractions but only two are represented in the model. These are a finer fraction of suspendable dust ($< \sim 200 \mu\text{m}$) and a courser fraction of non-suspendable dust/sand ($> \sim 200 \mu\text{m}$). The term suspendable in this case refers to the ability of traffic to remove the dust from the road system, even if the travel distances of the air born particles are not very far. The delineation between the finer and coarser fractions is intended to better represent the addition of traction sanding to the surface, which is mostly in the coarser fraction. Crushing of the coarser fraction may result in mass transfer to the finer fraction and abrasion may lead to generation in the fine fraction. The delineation at around $200 \mu\text{m}$ is intended to reflect the size distribution of road wear particles which are considered to be less than $200 \mu\text{m}$ so that road wear is all in the suspendable fraction. This may be updated at a later date as more information becomes available and the possibility of dividing the suspendable fraction into smaller size segregations may also be considered.

The suspendable and non-suspendable fractions, as well as salt mass, are indexed with m . The index for dust loadings is:

- suspendable wear particles; $m=dust(sus)$
- suspendable sand particles; $m=dust(sus-sand)$
- non-suspendable sand particles; $m=dust(non-sus)$

It is assumed that wear processes contribute only to the suspendable dust loading but that sanding can contribute to both suspendable and non-suspendable loadings, dependent on the size distribution of the sand applied. A separate index for suspendable sand ($dust(sus-sand)$) is given in order to trace the impact of sand in the model.

Salt can also be divided into different salt types, sodium, calcium or magnesium based salts or acetates, as these may have different retention properties. Currently only two type are included in the model. These are:

- sodium chloride $m=salt(na)$
- magnesium chloride $m=salt(mg)$

The mass balance equation is written as

$$\frac{\partial M_{road}^m}{\partial t} = P_{road}^m - S_{road}^m \quad (2.1)$$

Where M_{road}^m is the mass loading for the mass type m, P_{road}^m and S_{road}^m represent the production and sink terms respectively. The total suspendable road surface mass loading ($M_{road(total)}$) is given by

$$M_{road(total)} = \sum_m^{mass_type} M_{road}^m \quad (2.2)$$

2.3 Road dust and salt production

Road dust production is the sum of a number of sources. For the suspendable dust load these include: *retention* of wear particles on the road surface, *deposition* from ambient air, direct mass contribution from *sanding* in the suspendable size fraction ($f_{sanding}^{sus}$), abrasion of the road surface by the contact of the vehicle tyre with the non-suspendable dust loading (*sandpaper* effect) and *crushing* of the coarser non-suspendable loading to create finer particles in the suspendable fraction. Abrasion is difficult to separate from crushing as they will both be dependent on the amount of non-suspendable material available on the road surface and on the traffic volume and category. They may only be distinguished using measurements by chemical analysis of the dust loading (Kupiainen et al., 2005). In addition to these terms a *fugitive* rate production may be included. Fugitive production may include any process not described above. The road dust production can hence be written as:

$$P_{road}^{dust(sus)} = P_{retention} + P_{deposition} + P_{sanding} \cdot f_{sanding}^{sus} + P_{sandpaper} + P_{crushing} + P_{fugitive}^{dust(sus)} \quad (2.3)$$

For the non-suspendable production we include just two terms, this is the contribution of traction sanding in the non-suspendable size fraction ($1 - f^{sus}_{sanding}$) and a non-specific fugitive contribution. These fugitive sources may include road break up, road work activities, pavement sweeping, etc. These fugitive terms, if they are known, may also be included in the model.

$$P_{road}^{dust(non-sus)} = P_{sanding} \cdot (1 - f^{sus}_{sanding}) + P_{fugitive}^{dust(non-sus)} \quad (2.4)$$

As with sanding, there is only one source of salt production in the model (Equation 2.19), that being the addition of salt, dry or wet, related to defreezing or dust binding activities.

2.3.1 Road dust production through direct wear

A proportion of the dust produced from direct wear sources is emitted and removed from the road system, the rest is retained on the surface (*retention*) and contribute to the road dust production. These terms are parameterised in Equations 2.5-2.10. The rate of wear (WR_{source} [g.km⁻¹.hr⁻¹]) given in Equations 2.5 and 2.6, where *source* indicates either *roadwear*, *breakwear* or *tyrewear*, is determined by the number of vehicles ($N^{t,v}$ [veh.hr⁻¹]) and the wear parameter W_{source} [g.km⁻¹.veh⁻¹]. The wear parameter is dependent on a basic wear factor ($W_{0,source}^{t,v}$ [g.km⁻¹.veh⁻¹]) that is specified through user defined lookup tables for each vehicle category (*v*), tyre type (*t*) and wear source (*source*) This basis wear parameter may be adjusted by the pavement type factor (h^p_{pave}) for different pavements (*p*) or by a driving cycle factor ($h^d_{drivingcycle}$) for different driving cycles (*d*), dependent on the type of wear. The wear parameter is also considered to be functionally dependent on the vehicle speed (V^v_{veh} [km.hr⁻¹]) and on the depth of snow/ice on the road surface (*s* [mm.w.e.]). Other dependencies, such as on surface temperature, may also exist, but this is not included in the current model formulation.

The amount of retention is dependent on the fraction of wear that is lost from the road through direct wear emissions ($f_{0,dir-source}$) and by the surface wetness factor ($f_{q,source}$). This last term is dependent on the surface moisture, both liquid (g_{road}) or frozen (s_{road}) water and may be different for road and tyre wear sources (*roadwear*, *tyrewear*) than for brake wear (*brakewear*) since the later is not in direct contact with the road surface.

$$P_{retention} = \sum_{source=roadwear,tyrewear,brakewear} P_{retention-source} \quad (2.5a)$$

$$P_{retention-source} = \sum_{t=st,wi,su}^{tyre} \sum_{v=he,li}^{vehicle} WR_{source}^{t,v} \cdot [1 - f_{0,dir-source}^{t,v} \cdot f_{q,source}] \quad (2.5b)$$

The wear rates ($WR_{source}^{t,v}$) are given as follows for the different wear sources:

$$\begin{aligned} WR_{roadwear}^{t,v} &= N^{t,v} \cdot W_{roadwear}^{t,v} (W_{0,roadwear}^{t,v}, h^p_{pave}, V^v_{veh}, s_{road}) \\ WR_{tyrewear}^{t,v} &= N^{t,v} \cdot W_{tyrewear}^{t,v} (W_{0,tyrewear}^{t,v}, V^v_{veh}, s_{road}) \\ WR_{brakewear}^v &= N^v \cdot W_{brakewear}^v (W_{0,brakewear}^v, h^d_{drivingcycle}) \end{aligned} \quad (2.6)$$

The functional dependency of the road wear parameter ($W_{roadwear}^{t,v}$) is given as:

$$W_{roadwear}^{t,v} = W_{0,roadwear}^{t,v} \cdot h_{pave}^p \cdot f_{snow,road}(s_{road}) \cdot \left(\frac{V_{veh}^v}{V_{ref,roadwear}} \right)^{a_{wear}} \quad (2.7)$$

It is assumed that the vehicle speed dependency is linear ($a_{wear}=1$) but the power law dependence is included for flexibility. The term $f_{snow,road}$ indicates the impact of snow/ice on the road surface. It is a binary function whereby above a threshold ice/snow thickness ($s_{roadwear,thresh}$) no road or tyre wear occurs. A value of 3 mm w.e. is currently used.

$$\begin{aligned} f_{snow,road}(s_{road}) &= 1 \quad \text{for } s_{road} < s_{roadwear,thresh} \\ &= 0 \quad \text{for } s_{road} > s_{roadwear,thresh} \end{aligned} \quad (2.8)$$

Tyre wear follows a very similar description to the road wear but is not considered to be dependent on the pavement type.

$$W_{tyrewear}^{t,v} = W_{0,tyrewear}^{t,v} \cdot f_{snow,road}(s_{road}) \cdot \left(\frac{V_{veh}^v}{V_{ref,tyrewear}} \right)^{a_{wear}} \quad (2.9)$$

Brake wear is not considered to be dependent on tyre type or on the vehicle speed. It is better determined by braking activity than by vehicle speed, though there may be some relationship between these two (Boulter, 2005). We use a general ‘driving cycle’ factor that can alter the basis brake wear parameters if required. Driving cycle type may include highway, urban, congested, etc. and these are represented by the given ‘driving cycle’ factor.

$$W_{brakewear}^v = W_{0,brakewear}^v \cdot h_{drivingcycle}^d \quad (2.10)$$

There are a large number of terms included in the above description of road dust production. Not all of these need to be used in the model, however they are intended to reflect relevant processes and to provide the possibility to assess the impact of various changes. E.g. if the pavement type is changed from the reference type, for which the wear parameters have been derived, and there is experimental data indicating that this new pavement type alters the wear rate then this factor can be immediately included in the model calculations. The same is true for the driving cycle type, if the type of driving is altered (and its effect on wear is known) then its impact on the wear rates can be immediately included in the model. Describing the model in this way is intended to give it flexibility when carrying out management and planning activities.

2.3.2 Road dust production through deposition

The external deposition of material on the road surface is given by the background *TSP* concentration PM_{TSP} [$\mu\text{g}\cdot\text{m}^{-3}$] and deposition velocity w^{TSP} [$\text{m}\cdot\text{s}^{-1}$]. To

provide a production rate $P_{deposition}$ [$\text{g}\cdot\text{km}^{-1}\cdot\text{hr}^{-1}$] the deposition flux, $F_{deposition}$ [$\text{g}\cdot\text{km}^{-1}\cdot\text{hr}^{-1}\cdot\text{m}^{-1}$], is calculated, using appropriate conversion constants. This is multiplied with the width of the road area $n_{lanes}\cdot b_{lane}$ [m] to determine the production rate.

$$P_{deposition} = F_{deposition} \cdot n_{lanes} \cdot b_{lane} \quad (2.11a)$$

$$F_{deposition} = 3.6 \cdot w_{dep}^{TSP} \cdot PM_{TSP,background} \quad (2.11b)$$

TSP is rarely available and this can be replaced by PM_{10} . This term is likely to be very small except under special circumstances, such as Saharan dust episodes.

2.3.3 Road dust production through sanding

The contribution through sanding ($P_{sanding}$) is given by the mass of sand ($M_{sanding}$) distributed on the road within a particular hour. The contribution of mass through sanding is spread out over the time step of the model ($\Delta t = 1$ hour). The sand is split into two size fractions (suspendable and non-suspendable) using the factor $f^{sus}_{sanding}$ which represents the suspendable fraction of the applied sand. Some knowledge of the size distribution of the traction sand is thus required. Units for sanding are generally provided as [$\text{g}\cdot\text{m}^{-2}$] and the conversion factor to provide sanding rates ($P_{sanding}$) in [$\text{g}\cdot\text{km}^{-1}\cdot\text{hr}^{-1}$], assuming all of the sand arrives on the road surface, is included in equation 2.12.

$$P_{sanding} = \frac{M_{sanding}(t_{sanding})}{\Delta t} \cdot 1000 \cdot n_{lanes} \cdot b_{lane} \quad (2.12)$$

Applied sanding mass may be input directly to the model as a time series or may be calculated using a ‘sanding model’ which is intended to reproduce sanding activities based on user specified rules, Section 2.7.

2.3.4 Road dust production through abrasion with sand (sandpaper effect)

The sand paper effect, generation of road wear through abrasion with existing non-suspendable dust mass, is given by:

$$P_{sandpaper} = M_{road}^{dust(non-sus)} \cdot R_{sandpaper} \quad (2.13)$$

Where the wear rate is given as:

$$R_{sandpaper} = \sum_{t=st,wi,su}^{tyre} \sum_{v=he,li}^{vehicle} \frac{N^{t,v}}{n_{lanes}} \cdot f_{sandpaper}^{t,v} (f_{0,sandpaper}^{t,v}, V_{veh}^v, h_{pave}^p, s_{road}) \quad (2.14)$$

The term $f_{sandpaper}^{t,v}$ [veh^{-1}] has similar dependencies as the road wear parameter (Equation 2.7) as follows

$$f_{sandpaper}^{t,v} = f_{0,sandpaper}^{t,v} \cdot h_{pave}^p \cdot f_{snow,road}(s_{road}) \cdot \frac{V_{veh}^v}{V_{ref,sandpaper}} \quad (2.15)$$

The basis sandpaper factor ($f_{0,sandpaper}$) is the rate per vehicle at which the road surface is worn, dependent on the non-suspendable mass fraction. Though this term is included in the model the basic factors are quite unknown, however when non-suspendable dust is available on the surface this term may become significant (Kupiainen et al., 2005).

2.3.5 Road dust production through crushing of sand

Suspendable particles may be produced on the road surface by the physical crushing of existing non-suspendable dust, particularly from sanding, on the road surface. This is described by:

$$P_{crushing} = M_{road}^{dust(non-sus)} \cdot R_{crushing} \quad (2.16)$$

Where the crushing rate is given as:

$$R_{crushing} = \sum_{t=st,wi,su}^{tyre} \sum_{v=he,li}^{vehicle} \frac{N^{t,v}}{n_{lanes}} \cdot f_{crushing}^{t,v}(f_{0,crushing}, V_{veh}^v, s_{road}) \quad (2.17)$$

The functional dependence of ($f_{crushing}$) is not well defined so we apply the same dependencies as for road wear. i.e.

$$f_{crushing}^{t,v} = f_{0,crushing}^{t,v} \cdot f_{snow,road}(s_{road}) \cdot \frac{V_{veh}^v}{V_{ref,crushing}} \quad (2.18)$$

This term is very similar to the sandpaper term. The difference is that the crushing rate ($R_{crushing}$) is also a sink term in the non-suspendable dust mass balance, see Section 2.4.

2.3.6 Road salt production

Salting is an addition of mass ($M_{salting}$). As with sanding the instantaneous mass increase is spread out over the hour based on the timing, $t_{salting}$. Units for salting are provided as [gm^{-2}] and the conversion factor to [$g.km^{-1}.hr^{-1}$], assuming all of the salt arrives on the road surface, is included in Equation 2.19

$$P_{road}^{salt(i)} = \frac{M_{salting}^{salt(i)}(t_{salting})}{\Delta t} \cdot 1000 \cdot n_{lanes} \cdot b_{lane} \quad (2.19)$$

Applied salting mass may be input directly to the model as a time series or may be calculated using a 'salting model' which is intended to reproduce salting activities based on established local rules, see Section 2.7.

2.4 Road dust and salt sinks

The removal processes (sinks) are similar for both dust and salt, and both are considered to be dependent on the available mass. We can calculate the sinks

($S_{process}$) based on appropriate rates ($R_{process}$) for each process and apply these to all dust or salt masses individually as follows.

$$S_{process} = M_{road} \cdot R_{process} \quad (2.20)$$

Two of these sinks, suspension and windblown dust, are also related to emissions. It is assumed that the suspension of road dust is linearly proportional to the mass of road dust. This may be the case for low levels of dust loading but this may not be the case when dust loading is extensive, e.g. for unpaved roads. We write the various road dust sink terms for the various processes, indexed with m for the different mass types, as follows:

$$S_{road}^m = S_{suspension}^m + S_{windblown}^m + S_{drainage}^m + S_{cleaning}^m + S_{ploughing}^m + S_{spray}^m + S_{crushing}^m \quad (2.21)$$

Note that for suspendable (*sus*) mass types $S_{crushing}^{sus} = 0$ and that for non-suspendable (*non-sus*) mass types $S_{suspension}^{non-sus} = 0$ and $S_{windblown}^{non-sus} = 0$.

2.4.1 Road dust and salt reduction through traffic induced suspension

The reduction of road dust and salt loading through suspension is given by:

$$S_{suspension}^m = M_{road}^m \cdot R_{suspension}^m \quad (2.22)$$

$$R_{suspension}^m = \sum_{t=st,wi,su}^{tyre} \sum_{v=he,li}^{vehicle} R_{suspension}^{m,t,v} \quad (2.23)$$

$$R_{suspension}^{m,t,v} = \frac{N^{t,v}}{n_{lanes}} \cdot h_{0,suspension}^m \cdot f_{suspension}^{t,v}(f_{0,suspension}^{t,v}, V_{veh}^v) \cdot f_{q,suspension}(s_{road}, g_{road}) \quad (2.24)$$

Division of the number of vehicles ($N^{t,v}$) by the number of lanes (n_{lanes}) is required to account for the distribution of mass and traffic on the road. Note that it is assumed that all lanes carry the same amount of traffic. We note that even though the non-suspendable mass does not undergo ambient suspension it does undergo a similar process. i.e. the non-suspendable fraction can be removed from the road surface and deposited on the road shoulder or pavement by contact with the vehicle tyre.

The defining term in Equation 2.24 is the suspension factor ($f_{suspension}^{t,v}$) which defines the fraction of mass that is removed for each passage of each vehicle. This is dependent on a basic suspension factor ($f_{0,suspension}^{t,v}$ dependent on the vehicle type v and the tyre type t) as well as on vehicle speed (V_{veh}^v). The suspension rate for salt suspension is generally taken to be the same as for the suspendable road dust mass. To increase flexibility it is possible to specify salt, suspendable sand and non-suspendable sand suspension rates differently in the model using the

scaling factor ($h_{0,suspension}^m$). The suspension rate is given with a power law dependence on vehicle speed (a_{sus}). We include a site specific scaling factor (h_{sus}) that can be used to reflect different road macro-structures and their impact on the suspension rates. This is set to unity unless otherwise specified. Previous measurements have indicated that this may be linear or quadratic in nature.

$$f_{suspension}^{t,v} = h_{sus} \cdot f_{0,suspension}^{t,v} \cdot \left(\frac{V_{veh}^v}{V_{ref,sus}} \right)^{a_{sus}} \quad (2.25)$$

We note here again that the suspension rate may not simply be a rate determined by the passage of vehicles but may also represent the migration of off-road sources onto the road or the combined process of turbulence and tyre contact.

2.4.2 Road dust reduction through windblown suspension

The sink of suspendable particles by windblown dust from the road surface is given by

$$S_{windblown}^{sus} = M_{road}^{sus} \cdot R_{windblown}^{sus} \quad (2.26)$$

$$R_{windblown}^{sus} = f_{q,suspension}(s_{road}, g_{road}) \cdot R_{0,wind}(FF) \quad (2.27)$$

Where the index ‘sus’ represents all suspendable mass types. The rate dependency of $R_{0,wind}$ on the wind speed FF is given as:

$$R_{0,wind}(FF) = \frac{1}{\tau_{wind}} \cdot \left(\frac{FF}{FF_{thresh}} - 1 \right)^3 \quad \text{for } FF > FF_{thresh}$$

$$= 0 \quad \text{for } FF \leq FF_{thresh} \quad (2.28)$$

In this case the road mass is removed by wind under dry conditions at the rate $R_{0,wind} \cdot FF_{thresh}$ is the threshold wind speed below which no suspension occurs and τ_{wind} [hr] is the time scale at which suspension occurs at the given reference wind speed. Typical values may be found in the literature, though these do not consider available mass but consider mass to be continually available (e.g. Nicholson, 1993). Due to the lower wind speeds in the urban canopy this is generally not active in the model. Non-suspendable particles are assumed not to take part in this process.

2.4.3 Road dust reduction through drainage

The removal of dust and salt by drainage is related directly to the amount of surface water that is drained from the road $g_{road,drainable}$ (Section 3.4). This water will carry with it both dust and salt. The removal of dust and salt requires knowledge of the level of mixing in the drainage water. For salt, which is in solution, this will be fairly well mixed. For suspendable dust on the road surface this may not be well mixed and for non-suspendable dust the efficiency of removal by drainage may be very poor (Vaze and Chiew, 2002). To reflect this, a drainage efficiency parameter is used ($h_{drain-eff}^m$) which can range from 1, for the well mixed situation, to 0, when no mass is removed through drainage. An

additional aspect concerning drainage is that dust particles will stick to the snow surface, if snow is present, even though melting may lead to significant drainage. To this end a snow depth drainage limit ($s_{\text{drain-limit}} = 2 \text{ mm}$) is set so that dust is not removed when the snow depth is greater than this limiting value.

In Section 3.4, that describes the model drainage process, the drainable water is removed instantaneously. This means that the surface reservoir of non-drainable water ($g_{\text{road,drainable-min}}$) is considered to be continuously replenished by clean water that is continuously drained at the same rate. Assuming this, and that the dust and salt is continuously mixed with an efficiency ($h_{\text{drain-eff}}^m$) in the surface reservoir, then the total sink of mass in the drainage water will be

$$S_{\text{drainage}}^m = \frac{M_{\text{road}}^m}{\Delta t} \cdot \left(1 - \exp\left(-h_{\text{drain-eff}}^m \cdot \frac{g_{\text{road,drainable}}}{g_{\text{road,drainable-min}}}\right) \right) \quad \text{for } s_{\text{road}} < s_{\text{drain-limit}}$$

$$= 0 \quad \text{for } s_{\text{road}} > s_{\text{drain-limit}}$$

(2.29)

In the case of salt only the dissolved salt is considered to be drainable. The removal of mass through drainage occurs, as is the case of water, after the other production and sink terms have been calculated. An example is given in Figure 2.1 for four different efficiency rates assuming a minimum drainable depth ($g_{\text{road,drainable-min}}$) of 1 mm.

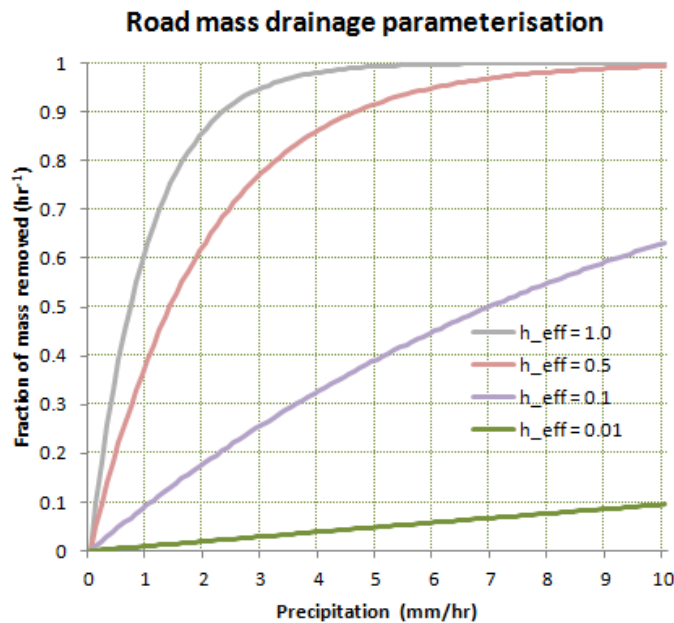


Figure 2.1. The impact of different drainage efficiency parameters on the drainage for a minimum drainage threshold of 1 mm, over the period of one hour for a range of precipitation rates (0-10 mm/hr). It is assumed that the surface moisture content is at the threshold level before the precipitation

2.4.4 Road dust reduction through cleaning and ploughing

For cleaning and ploughing we describe the efficiency of these activities using the factor $h^m_{\text{cleaning-eff}}$ and $h^m_{\text{ploughing-eff}}$. i.e. cleaning or ploughing removes this fraction of the surface mass. $h^m=1$ indicates that all the mass is removed. The different mass types may have different efficiencies, e.g. that road cleaning is more efficient in removing the coarser particles than the finer particles from the road surface. To be consistent with the other removal and addition processes, we solve these sink processes assuming that the reduction occurs over the model time step Δt , rather than instantaneously. In order that the mass reduction over the time period Δt corresponds to the implied instantaneous mass reduction, when solved using Equation 4.2, then we write the sinks for cleaning and ploughing as follows:

$$S^m_{\text{cleaning}} = M^m_{\text{road}} \cdot \frac{-\log(1 - h^m_{\text{cleaning-eff}})}{\Delta t} \cdot \delta(t_{\text{cleaning}}) \quad (2.30)$$

$$S^m_{\text{ploughing}} = M^m_{\text{road}} \cdot \frac{-\log(1 - h^m_{\text{ploughing-eff}})}{\Delta t} \cdot \delta(t_{\text{ploughing}}) \quad (2.31)$$

In this way the rates are defined so that at the end of the time step the resulting mass is equivalent to $(1 - h^m)$, as it would be if the reduction was instantaneous. We use the delta function (δ) to indicate the hours when these activities occur. Note that $h^m=1$ (complete efficiency) is not possible using this formulation and this is numerically dealt with by reducing the efficiency by a very small amount.

2.4.5 Road dust reduction through spray and splash

Removal of mass from the road surface due to splash and spray processes is treated in a similar way to drainage. The rate of water removal by splash and spray $R_{g,\text{spray}}$ (Section 3.5) provides the basis of the mass removal. The efficiency of the mixing in the spray is given by the factor $h^m_{\text{spray-eff}}$ for the different mass types (dust/salt). Dust and non-dissolved salt will have a lower efficiency of removal. We can thus write the spray sink for both dust and salt as:

$$S^m_{\text{spray}} = M^m_{\text{road}} \cdot R_{g,\text{spray}} \cdot h^m_{\text{spray-eff}} \quad (2.32)$$

No consideration is given to snow surfaces, i.e. the spray process applies only to surface water.

2.4.6 Non-suspendable dust reduction through crushing

Crushing of sand is a sink for the non-suspendable dust and is equivalent to the production of suspendable dust through crushing, Section 2.3.5, i.e.

$$S^{\text{dust(non-sus)}}_{\text{crushing}} = P_{\text{crushing}} \quad (2.33)$$

2.5 Emissions

2.5.1 Total emissions

The total emission (E^x) from wear and surface suspension sources for a particular PM size fraction (x), e.g. $x = TSP, 10, 2.5, 1 \mu m$, is given by

$$E^x = E_{direct}^x + E_{suspension}^x \quad (2.34)$$

2.5.2 Direct emissions through road, brake and tyre wear sources

The direct emissions, from the wear sources, is written in the following way:

$$E_{direct}^x = \sum_{source=roadwear,tyrewear,brakewear} E_{dir-source}^x$$

$$E_{dir-source}^x = \sum_{t=st,wi,su}^{tyre} \sum_{v=he,li}^{vehicle} WR_{source}^{t,v} \cdot f_{0,dir-source}^{t,v} \cdot f_{q,source} \cdot f_{PM,dir-source}^{x,t} \quad (2.35)$$

Here, as elsewhere, *source* refers to the *roadwear*, *brakewear* and *tyrewear* sources

2.5.3 Suspension from the road

The suspension is assumed to be linearly dependent on the road dust loading (M_{road}) and follows the same form as the sink term for suspension, Equations 2.22-2.24.

$$E_{suspension}^x = E_{sus-road}^x + E_{wind-road}^x \quad (2.36a)$$

$$E_{sus-road}^x = \sum_{m=sus} M_{road}^m \cdot \sum_{t=st,wi,su}^{tyre} \sum_{v=he,li}^{vehicle} R_{sus-road}^{t,v} \cdot f_{PM,sus-road}^{x,t} \quad (2.36b)$$

$$E_{wind-road}^x = \sum_{m=sus} M_{road}^m \cdot R_{windblown}^{sus} \cdot f_{PM,sus-road}^x \quad (2.36c)$$

2.5.4 Dependency of road wear PM size fraction on wear and speed

The fraction of wear in any particular PM size category may also be dependent on pavement type, tyre type and on vehicle speed, particularly in regard to studded tyres. We define the dependency of the direct and suspended emission fraction on vehicle speed in a linear form (Snilsberg at al., 2008) such that

$$f_{PM,dir-roadwear}^{x,t} = \sum_v^{vehicle} f_{PM,ref,roadwear}^{x,t} \cdot \frac{(1 + c_{PM-fraction}^x \cdot V_{veh}^v)}{(1 + c_{PM-fraction}^x \cdot V_{ref,PM-fraction})} \quad (2.37a)$$

The coefficient $c_{PM-fraction}$ and the reference PM_x fraction ($f_{PM,ref,roadwear}$) at the reference speed ($V_{ref,PM-fraction}$) must be determined, see Section 5.1.2. Equation 2.37a is written in this form so that the user can define a PM fraction at a given reference speed. To be consistent with the road wear size distribution the size fraction of suspended particles is given in the same way:

$$f_{PM,sus-road}^{x,t} = \sum_v^{vehicle} f_{PM,ref,sus-road}^{x,t} \cdot \frac{(1 + c_{PM-fraction}^x \cdot V_{veh}^v)}{(1 + c_{PM-fraction}^x \cdot V_{ref,PM-fraction})} \quad (2.37b)$$

The size fraction for suspendable dust is defined as being the same for all wear sources, whilst these may be different for direct emissions from wear sources. In any future development of the model it may be desirable to define the suspended size fraction individually for each source. This would effectively lead to a size segregation within the suspendable dust mass in the model.

2.6 Conversion of emissions to concentrations

When comparing model results to observed concentrations it is necessary to convert emissions to concentrations. As in Omstedt et al. (2005) this is done with the help of observed NO_X concentrations and calculated NO_X emissions. This provides a conversion factor (f_{conc}) that converts emissions to concentrations. This avoids the use of dispersion models which would bring in additional uncertainty.

$$[PM_x^{model}] = f_{conc} \cdot E_{source}^x \quad (2.38a)$$

$$f_{conc} = \frac{[NO_X^{net}]}{NO_X^{emission}} \quad (2.38b)$$

$$[NO_X^{net}] = [NO_X^{traffic}] - [NO_X^{background}] \quad (2.38c)$$

To avoid uncertainties when using low NO_X values we apply lower limits to both the emissions and the net concentration values. These values tend to exclude early morning concentrations.

$$NO_X^{net,min} = 5 \mu g m^{-3}$$

$$NO_X^{emission,min} = 50 \text{ g/km/hr}$$

The conversion to concentrations using NO_X as a tracer, though considered to be more certain than dispersion modelling, also brings into play the uncertainty of the NO_X emission factors and under some meteorological conditions (e.g. very stable) the measured NO_X concentrations may not be reflected at all by the NO_X emissions due to the build up of NO_X over many hours.

2.7 Salting and sanding by rule

Since activity data is generally missing from the available datasets an estimate must be made concerning the application of salt or sand. To do this a number of rules concerning these activities are prescribed and the salt and sand added appropriately. The rules follow the following logic.

A window of time is established (t_{window}), that can be used both backwards and forwards, around the current time (t_0) at predefined times of the day (t_{hour}). A minimum time between salting/sanding events is prescribed (t_{delay}). Within this window a number of meteorological parameters are searched for. If these parameters are found within specified bounds then salt or sand will be applied

($t_{application}$). The following rules apply for temperature (T), Humidity (RH) and precipitation ($Prec$) and may be specified separately for salting and sanding.

If $t_0 = t_{hour}$ and $t_0 > t_{application} + t_{delay}$ then (check meteorological parameters)
If $T_{min} < T(t) < T_{max}$ for $t = t_0$ to $t_0 + t_{window}$ then $T_{allowed}$ is true
If $RH(t) > RH_{min}$ for $t = t_0$ to $t_0 + t_{window}$ then $RH_{allowed}$ is true
If $Prec(t) > Prec_{min}$ for $t = t_0 - t_{window}$ to $t_0 + t_{window}$ then $Prec_{allowed}$ is true
If $T_{allowed}$ and ($RH_{allowed}$ or $Prec_{allowed}$) then $t_{application} = t_0$ (apply salt/sand)

In addition to the above rules an additional rule concerning wetting of the salt or sand is included, at a predefined solution (e.g. 20% salt). This is based on whether the road surface is wet or not and depends on the modelled surface moisture at the time of application, i.e. water (g_{road}) or snow (s_{road}) see Section 3. It simply infers that wet salting/sanding occurs when the surface is dry such that:

If $g_{road} + s_{road} > g_{min}$ at $t = t_0$ then $t_0 = t_{wetting}$ (salt/sand in dilution)

Tables providing first estimates of these parameters, which will be strongly dependent on the local authorities applying the salt/sanding, are given in Appendix C.3.

3 Road moisture model formulation

An essential part of the road dust model is the description of the surface moisture which is the factor that determines the retention of wear particles on the surface. So, in addition to the mass balance equation for road dust, a mass balance equation governing liquid and frozen water content (generally termed ‘moisture’) on the road surface is required. The moisture mass balance and its related source and sink terms are used in the road dust balance to determine:

- the surface retention factors (f_q)
- the surface dust mass sinks due to drainage
- the surface dust mass sinks due to spraying
- the salt dilution on the road surface
- the reduction of road and tyre wear due to ice on the road surface

3.1 Mass balance for road water and snow/ice

As with the dust loading we establish a mass balance equation for water and ice and determine the production and sink terms for the road moisture balance. The road moisture is separated into water (g_{road}) and snow/ice (s_{road}). The surface moisture mass balance is then given by

$$\frac{\partial g_{road}}{\partial t} = P_g - S_g \quad (3.1)$$

$$\frac{\partial s_{road}}{\partial t} = P_s - S_s \quad (3.2)$$

The production of road water is determined by the processes of rain, snow melt, wetting (during cleaning or salting) and condensation

$$P_g = P_{g,rain} + P_{g,snowmelt} + P_{g,wetting} + P_{g,condens} \quad (3.3)$$

The sink terms for the road surface water include drainage, spray, evaporation and freezing (converting water to ice).

$$S_g = S_{g,drain} + S_{g,spray} + S_{g,evap} + S_{g,freeze} \quad (3.4)$$

Note that evaporation/condensation are the same process but in reverse directions. The production of road snow/ice is determined by the processes of snow fall, freezing and deposition (condensation of ice)

$$P_s = P_{s,snow} + P_{s,freeze} + P_{s,condens} \quad (3.5)$$

The sink terms for the road surface snow/ice include snow melt, ploughing and sublimation (evaporation of ice)

$$S_s = S_{s,snowmelt} + S_{s,ploughing} + S_{s,evap} \quad (3.6)$$

In the following Sections 3.2 – 3.8 these production and sinks terms are described.

3.2 Precipitation

Precipitation in the form of rain or snow is added to the road surface. The rate of production by precipitation (mm/hr) is simply written as

$$P_{g,rain} = \frac{Rain}{\Delta t} \quad \text{and} \quad P_{s,snow} = \frac{Snow}{\Delta t} \quad (3.7)$$

Where the total rain/snow for the period Δt is given in mm (water equivalent). When only the total precipitation is given then snow is defined as being precipitation for atmospheric temperatures < 0 °C.

3.3 Wetting

This reflects the addition of water and salt solutions to the surface or if wetting is used for cleaning the surface. Its addition is implemented in a corresponding way to dry salt (Section 2.3.6)

$$P_{g,wetting} = \frac{g_{road-wetting}(t_{wetting})}{\Delta t} \quad (3.8)$$

where $g_{road-wetting}$ is the amount of water used in the wetting (mm or litre/m²). If salt is provided in solution then the amount of water applied will depend on the salt solution concentration.

3.4 Drainage

Drainage is treated in the model as an instantaneous process, since the time scale for drainage is assumed to be much less than the typical model time step, i.e. one hour. The amount of water drained from the road in the period Δt is thus specified by

$$g_{road,drainable} = \max[g_{road} - g_{road,drainable-min}, 0] \quad (3.9)$$

and the water sink rate is specified by

$$S_{g,drain} = g_{road,drainable} / \Delta t \quad (3.10)$$

The parameter $g_{road,drainable-min}$ indicates the minimum moisture level below which drainage does not occur. Typically drainage will stop once the water levels are similar to the surface roughness elements and viscous forces are in place. Values for $g_{road,drainable-min}$ are unknown but, as in Omstedt et al. (2005), this will be around the 1 mm value. The drainage process is implemented in the model after the addition of rain and other production and sink processes.

Drainage is likely to be particularly important for the removal of salt and the formulation for this is provided in Section 2.4.3.

3.5 Spray and splash

Splash and spray are the mechanisms by which water, or snow/sludge, are emitted from the road surface through contact of the tyre with the road surface water. Spray occurs for all road moisture values but splash will only occur for higher levels of road water. Spray and splash will remove water from the wheel tracks and redistribute it onto the road surface or remove it completely from the road. We consider here the process purely as spray, using a rate factor that is vehicle type and vehicle speed dependent. For heavy duty vehicles spray removal will be larger than for light duty vehicles. In addition spray removal will be dependent on wind speed perpendicular to the road, Möller (2007). In the current formulation wind speed dependence is not included.

We consider spray as a road moisture sink term that can be described using a rate equation and that occurs down to a threshold surface moisture level ($g_{road,sprayable-min}$.)

$$\begin{aligned} S_{g,spray} &= R_{g,spray} \cdot g_{road} & \text{for } & g_{road} > g_{road,sprayable-min} \\ &= 0 & \text{for } & g_{road} < g_{road,sprayable-min} \end{aligned} \quad (3.11)$$

We suggest a value of $g_{road,sprayable-min}$ to be:

$$g_{road,sprayable-min} = 0.1 \text{ mm}$$

which must also be representative of the fact that drying will occur more quickly in the wheel tracks than on the rest of the road, taking into account that the g_{road} values are considered to be representative of the entire road surface.

The rate equation is dependent on traffic volume (N^v), a spray rate factor (f^v_{spray}) and the vehicle speed (V^v_{veh}). This is summed over heavy (*he*) and light (*li*) vehicle types.

$$R_{g,spray} = \sum_{v=he,li} \frac{N^v}{n_{lanes}} \cdot f^v_{spray}(V^v_{veh}) \quad (3.12)$$

where the spray factor f_{spray} [veh^{-1}] is given by a quadratic dependence on vehicle speed

$$f^v_{spray}(V^v_{veh}) = f^v_{0,spray} \left(\frac{V^v_{veh}}{V_{ref,spray}} \right)^2 \quad (3.13)$$

3.6 Snow ploughing

Ploughing of the road will remove snow. A similar treatment, as given for mass loading, can be used here. In this case we write the road snow sink rate due to ploughing as being

$$S_{s,ploughing} = s_{road} \cdot \frac{-\log(1 - h^{snow}_{ploughing-eff})}{\Delta t} \cdot \delta(t_{ploughing}) \quad (3.14)$$

The efficiency of the ploughing, i.e. the fraction of snow removed by the ploughing, is given by the factor $h^{snow}_{ploughing-eff}$. This should be fairly high and is set at 0.8 in the model.

3.7 Evaporation, condensation and energy balance modelling

Both evaporation and condensation processes will impact on the road wetness and these are described by the flux of water vapour to, or from, the surface. Physically the water vapour flux is a product of the energy balance of the road surface which also determines the surface temperature and surface humidity. In order to describe these processes an energy balance model has been developed and applied. Such a model is similar to road weather models that are used to predict road surface conditions, e.g. Sass (1997) and Karlsson (2001).

The surface energy balance, i.e. the net energy passing through the top of the road surface, is given by the following:

$$G_s = R_{net,s} - H_s - L_s + H_{traffic} \quad (3.15)$$

where we use the convention that sensible (H_s) and latent (L_s) energy fluxes are positive out of the surface and net radiation fluxes ($R_{net,s}$) are positive into the surface, as in Garrett (1994). An addition energy flux into the surface is that from traffic ($H_{traffic}$) which may be through radiation, through conduction (contact with

tyres) or through turbulent exchange. If the surface heat flux (G_s) is positive then this means that the surface is being warmed.

3.7.1 Net radiation

The net radiation flux at the surface ($R_{net,s}$) is given by

$$R_{net,s} = RS_{in,s}(1 - \alpha_{road}) + RL_{in,s} - RL_{out,s} \quad (3.16)$$

where $RS_{in,s}$ is the incoming short wave global radiation, α_{road} is the road surface albedo (0.1 - 0.3 for road, 0.6 for snow) and $RL_{in,s}$ and $RL_{out,s}$ are the incoming and outgoing long wave radiation respectively. The incoming radiation values may be available from meteorological models or measurements, but these can also be parameterised. Parameterised versions will require information on latitude, longitude, cloud cover (also possibly cloud base height), as well as temperature and often humidity.

3.7.1.1 Incoming short wave radiation

The incoming short wave radiation is preferably a measured quantity or can be determined using

$$RS_{in,s} = \tau_{clear} \cdot \tau_{cloud} \cdot RS_{in,0} \quad (3.17)$$

where the transmission functions for clear sky (τ_{clear}) and cloudy sky (τ_{cloud}) attenuate the short wave radiation at the top of the atmosphere ($RS_{in,0}$) based on the calculated azimuth and zenith angles (Iqbal, 1983). The attenuation factors for clear and cloudy skies are determined using the parameterisations from Konzelmann et al. (1994).

The calculated clear sky short wave radiation ($RS_{clear,s}$) may also be used to estimate the cloud coverage (n_c) if observed global radiation ($RS_{in,obs}$) is available. By assuming that overcast conditions reduce the clear sky radiation by a factor 0.9 then cloud cover is estimated using the equation:

$$n_c = \min\left(1, \frac{1}{0.9} \left(1 - \frac{RS_{in,obs}}{RS_{clear,s}}\right)\right) \quad (3.18)$$

For street canyons shading of the street by the canyon walls is included. Given a street configuration that includes the street orientation, the width of the canyon, the height of the building facade (with different heights on the northern and southern side) and the width of the road, then the fraction of the road surface in shadow can be calculated ($f_{road-shadow}$) assuming an infinite canyon length and given the solar zenith and azimuth angle. From this, the effective radiation on the road surface is determined by separating the incoming radiation into a diffuse and a direct component:

$$\begin{aligned}
RS_{in,diffuse} &= RS_{in,s} (\tau_{diffuse} + (1 - \tau_{diffuse}) \cdot n_c) \\
RS_{in,direct} &= RS_{in,s} - RS_{in,diffuse} \\
RS_{in,road-shadow} &= RS_{in,diffuse} + (1 - f_{road-shadow}) RS_{in,direct}
\end{aligned} \tag{3.19}$$

The factor $\tau_{diffuse} = 0.2$ is the component of the clear sky radiation that is considered to be diffuse. For totally overcast skies the global radiation is assumed to be completely diffuse.

3.7.1.2 Incoming long wave radiation

The incoming long wave radiation is based on the Boltzmann equation for blackbody radiation written as

$$RL_{in,s} = \varepsilon_{eff} \sigma TK_a^4 \tag{3.20}$$

Where TK_a is the atmospheric temperature in Kelvin ($TK_0 = 273.15$ K) and σ is the Stefan-Boltzmann constant (Appendix A). The effective emissivity (ε_{eff}) is parameterised as a function of cloud cover (n_c) and atmospheric water vapour pressure (e_a). We use a version from Konzelmann et al. (1994) given as

$$\varepsilon_{eff} = \varepsilon_{cs} (1 - n_c^2) + \varepsilon_{cl} n_c^2 \tag{3.21}$$

Where the clear sky emissivity (ε_{cs}) is further parameterised as:

$$\varepsilon_{cs} = 0.23 + 0.443 \cdot \left(\frac{e_a}{TK_a} \right)^{1/8} \tag{3.22}$$

Typical clear sky emissivity values will be in the range of 0.6 – 0.8. The cloudy sky emissivity (ε_{cl}) will depend on the cloud type. For low lying clouds this will be large and for high clouds this will be smaller. We use a constant value similar to that suggested by Konzelmann et al. (1994) of 0.97.

Within the urban environment buildings will also emit long wave radiation which will contribute to the incoming surface long wave radiation flux. The contribution from the street canyon building facade to the surface energy flux in the centre of the street canyon is calculated assuming the road to be surrounded by a cylindrical wall at a height and diameter equivalent to the facade height and canyon width. This cylindrical wall is assumed to have a surface temperature equivalent to the atmospheric temperature and to radiate as a black body. The fraction of the sky area covered by the facade ($f_{RL,canyon}$) is then determined using

$$f_{RL,canyon} = 1 - \sin \left(\tan^{-1} \left(\frac{b_{canyon}}{2h_{canyon}} \right) \right) \tag{3.23}$$

and the total incoming long wave radiation flux is then calculated by

$$RL_{in,s} = \varepsilon_{eff} \left(1 - f_{RL,canyon}\right) \cdot \sigma TK_a^4 + f_{RL,canyon} \cdot \sigma TK_a^4 \quad (3.24)$$

When $f_{RL,canyon} = 0$ this is equivalent to the open sky long wave radiation flux. Currently the surface temperature of the buildings is assumed to be the same as the air temperature. However this may not be the case, particularly during winter, when buildings are heated internally or in the summer when they absorb shortwave radiation. This information is not easily obtainable and so the atmospheric temperature is used.

3.7.1.3 Outgoing long wave radiation

The outgoing long wave radiation will depend on the surface temperature following Boltzmanns law,

$$RL_{out,s} = \varepsilon_s \sigma TK_s^4 \quad (3.25)$$

It is useful to linearise this equation for the surface temperature (TK_s), around the near surface atmospheric temperature (TK_a), when solving the surface temperature (Equation 3.35). Equation 3.25 can thus be rewritten as:

$$\begin{aligned} RL_{out,s} &\cong RL_{out,a} + (TK_s - TK_a) \cdot \frac{\partial RL_{out,a}}{\partial TK_a} \\ &= RL_{out,a} \cdot \left[\left(1 - \frac{4TK_a}{TK_a}\right) + \frac{4TK_s}{TK_a} \right] \end{aligned} \quad (3.26)$$

where

$$RL_{out,a} = \varepsilon_s \sigma TK_a^4 \quad (3.27)$$

Here we distinguish temperatures in degrees Kelvin using TK ($TK_0 = 273.15$ K). The surface emissivity (ε_s) is taken to be unity, even though this is may not usually be the case it is a good approximation since the incoming long wave radiation is reflected by the factor $(1 - \varepsilon_s)$.

3.7.2 Latent and sensible heat fluxes

We use a bulk atmospheric surface layer formulation (Garratt, 1992) to describe the latent and sensible heat fluxes as:

$$H_s = -\rho_a \cdot C_p \cdot (T_a - T_s) / r_T \quad (3.28)$$

$$L_s = -\rho_a \cdot \lambda_s \cdot (q_a - q_s) / r_q \quad (3.29)$$

where T_a and T_s are the atmospheric and surface temperatures, q_a and q_s are the atmospheric and surface specific humidity, r_T and r_q are the aerodynamic resistances for temperature and specific humidity. The latent heat constants (λ_s) are slightly different for water and ice surfaces and are provided, along with the

heat capacity of dry air (C_p), in Appendix A (A.1). The surface and atmospheric specific humidity, along with the atmospheric density (ρ_a), are calculated using the equations listed in Appendix A (A.2).

3.7.2.1 Wind and traffic induced exchange coefficients

In the energy balance model use is made of the aerodynamic resistance factor r_q and r_T (Equation 3.28 and 3.29). For wind induced turbulence these ‘resistance factors’ or ‘bulk turbulence exchange coefficients’, when inverted, are described using classic similarity theory under neutral conditions. i.e.

$$\frac{1}{r_{q,T}^{wind}} = \frac{FF(z) \cdot \kappa^2}{\log(z/z_0) \cdot \log(z/z_{q,T})} \quad (3.30)$$

Where the subscripts q and T represent water vapour and temperature, κ is the von Karman constant (0.4) and $z_{0,q,T}$ are the respective roughness lengths. We follow Garratt (1992) and write $z_{q,T} = z_0/7.4$.

Within street canyons it is sometimes appropriate to reduce the wind speed (FF), if it is measured at roof top as is often the case. A wind speed scaling factor can be applied in the model to reduce the wind speed to an appropriate level representative of the canyon.

In addition to the exchange coefficient due to wind shear we wish also to include the enhanced exchange through traffic induced turbulence. This will be dependent on the vehicle type (v) the vehicle speed (V_{veh}^v) and the number of vehicles of any given type (N^v). Heavy duty vehicles will induce more turbulence than light duty. We relate these parameters as simply as possible to each other in the following way

$$\frac{1}{r^{traffic}} = \frac{1}{3600 \cdot 3.6} \sum_{v=li,he} a_{traffic}^v \cdot \frac{N^v}{n_{lanes}} \cdot V_{veh}^v \quad (3.31)$$

where the constants convert the traffic speed [km/hr] and volume [veh/hr] to units of [m/s] and [veh/s] respectively. The coefficient $a_{traffic}$ has units of [s/veh] and represents the aerodynamics of the vehicle in question. Larger values of $a_{traffic}$ indicate the creation of more turbulence. We suggest values of around 1×10^{-3} and 1×10^{-2} [s/veh] for light duty and heavy duty vehicles respectively. These will be the same for both water vapour and temperature.

The total aerodynamic resistance is then calculated using

$$\frac{1}{r} = \frac{1}{r^{traffic}} + \frac{1}{r^{wind}} \quad (3.32)$$

3.7.2.2 Surface relative humidity

To determine the surface specific humidity q_s in Equation 3.29 the surface relative humidity (RH_s) is specified. RH_s is expected to decrease once the surface moisture content starts to fall below a threshold value. This mimics the patchiness of the drying surface and moisture contained within the pores of the road surface. Within the model we write this either as a discontinuous linear function

$$RH_s = \frac{g_{road} + s_{road}}{g_{road, evap-thresh}} \cdot 100 \quad \text{for } g_{road} < g_{road, evap-thresh} \quad (3.33a)$$

or as a continuous exponential function

$$RH_s = \left(1 - \exp\left(-2 \frac{g_{road} + s_{road}}{g_{road, evap-thresh}}\right) \right) \cdot 100 \quad (3.33b)$$

The factor 2 in the exponential is used so that the integral of both methods is equal, making the two methods comparable for the same evaporation threshold value. This threshold value is currently taken to be 0.05 mm. This parameter is essential for calculating latent heat and evaporation on relatively dry surfaces. Figure 3.1 shows the relative humidity as a function of surface moisture for the two formulations assuming a value for the evaporation threshold of 0.05 mm.

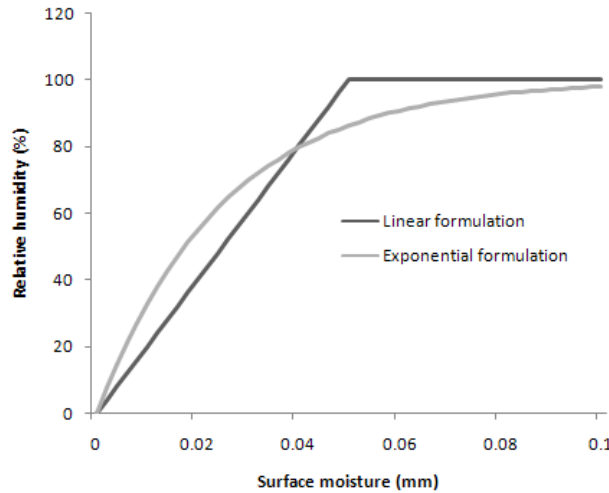


Figure 3.1. Two formulations for the surface humidity based on an evaporation threshold value of 0.05 mm.

3.7.3 Vehicle induced heat flux

Heat fluxes, through radiation, conduction and as sensible heat flux, are produced by vehicles due to both motor warmth and friction of tyres with the surface. This is parameterised in the model using the following form

$$H_{traffic} = \sum_{v=li,he} H_{veh}^v \cdot \max\left(1, \frac{N^v}{n_{lanes}} \cdot \frac{l_{veh}^v}{V_{veh}^v} \cdot 10^{-3}\right) \quad (3.34)$$

Here the traffic induced heat flux ($H_{traffic}$ [W.m^{-2}]) is determined by the individual heat flux from a single vehicle (H_{veh} [$\text{W.m}^{-2}.\text{veh}^{-1}$]), the number of vehicles in the vehicle category v (N^v) and the time of the vehicle spent over any part of the road, determined by the vehicle speed (V_{veh}^v) and the vehicle length (l_{veh}^v). The heat flux is added to the radiation fluxes in the energy balance equation and is defined as positive towards the surface. A maximum value is chosen here so that the maximum heat flux is not exceeded, i.e the heat flux if the vehicles are queued and not moving on the road. Typical heat flux per light vehicle is given as $H_{veh}^v = 50 \text{ W.m}^{-2}.\text{veh}^{-1}$. Heavy vehicles are considered to be three times as long and to give off three times as much. These parameter values are considered to be first estimates and their impact on the moisture is assessed in Section 5.9.1.

3.7.4 Surface heat flux and temperature

The surface heat flux G_s is used to warm a surface layer slab of depth Δz_s as follows

$$\frac{\partial T_s}{\partial t} = \frac{1}{\rho_s c_s} \frac{G_s - G_{sub}}{\Delta z_s} \quad (3.35)$$

where G_{sub} is the flux out of the slab into the under laying sub-surface. To solve this equation the sub-surface flux is specified using a relaxation term in Equation 3.35 as

$$G_{sub} = \mu(T_s - T_{sub}) \quad (3.36)$$

where T_{sub} is the unchanging subsurface temperature for the period considered, in this case several days. To determine the parameter μ the coefficients in the Equations 3.35 and 3.36 are set so that the model provides the correct surface temperature for a sinusoidal varying surface flux with a period of one day, representing the daily cycle with angular velocity Ω , similar to the force restore method described in Garratt (1992). Given this then the parameters would be specified as

$$\Delta z_s = \left(\frac{k_s}{\rho_s c_s 2\Omega} \right)^{1/2} \quad (3.37a)$$

$$\mu = \Omega \rho_s c_s \Delta z_s \quad (3.37b)$$

Given the angular velocity of the earth of $\Omega = 7.3 \times 10^{-5} \text{ rad.s}^{-1}$ and typical road parameters of density $\rho_s = 2400 \text{ kg/m}^3$, specific heat $c_s = 800 \text{ J/kg/K}$ and thermal conductivity $k_s = 2.0 \text{ Wm}^{-1}\text{K}^{-1}$ then we find that the appropriate choice of $\Delta z_s = 0.08 \text{ m}$ and that $\mu = 11.8 \text{ Wm}^{-2}\text{K}^{-1}$. The value of T_{sub} can be specified by climatology or can be derived from the average atmospheric temperature over the previous few days. We use the running mean atmospheric temperature over the past 3 days to specify the subsurface temperature T_{sub} .

The alternative to the slab with sub-surface relaxation model is to apply a depth resolving temperature diffusion model, however the slab model formulation is a simple and seemingly appropriate method for the current application. Given the linearised form of the outgoing long wave radiation the surface temperature can be prognosed implicitly and calculated for each time step, see Section 4.2.

3.7.5 Implementation of evaporation and condensation

Using the energy balance and related equations (Equations 3.15 – 3.37) the surface temperature is prognosed and the latent heat flux diagnosed. From this the evaporation is calculated from

$$evap_{road} = \frac{L_s}{\lambda_s} \quad (3.38)$$

Where the coefficients of latent heat (λ_s) depend on whether the surface is snow or water. When both snow and water are present the latent heat flux, evaporation and latent heat coefficients are distributed between the two, based on a weighting of their depths.

The evaporation of a wet surface is not dependent on the surface wetness itself, as long as it remains moist. However, as with other sink terms, evaporation rates per hour may exceed the available surface moisture. To implement this in the model we consider the evaporative sink term to be proportional to the available surface moisture normalized with the current surface moisture. This avoids negative surface moisture values and gives the correct rate of decrease when the evaporation rate per hour is much less than the available moisture. Given that evaporation is defined as a positive value and condensation as a negative value we write the sink and production due to evaporation/sublimation and condensation/deposition as

$$S_{g,evap} = \frac{g_{road}}{g_{0,road}} \cdot \max(0, evap_{road}) \quad (3.39a)$$

$$P_{g,condens} = \min(0, evap_{road}) \quad (3.39b)$$

The above formulation for the evaporative sink reflects the fact that, physically, evaporative processes cannot remove more surface moisture than is on the surface. To be consistent with this formulation the latent heat flux at the surface is also limited so that the evaporation at the surface cannot lead to more latent heat flux than the available moisture allows at each time step. This means that

$$L_s = \min(L_s, L_{s,lim}) \quad (3.40a)$$

where the limit to the latent heat flux is given by

$$L_{s,lim} = \frac{\lambda \cdot g_{0,road}}{\Delta t} \quad (3.40b)$$

3.8 Melting and freezing

Snow can melt once the snow temperature, i.e. surface temperature, reaches the melting point (T_{melt}). For pure water this is 0°C but when salt is present this will be lower. The amount of melt depends on the surface energy flux and is given as a sink term for the surface snow and as a production term for the surface water

$$\begin{aligned} S_{s,snowmelt} &= \frac{G_s}{\lambda_m} && \text{for } G_s > 0 \text{ and } T_s \geq T_{melt} \\ P_{g,snowmelt} &= S_{s,snowmelt} \end{aligned} \quad (3.41)$$

where λ_m is the latent heat of fusion of ice. The amount of melt is limited by the amount of surface snow/ice and cannot exceed that amount.

Similar to snow melt, surface water may freeze when the surface temperature is at the melting temperature ($T_s = T_{melt}$) and the surface heat flux is negative ($G_s < 0$). The amount of freezing depends on the surface energy flux and is given as a sink term for the surface water and as a production term for the surface snow/ice

$$\begin{aligned} S_{g,freeze} &= -\frac{G_s}{\lambda_m} && \text{for } G_s < 0 \text{ and } T_s \leq T_{melt} \\ P_{s,freeze} &= S_{g,freeze} \end{aligned} \quad (3.42)$$

The amount of freezing is limited by the amount of available surface water and cannot exceed that amount.

3.9 Vapour pressure and melt temperature dependence on salt concentration

The addition of salt changes the vapour pressure of the surface moisture which may impact significantly on the evaporation and condensation. The vapour pressure of a salt solution can be described as depending on the salt content, salt type and temperature. Vapour pressure over saturated salt solutions can be found by fitting Antoine's function to experimental data (Morillon et al., 1999). Antoine's function is described using three parameters

$$\log_{10}(e_{salt}^*) = A_{salt} - \frac{B_{salt}}{C_{salt} + T} \quad (3.43)$$

where the saturated vapour pressure of the salt solution e_{salt}^* [mm.Hg] is determined by the temperature (T) and the experimentally fitted coefficients A_{salt} , B_{salt} and C_{salt} . Values for these parameters are given in Table 3.1 and Equation 3.43 is plotted in Figure 3.2 for water/ice, NaCl and MgCl₂.

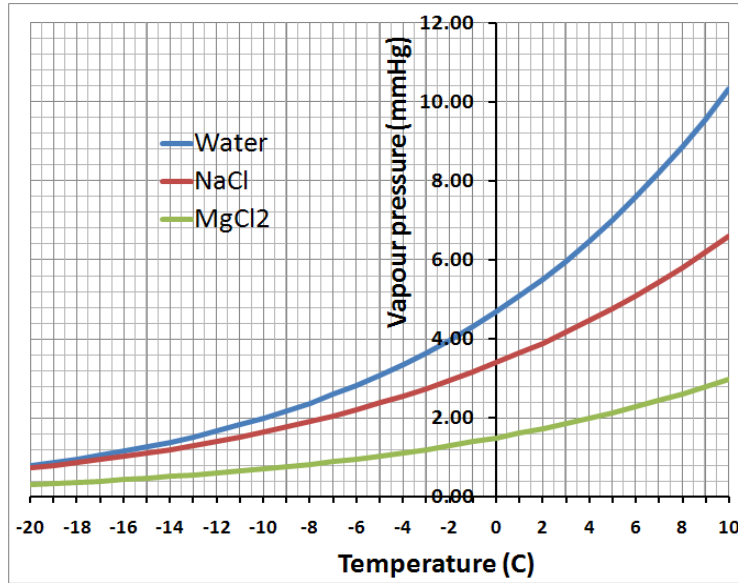


Figure 3.2. Dependence of vapour pressure on temperature for water and two saturated salt solutions (NaCl and MgCl₂) according to Equation 3.43.

In this application we are dealing with mass of salt in [g.m⁻²] and mass of water in mm [kg.m⁻²]. We can thus write the number of moles of salt and water on the road surface [mol.m⁻²] as

$$N_{\text{moles,salt}} = \frac{M_{\text{road}}^{\text{salt}}}{M_{\text{atomic,salt}}} \quad \text{and} \quad N_{\text{moles,water}} = \frac{1000 \cdot g_{\text{road}}}{M_{\text{atomic,water}}} \quad (3.44)$$

and the salt in solution (as a molar fraction) then becomes

$$\text{Solution}_{\text{salt}} = \frac{N_{\text{moles,salt}}}{N_{\text{moles,water}} + N_{\text{moles,salt}}} \quad (3.45)$$

Values for the saturated molar solutions and atomic weights for water, NaCl and MgCl₂ are provided in Table 3.1.

As the constants A_{salt} , B_{salt} and C_{salt} are given only for saturated solutions we assume a linear dependence of the vapour pressure, for non-saturated solutions, on the molar fraction of salt in solution, relative to the saturated molar fraction. The vapour pressure (e_{salt}) for a salt solution at surface temperature T_s is then approximated by

$$e_{\text{salt}}(T_s) = \left(1 - \frac{\text{Solution}_{\text{salt}}}{\text{Saturated}_{\text{salt}}}\right) \cdot e_{\text{ice}}(T_s) + \frac{\text{Solution}_{\text{salt}}}{\text{Saturated}_{\text{salt}}} e_{\text{salt}}^*(T_s) \quad (3.46)$$

where e_{salt}^* is the saturated vapour pressure of the salt and e_{ice} is the vapour pressure of ice/water. $\text{Solution}_{\text{salt}}$ is determined using equation 3.45 and $\text{Saturated}_{\text{salt}}$ is taken from Table 3.1.

The melt temperature is found when the vapour pressure of ice becomes lower than that of the salt solution, i.e. when $e_{salt}(T_{melt}) = e_{ice}(T_{melt})$. Using Antoine's equation this leads to a quadratic equation with solution

$$T_{melt} = \frac{-BB + \sqrt{(BB^2 - 4 \cdot AA \cdot CC)}}{2 \cdot AA} \quad (3.47a)$$

where

$$\begin{aligned} AA &= A_{ice} - A_{salt} - A_{solution} \\ BB &= (A_{ice} - A_{salt} - A_{solution}) \cdot (C_{ice} + C_{salt}) - B_{ice} + B_{salt} \\ CC &= (A_{ice} - A_{salt} - A_{solution}) \cdot C_{ice} \cdot C_{salt} - B_{ice} \cdot C_{salt} + B_{salt} \cdot C_{ice} \end{aligned} \quad (3.47b)$$

and

$$A_{solution} = \log_{10} \left[\frac{e_{salt}(T_s)}{e_{salt}^*(T_s)} \right] \quad (3.47c)$$

To determine the surface relative humidity (RH_s), given in Equation 3.33, with the inclusion of the salt solution we adjust RH_s by:

$$RH_{s,salt} = \frac{e_{salt}(T_s)}{e_{ice}(T_s)} \cdot RH_s \quad (3.48)$$

For saturated salt solutions this reduces the surface relative humidity significantly. For NaCl the relative humidity is reduced by a factor of 0.75 and for $MgCl_2$ by 0.33.

Table 3.1. Antoine coefficients and other parameters for saturated salt solutions in the temperature range 10 °C to -25 °C, Morillon et al. (1999).

| Variable | Units | Water/ice | NaCl | MgCl ₂ |
|--|---------------------|-----------|------|-------------------|
| Atomic weight ($M_{atomic,salt}$) | g.mol ⁻¹ | 18.0 | 58.4 | 95.2 |
| Saturated freezing temperature ($T_{melt,salt-saturated}$) | °C | 0 | -21 | -33 |
| Saturated solution by molar fraction ($Saturated_{salt}$) | % | | 22 | 23 |
| Saturated relative humidity ($RH_{s,salt-saturated}$) | % | 100 | 75 | 33 |
| A_{salt} | | 10.3 | 7.4 | 7.2 |
| B_{salt} | | 2600 | 1566 | 1581 |
| C_{salt} | | 270 | 228 | 225 |

3.10 Surface moisture retention parameters

The retention parameters that inhibit emissions based on road wetness conditions are given in two forms. The first is a discontinuous linear dependence:

$$f_{q,source} = \max(0, \min[1, 1 - g_{ratio,source}]) \quad (3.49a)$$

and the second a continuous exponential dependence:

$$f_{q,source} = \exp(-2 \cdot \max[0, g_{ratio,source}]) \quad (3.49b)$$

where

$$g_{ratio,source} = \frac{(g_{road} + s_{road} - g_{retention-min,source})}{(g_{retention-thresh,source} - g_{retention-min,source})} \quad (3.49c)$$

and *source* is any one of the various emission sources (i.e. direct road, direct brake, suspended road). In both cases a minimum retention threshold value ($g_{retention-min,source}$) defines the minimum surface moisture that inhibits suspension. Below this value $f_{q,source} = 1$. A threshold value ($g_{retention-thresh,source}$) defines the upper limit for retention for which, in the linear case, $f_{q,source} = 0$. In the exponential formulation $f_{q,source} \rightarrow 0$ for $g_{road} + s_{road} > g_{retention-thresh,source}$. The factor 2 in the exponential form is used so that the integral of both methods are equal, making the two methods comparable for the same evaporation threshold value. An example is shown in Figure 3.3.

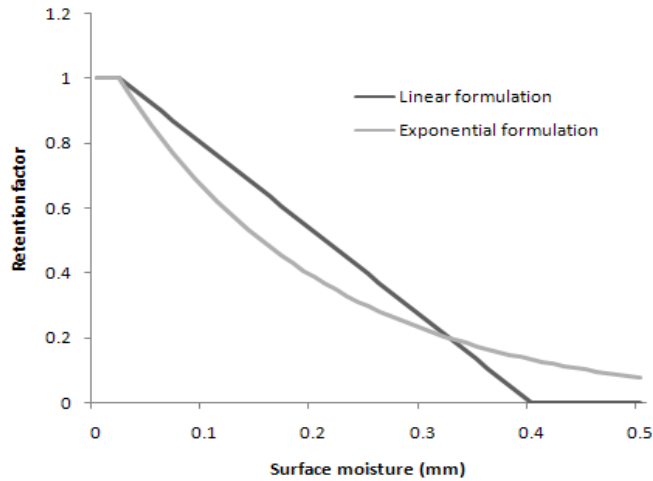


Figure 3.3. Retention factor formulations for values of $g_{retention-thresh} = 0.4$ and $g_{retention-min} = 0.02$;

4 Analytical and numerical solutions to the road dust model

4.1 Time integrated mass balance solution

Most of the model is direct application of the equations. For the time integration, which is carried out in steps of one hour, it is necessary to introduce a short term solution to the mass balance equations to ensure stability. For generalised sink ($S = R \cdot M$) and production (P) terms the equations can be written

$$\frac{\partial M}{\partial t} = P - R \cdot M \quad (4.1)$$

This has an analytical solution when P and R are constant during the time integration from t_0 to $t_0 + \Delta t$ given by

$$M(t_0 + \Delta t) = \frac{P}{R} + \left(M(t_0) - \frac{P}{R} \right) e^{-R \cdot \Delta t} \quad (4.2a)$$

or

$$M(t_0 + \Delta t) = \frac{P}{R} (1 - e^{-R \cdot \Delta t}) + M(t_0) \cdot e^{-R \cdot \Delta t} \quad (4.2b)$$

where R^{-1} is the time scale of the equation.

This has a singularity when $R = 0$ (or for calculation purposes when $R \ll P$) which will occur when there are no sink terms. In that case the solution to the equation becomes simply

$$M(t_0 + \Delta t) = M(t_0) + P \cdot \Delta t \quad (4.3)$$

For some loss terms, e.g. drainage and melt, it is more appropriate to use a simpler form of Equation 4.2, due to the way the model describes the processes. In these cases the change in mass is specified by

$$M(t_0 + \Delta t) = M(t_0) - S \cdot \Delta t \quad (4.4)$$

and is carried out after the implementation of Equation 4.2 in the model for the other production and sink terms.

4.2 Implicit surface temperature solution

The prognostic equation for surface temperature is solved implicitly to avoid numeric instability. We write the time integrated solution of the temperature equation (Equation 3.35) as

$$\begin{aligned}
T_s(\Delta t) &= T_s(0) + \Delta t \cdot a_G \cdot (G_s - G_{sub}) \\
&= T_s(0) + \Delta t \cdot a_G \cdot \left(\begin{aligned} &RS_{in,s}(1 - \alpha_{road}) + RL_{in,s} - RL_{out,s} \\ &+ H_{traffic} - L_s - H_s - \mu \cdot (T_s(\Delta t) - T_{sub}) \end{aligned} \right) \\
&= T_s(0) + \Delta t \cdot a_G \cdot \left(\begin{aligned} &a_{rad} - a_{RL} - b_{RL} \cdot T_s(\Delta t) - L_s \\ &+ a_H \cdot (T_a - T_s(\Delta t)) - \mu \cdot (T_s(\Delta t) - T_{sub}) \end{aligned} \right) \\
&= \frac{T_s(0) + \Delta t \cdot a_G \cdot (a_{rad} - a_{RL} - L_s + a_H \cdot T_a + \mu \cdot T_{sub})}{1 + \Delta t \cdot a_G \cdot (a_H + b_{RL} + \mu)}
\end{aligned} \tag{4.5}$$

where

$$\begin{aligned}
a_G &= \frac{1}{\rho_s c_s \Delta z_s} \\
a_{rad} &= RS_{in,s}(1 - \alpha_{road}) + RL_{in,s} + H_{traffic} \\
a_{RL} &= \varepsilon_s \sigma T K_a^4 \cdot \left(1 - \frac{4T_a}{TK_a} \right) \\
b_{RL} &= 4\varepsilon_s \sigma T K_a^3 \\
a_H &= \frac{\rho_a \cdot C_p}{r_T} \\
\mu &= \Omega \rho_s c_s \Delta z_s
\end{aligned}$$

4.3 Numerical limitations when calculating surface moisture

The finite time step of the surface moisture mass balance can lead to instabilities (oscillations) in the evaporation and surface moisture when the surface moisture values are comparable to evaporation over the time step used. Basically this is the result that evaporation at one time may reduce the surface moisture content to a level where condensation occurs in the next time step. Condensation rates then over predict the next time step and then evaporation occurs again, over predicting the evaporation, and so on. In reality this oscillation would not occur with continuously varying evaporation rates and surface moisture content. This generally occurs when turbulent exchange coefficients are high and surface moisture contents are low. To avoid this, the evaporation and condensation is limited not just to the available moisture content but is limited as to not allow a change of evaporation sign from one time step to the next when this is caused by the finite time step.

The ‘no evaporation/condensation’ condition occurs, when based on the linear definition of the surface relative humidity, when

$$g_{road,noevap} = \frac{q_a}{q_s^*} \cdot g_{road,evap-thresh} \quad \text{for } g_{road} < g_{road,evap-thresh} \tag{4.6a}$$

or when based on the exponential definition this is

$$g_{road,noevap} = -0.5 \log\left(1 - \frac{q_a}{q_s}\right) \cdot g_{road,evap-thresh} \quad \text{for } g_{road} < g_{road,evap-thresh} \quad (4.6b)$$

The threshold evaporation/condensation then becomes

$$evap_{road,evap-thresh} = \frac{(g_{road} - g_{road,noevap})}{\Delta t} \quad (4.7)$$

and the threshold latent heat flux becomes

$$L_{s,,evap-thresh} = \frac{\lambda \cdot (g_{road} - g_{road,noevap})}{\Delta t} \quad (4.8)$$

5 Parameter estimation and sensitivity analysis

There are a large number of parameterisations and parameters required for the model calculations. Definition of these parameters can come from three separate sources:

- independent measurements and experiments
- calibration of the model to a range of datasets
- best estimates combined with sensitivity studies

The first of these options is the preferred basis for the parameters but this is not always possible as there are many unmeasured parameters required for the model. Within this section the basis for the parameter choice and their uncertainty is provided.

5.1 Road wear, PM fractions and their functional dependencies

5.1.1 Basic road wear for studded tyres

Total road wear is the basis for the modelled road dust contribution. For the studded tyre wear, use is made of the already existing Swedish road wear model (Jacobson and Wågberg, 2007) which uses input data concerning maximum stone size (MS), Nordic ball mill (NBM) value for hardness and percentage of stone size $> 4\text{mm}$ ($S_{>4mm}$) to determine the basic road wear parameter ($W_{0,roadwear}$) and the pavement type factor (h_{pave}) used in Equation 2.7. The Swedish road wear model uses a reference pavement type (ABS16 with porphyry from Älvdalen) with a wear rate of 2.88 g/km/veh at the reference speed of 70 km/hr. We thus set the reference wear parameter for studded light duty vehicles to

$$W_{0,roadwear}^{st,li} = 2.88 \text{ g/km/veh}$$

The road surface data is used to calculate the pavement type factor for a particular pavement p as:

$$h_{pave}^p = 2.49 + 0.144 \cdot NBM^p - 0.069 \cdot MS^p - 0.017 \cdot S_{>4mm}^p \quad (5.1)$$

Swedish roads often use MS=16 mm and NBM=5, though this can range from 4 – 15. For Norwegian roads smaller stone sizes are favoured with similar ball mill values (e.g. MS=11mm and NBM=6), Snilsberg et al. (2008). The percentage of stones > 4 mm is taken to be 75% in most cases. Typical wear rates are thus 2 – 5 g/km/veh. Unfortunately knowledge of these parameters is not always possible and so there can be significant uncertainty in the final wear factor.

In the NORTRIP model, road wear is functionally dependent on vehicle speed since speed dependence has been shown in a range of laboratory experiments (e.g. Gustafsson et al., 2008; Snilsberg et al., 2008). The PM₁₀ concentration measured in the laboratory (VTI road simulator) is seen to be linear over a large range (30 – 70 km/h). However, direct fits to these data indicate that the linear relation does not pass through 0, which is the assumption used in the model (Equation 2.7), but rather infers wear to approach 0 at around 20 km/hr. The Swedish road wear model, however, does apply a fit that passes close to 0. Measurements of ambient PM concentrations in the laboratory to indicate wear rates are affected by the deposition and mixing processes in the laboratory. It is not clear from such measurements if the relationship with speed is also partly due to the induced turbulence from the road simulator and its impact on mixing and deposition.

Within the NORTRIP model light duty vehicle road wear rates are enhanced by a factor of 10 for heavy duty vehicles. In the literature a range of values is available, from 5 – 100 (Boulter, 2005), for the increased emission from heavy duty vehicles (HDV). However, it is often difficult to distinguish between suspended and direct road wear in these studies. This uncertainty is significant especially if the wear from HDV is significantly higher (order 100) since the HDV often make up from 3-10% of the total traffic and can thus dominate road wear. It is also worth noting that the percentage of studded tyres on HDV is often quite low, or none at all, and so the studded tyre contribution from HDV's may not be very significant.

5.1.2 *PM₁₀ fraction of studded tyre road wear*

The proportion of total wear in the various PM fractions is an important parameter for the PM emissions. Measurements carried out at VTI with the road wear simulator have attempted to address exactly this question. Using a laser scanner to measure the road wear directly in the road simulator and by determining the emission factors for PM₁₀, a parameterised form of the fraction of PM₁₀ has been developed as part of the NORTRIP project (Johansson et al., 2012), and expressed in terms of the same pavement wear parameters *MS* and *NBM* as follows

$$f_{PM,ref,d\dot{ir}-roadwear}^{10,st,li} = (8.2 - 0.2 \cdot NBM + 0.1 \cdot (MS - 11)) / 100 \quad (5.2)$$

The reference speed for this relationship is 50 km/hr and the equation is shown in Figure 5.1 for a range of NBM values

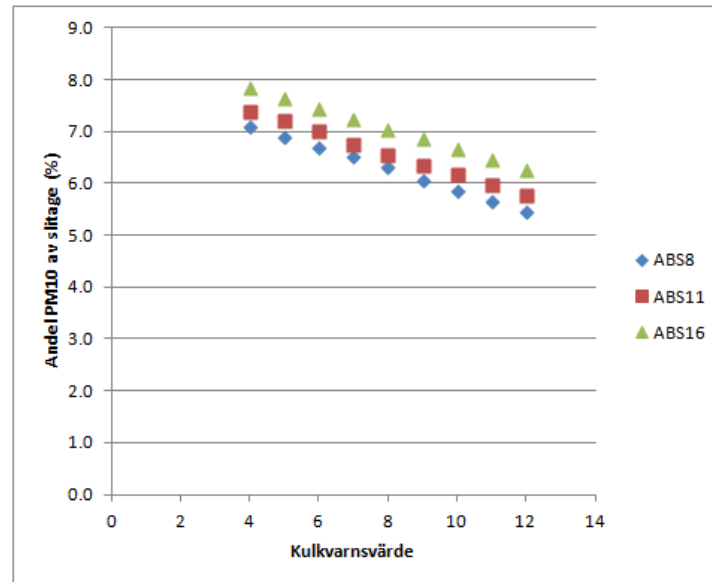


Figure 5.1. Percentage of road wear in PM_{10} fraction (Andel PM_{10} av slitage) plotted against NBM (Kulkvarnsvärde) for three different ABS pavements with $MS = 8, 11$ and 16 according to the relationship in Equation 5.2. Figure provided by VTI.

In addition to these measurements Snilsberg et al. (2008) has also assessed the impact of vehicle speed, using the same road simulator, on the fraction of PM_{10} and $PM_{2.5}$. In that case dust from studded tyres was collected directly behind the tyre and the size distribution was analysed. Speed dependence of the size distributions was determined, Figure 5.2.

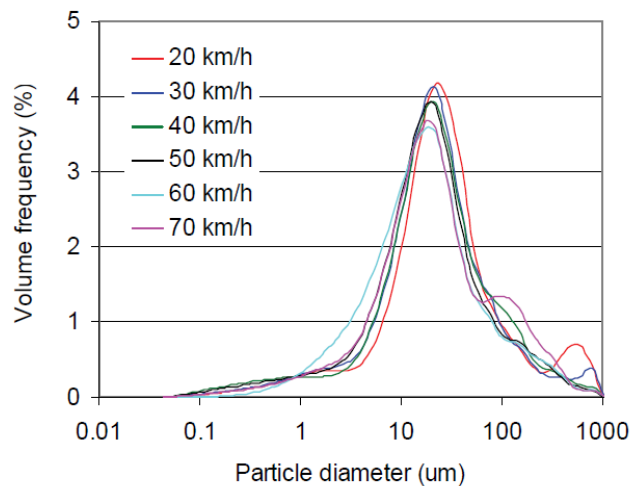


Table 1. Cumulative volume (%) of PM₂₀, PM₁₀ and PM_{2.5} as a function of driving speed

| Speed (km/h) | 20 | 30 | 40 | 50 | 60 | 70 |
|-----------------------|-----|-----|-----|-----|-----|-----|
| PM ₂₀ (%) | 37 | 44 | 44 | 48 | 53 | 47 |
| PM ₁₀ (%) | 20 | 26 | 26 | 30 | 35 | 29 |
| PM _{2.5} (%) | 7.0 | 7.6 | 8.1 | 8.5 | 8.6 | 7.6 |

Figure 5.2. Experimental setup and resultant size distributions and tabulated PM₁₀ fractions for a range of simulator speeds. Taken from Snilsberg et al. (2008).

These measurements indicate a much higher proportion of the wear to be PM₁₀, between 20 – 30%, and also indicate a significant vehicle speed dependence. It is likely that not all of the dust wear was collected behind the wheel with the instrumentation but if the size distributions are representative then this is in conflict with the VTI results. Of course some of the larger fractions, > 1mm, may have not been captured and this would tend to increase the apparent contribution of the smaller fractions.

Based on the above information we propose a speed dependence, provided in Equation 2.37, based on a linear fit to the Snilsberg et al. (2008) data (Figure 5.2). This fit provides a speed dependence slope $c_{PM-fraction} = 0.012 \text{ (km.hr}^{-1}\text{)}^{-1}$. At a reference speed of $V_{ref,PM-fraction} = 50 \text{ km/hr}$ the fit also implies a reference PM₁₀ wear fraction ($f_{PM,ref,roadwear}$) of 28%, according to Snilsberg et al. (2008), or of around 6-8%, according to Equation 5.2. Due to the significant differences between the two results, definition of this reference size fraction is to be determined by comparison with real world application of the model, as outlined below. The optimal choice lies somewhere between these two values, at around 18% (Section 5.1.3). This fit, though derived for PM₁₀ only, will be applied to all size fractions and requires the definition of the reference size fraction ($f_{PM,ref,dir-roadwear}$).

5.1.3 PM₁₀ wear rate fraction for studded tyre road wear based on model calibration

It is possible to derive the studded tyre PM₁₀ wear rate (combination of wear and PM₁₀ size fraction) for the datasets available using the model. This is done by

running the model and calculating the required studded tyre PM_{10} wear rate needed to achieve the observed mean concentrations assuming there is no loss of particles through any process other than suspension. Because it is not possible to differentiate between the total wear and the fractional size distribution we determine the proportion of the wear in PM_{10} . This method works best on well defined and long datasets, such as Hornsgatan (Appendix D.1), where surface moisture measurements are available and a strong concentration signal is available in the street canyon. The methodology will require more effort to properly assess the uncertainties (e.g. salt may have a large and unknown impact) but the results are indicated in Figure 5.3 where the calculated studded tyre PM_{10} wear rate is plotted as a function of average vehicle speed. Included in the plot is also the wear rate for PM_{10} derived from the model using the above wear parameters assuming:

- A **constant PM_{10} fraction** based on Equation 5.2 (~7.2 %) and a linear wear dependence on speed based on Equation 2.7. Two road types with maximum stone sizes of $MS=16$ and $MS=11$, both with $NBS=6$, are used. This corresponds to the application of Equations 2.7, 5.1 and 5.2.
- As above but Equation 5.2 is replaced with a **linear speed dependent PM_{10} fraction** (Equation 2.37a). Chosen reference value is $f_{PM,ref,dir-roadwear} = 18\%$ at 50 km/hr and $c_{PM-fraction} = 0.012 [(\text{km.hr}^{-1})^{-1}]$.

In making this calculation the same size fraction is assumed for both suspended and direct wear emissions.

Using the Swedish Road wear model values with a fixed PM_{10} fraction, solid lines in Figure 5.3, clearly under predicts the observed studded tyre wear rates. For Hornsgatan this is around a factor of 2 and for RV4, Essingeleden and Mannerheimintie this is around a factor of 3. For RV4, which is likely to have used smaller stone sizes ($MS=11$), this wear rate may be higher ($W_0 = 3.1$ g/km/veh, green solid line) but even so there is a clear under prediction. The wear rate of Mannerheimintie is unknown as the surface is made of cobble stones. Inclusion of the speed dependence on the PM_{10} fraction (dashed lines) clearly improves the results, though the choice of $f_{PM,ref,dir-roadwear} = 18\%$ in Equation 2.37 is intended to fit the observed data.

For further application of the model use is made of Equation 2.7 and 5.1 to determine studded tyre wear, and Equation 2.37 to determine PM_{10} fraction.

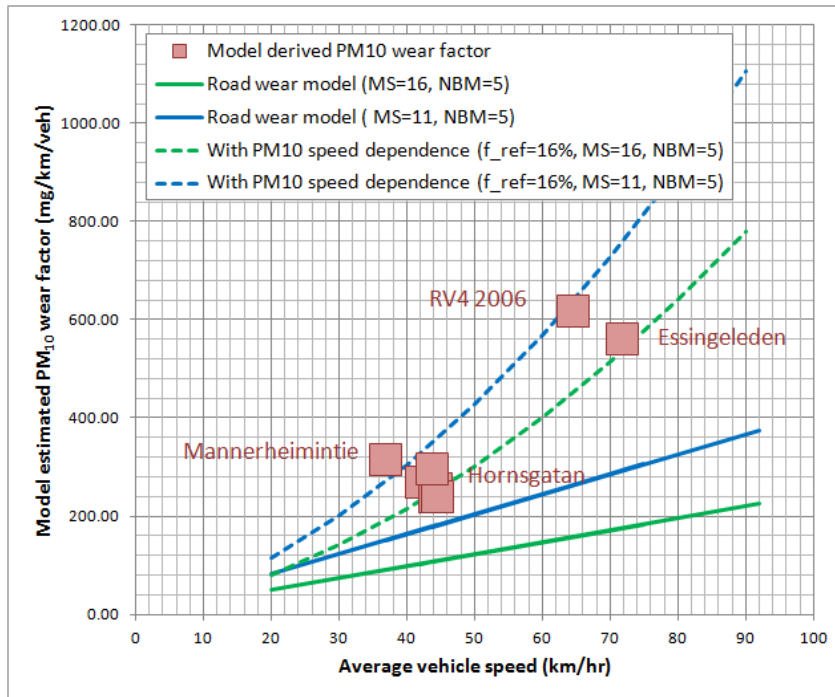


Figure 5.3. Required PM_{10} wear factor necessary to obtain the annual mean concentrations for a number of different datasets (red squares). PM_{10} fraction is the same for both direct and suspended particles. Also shown is the road wear model estimates for PM_{10} wear factor based on a **constant PM_{10} fraction** (Equations 2.7, 5.1 and 5.2, solid lines) and a **linear speed dependent PM_{10} fraction** (Equations 2.7, 5.1 and 2.37), dotted lines.

5.1.4 Non-studded road wear and PM_{10} fraction

Nominal values for the friction and summer tyre road wear are based on VTI measurements (Snilsberg et al., 2008 and Gustafsson et al., 2008) that indicate that non-studded tyre road wear is around 20 - 30 times less than studded tyre wear. These road wear values are also supported by other emission inventories. Combined with a PM_{10} fraction of 18% road wear rates of 0.1 g/km/veh are equivalent to 18 mg/km/veh. This is more twice the value given by Boulter (2005) of 7.5 mg/km/veh but no speed dependence is included in that case.

Whilst the emission factor for non-studded road wear may not have significance when a large fraction of cars are studded, it does become important for summer and in areas where non-studded winter tyres are dominant.

5.1.5 $PM_{2.5}$ size distribution of road wear particles

For $PM_{2.5}$, estimates from Kupiainen et al. (2005) provide a $PM_{2.5}/PM_{10}$ ratio of around 10%. From Snilsberg et al. (2008) this is around 20%. Comparison of observed $PM_{2.5}$ and PM_{10} from the available datasets is sometimes contradictory but a ratio of around 5% is closer to that observed. Note that there is sometimes confusion in that the measured $PM_{2.5}$ also includes exhaust particles which is a significant contributor.

In Figure 5.4 we show the observed non-exhaust $PM_{2.5}/PM_{10}$ for the available datasets. This has been calculated using the equation

$$PM_{2.5}/PM_{10} = \frac{(\overline{PM}_{2.5} - \overline{PM}_{exhaust})}{(\overline{PM}_{10} - \overline{PM}_{exhaust})} \quad (5.3)$$

Where the over bars indicate that they are the average concentrations for the period. Exhaust concentrations are calculated based on exhaust emission factors and the conversion using NO_x as a tracer. The calculated ratio, given in %, is uncertain, and can be negative, when the calculated exhaust concentrations are close to the measured $PM_{2.5}$ concentrations.

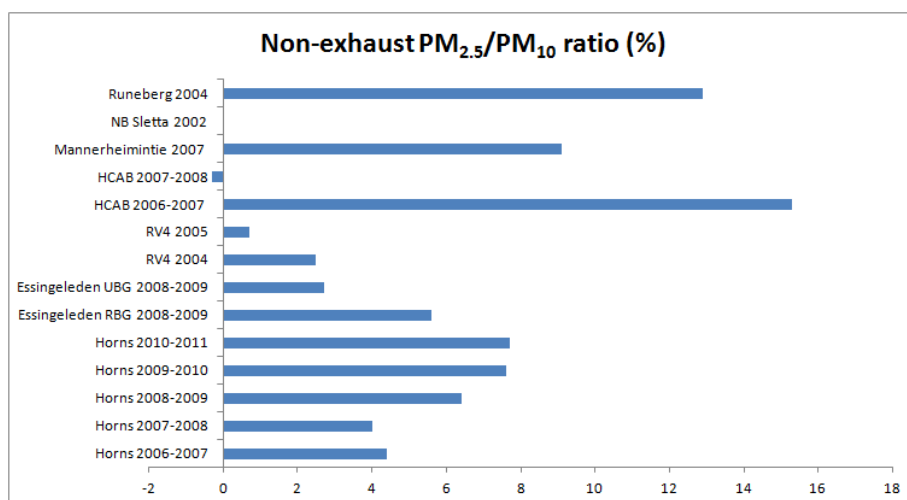


Figure 5.4. Calculated ratio of non-exhaust $PM_{2.5}$ to PM_{10} based on the observational data after subtraction of the modelled exhaust contribution.

Based on the Hornsgatan data, which is considered the best available dataset, the measured $PM_{2.5}/PM_{10}$ ratio is 3 – 7 %. We choose a value of 5%. This appears to be lower than other studies would indicate.

The question of whether direct wear emission $PM_{2.5}/PM_{10}$ ratios are the same as suspended emission $PM_{2.5}/PM_{10}$ ratios needs also to be addressed. Measurements (e.g. Snilsberg et al., 2008) of surface dust loading or deposited dust indicate a $PM_{2.5}/PM_{10}$ ratio that is larger, but these do not take into account the exhaust emissions or other processes affecting the concentrations. E.g. Snilsberg et al. (2008) found a deposited $PM_{2.5}/PM_{10}$ ratio of around 20% and laboratory ratios of 20 – 30% (no exhaust). Ketzler et al. (2007) found a $PM_{2.5}/PM_{10}$ ratio in Denmark of around 25% after subtraction of exhaust emissions. In addition Snilsberg et al. (2008) found that studded tyres produced a higher proportion of $PM_{2.5}$ than did non-studded tyres. For the current application of the model we apply the same size fractions for both direct and suspended emissions and for all tyre and vehicle types.

5.2 Tyre and brake wear

Tyre and brake wear have been taken from the literature (Boulter, 2005). No speed dependency is currently implemented in the model for brake wear. Selected parameters are provided in Appendix C (C.1).

5.3 Suspension rates and dependencies

The rate of suspension from the road surface is the result of a number of processes. In the model the suspension rates are described by a single value, dependent on the tyre and vehicle type and some functional dependence on vehicle speed. It is assumed that the suspension is directly proportional to the mass loading. In addition it is possible to provide sand and salt, applied to the surface, with different suspension rates.

The processes affecting the suspension are not just the turbulent and mechanical suspension from the road surface, though this is the mechanism by which suspension will finally occur. It is also governed by the availability of the dust, e.g. from road or the shoulder/pavement sources, on the cohesive forces on the dust, e.g. salt and hygroscopic properties of dust, and also on the surface structure. Experiments with a suspension simulator (Blomqvist et al., 2011) have shown a strong dependence of turbulence induced suspension on the surface texture (macro-structure).

As part of the NORTRIP and REDUST (www.redust.fi) projects, Sniffer (Pirjola et al., 2009) emission factor data were analysed and compared to vehicle speed. The results are presented in Section 6.2 of Johansson et al. (2012) and indicate a roughly linear dependence of the Sniffer emission factors with vehicle speed. This dependence however is not well defined and a constant value for the Emission rates would have been equally suitable for speeds above 30 km/hr.

Some experiments have been carried out to determine the suspension rates of dust distributed on the road surface (e.g. Langston et al., 2008). These indicate that applied deposited dust is quickly removed from the surface, with suspension rates of the order of $10^{-2} - 10^{-3} \text{ veh}^{-1}$. i.e. an e-folding time of 100 to 1000 vehicles. Patra et al. (2008) estimated this rate to be $3 \times 10^{-4} \text{ veh}^{-1}$ based on distributions of rock salt on a road in London. Kupiainen and Pirjola (2011) found that traction sanding, added to the surface under dry conditions, increased the suspended emissions by a factor of 15 but that the PM_{10} emissions reduced quickly, over a matter of hours. Clearly these suspension rates are not commensurate with the suspension seen during and after the studded tyre season where the dust loading and suspension extend well beyond the studded tyre season.

It would appear that suspension of freshly laid dust/sand and the retained dust from wear sources during wet periods have a different adhesive quality and distribution, and hence suspension rate. So it is necessary to separate the short term suspension after dry sanding and the long term suspension due to the other processes affecting cohesion and availability of the dust loading.

Model sensitivity analysis is carried out to help define the required long term suspension rates. In Figure 5.5 a large number of different suspension rates have

been applied to the available datasets (Section 7). Since the suspension rates impact on the temporal development of the emissions then correlation of daily mean concentrations is used to assess the impact of the suspension rates. Correlation is also strongly dependent on the surface moisture so whenever possible observed moisture is used. Some correlations are quite low and the ability to determine optimal suspension rates in some datasets is limited.

Visual inspection of the data and models (Appendix D) is very instructive in assessing suspension rates. Three different situations can be defined that can differentiate between direct and suspended emissions and their rates. These are:

1. Enhanced emissions at the start of the studded tyre season where dust loading, and hence suspension, are low. This is indicative of the direct emissions.
2. Enhanced emissions that occur after a long wet period. This peak provides evidence, not just of the suspension rate, but also of the accumulated mass.
3. Decay of emissions at the end of the studded tyre season. This decay is a clear indicator of the long term suspension rates.

All three of these situations must be well modelled if the temporal signal, in this case expressed in terms of correlation, is to be well simulated.

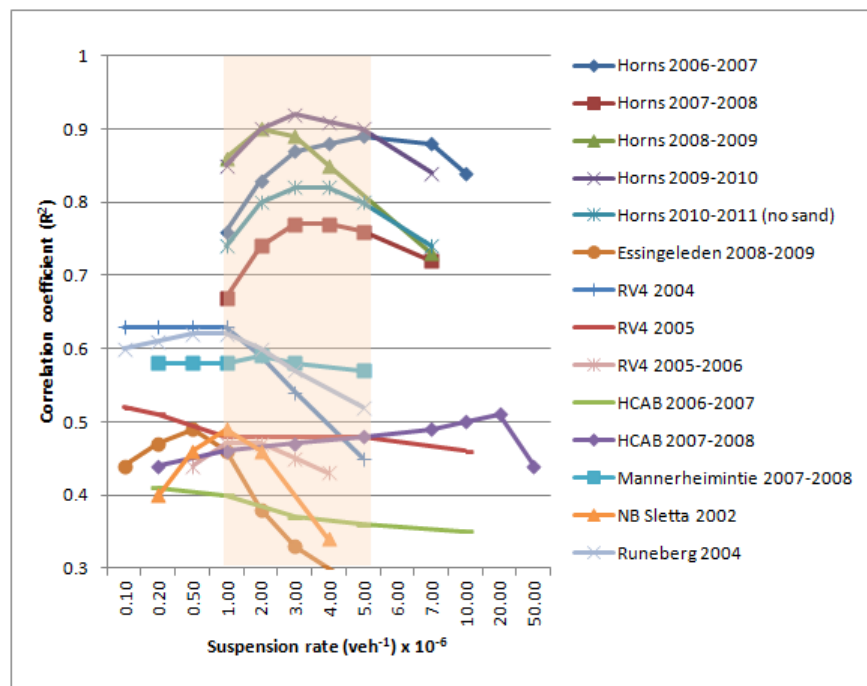


Figure 5.5. Sensitivity study of the model daily mean correlation for various datasets to the model suspension rate.

From Figure 5.5 the optimal suspension rate is in the range from $0.5 - 5 \times 10^{-6}$ veh^{-1} (orange band). Optimal suspension rates are more certain for the datasets with the highest correlation, i.e. Hornsgatan using observed moisture, however the roads with the highest vehicle speeds (70 – 90 km/hr for RV4, Essingeleden and NB Sletta) all show lower optimal suspension rates than Hornsgatan with an average vehicle speed of around 45 km/hr. This is counter intuitive but may be the

result of different surface textures on the different road surfaces rather than the impact of vehicle speed. For some datasets no optimum value was obtained (e.g. RV4, HCAB). An optimal value chosen is $2 \times 10^{-6} \text{ veh}^{-1}$ at a reference speed of 50 km/hr. Even though the model optimisation indicates lower suspension rates for roads with higher vehicle speeds the evidence from other studies is quite strong and so a linear dependence of suspension rate on vehicle speed is chosen, i.e. $a_{sus} = 1$ in Equation 2.25. This infers that the suspension rate at the highway sites is lower than the current model estimates. This could be due to the macro-structure of the surfaces or other processes, e.g. that there is less lane changing, parking and meandering on highways that can redistribute the dust.

The above analysis was carried out assuming that no wear is retained on the road when the surface is dry. It is also possible to set the model parameter ($f_{0,dir-source}$) so that dry wear is also deposited on the surface, i.e. no direct emissions, and so the wear particles must then all be suspended. In general there is little change to the model results when doing this in terms of correlation, though there is a slight decrease in correlation for most datasets. The exception is the highway dataset from Essingeleden which shows some improvement in the correlation. The wear particles are thus assumed to be directly emitted when the surface is dry, i.e. $f_{0,dir-source} = 1$ (Equation 2.5b).

5.4 Sanding parameters: suspension, size distribution, abrasion and crushing

Assessing the impact of sanding on emissions is one of the major, but ambitious, aims of the model. The model treats the impact of sand in 3 different ways. These are:

- A fraction of the distributed sand is suspendable and will join the road wear dust on the surface to increase the dust loading
- The non-suspendable sand fraction can lead to additional abrasion of the road surface (sand paper effect)
- The passage of vehicle tyres over the non-suspendable sand will lead to crushing of the sand and the generation of suspendable sand mass.

The amount of data concerning these three aspects is limited, particularly the last two. Though the model includes these processes there is insufficient information at the moment to include them. As a result the abrasion and crushing are not activated in the model.

For the fraction of suspendable sand, measurements of sand size distribution are required. These are available from Stockholm in a report on the sand size distribution (VTIInr: 11-081), shown in Figure 5.6. These indicate that in total 0.8% of the sand is $< 10 \mu\text{m}$ in diameter. In the model we use the concept of suspendable and non-suspendable sand with the cut off around $200 \mu\text{m}$ (This cut off is used for practical reasons and also because the vast majority of wear is expected to occur within this size range). Based on the data in Figure 5.6 the suspendable fraction is then 6%, and the fraction of this that is PM_{10} is 16%. This value of 16% is close to that chosen for the road wear contribution (18% at 50 km/hr).

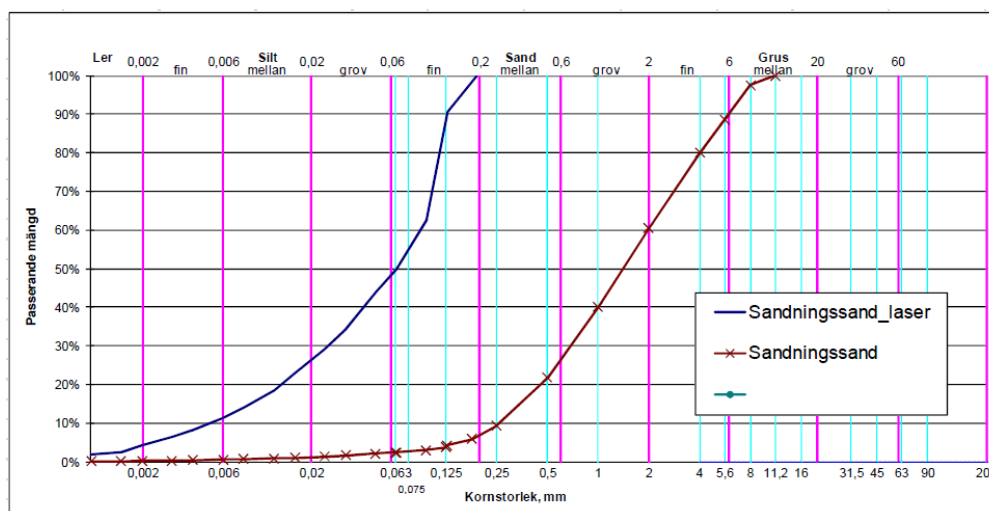


Figure 5.6. Size distribution of particles in traction sand used in Stockholm (VTInr: 11-081).

There is only one data set available (Hornsgatan 2010-2011) where it is known when and how much sand has been applied to the surface. Using the above model parameter ($f_{sus-sanding} = 6\%$) sand is applied to the surface and the applied sand is allowed to be removed by suspension only, at the same rate as the wear particles. Applying the model in this way leads to a significant increase (factor of 2) in the modelled concentrations. Assuming that the size distributions for sand are correct the inference is that sand is either less readily suspended than wear particles or that suspendable sand is more efficiently removed from the surface than wear particles. Information on this is not currently available.

The sensitivity of the model to the addition of sand is analysed for Hornsgatan 2010-2011. The addition of 1 % suspendable sand slightly increased the correlation (by 0.01) and leads to an average contribution of around $2.7 \mu\text{g}/\text{m}^3$ compared to the contribution from road wear which is $7.8 \mu\text{g}/\text{m}^3$. In Figure 5.7 the impact of sanding for different suspendable fractions is shown for the annual mean and the number of days above the limit value of $50 \mu\text{g}/\text{m}^3$.

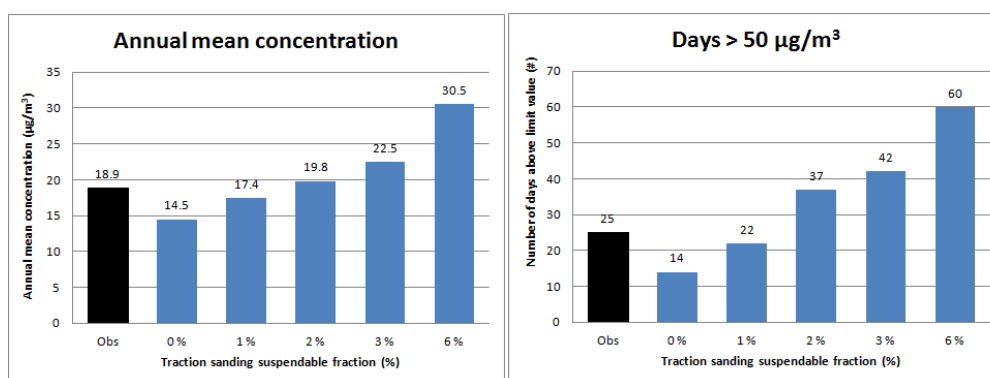


Figure 5.7 Impact of traction sanding suspendable fraction ($< 200 \mu\text{m}$) on the annual mean and days above limit value ($50 \mu\text{g}/\text{m}^3$) for the Hornsgatan 2010-2011 period. Also included are the observed values. Note that all concentrations are net concentrations, not including background.

Given that the Hornsgatan datasets are fairly well modelled for most years without the use of sand then it appears that sand is not a significant contributor to the total emissions. The current analysis sets a range of 0.5 – 2% to the amount of suspendable material in the sand that is active for suspension. We choose a value of $f_{sus-sanding} = 1\%$.

5.5 Salting: drainage and spray efficiencies

There have been a number of studies concerning salting (e.g. Blomqvist et al., 2012; Lysbakken and Norem, 2012) mostly in regard to the removal of salt from the surface through the interaction with traffic. However, at the moment the efficiency of salt removal through drainage is unknown, Section 2.4.3. Of all the datasets only the RV4 data has filter samples that have been chemically analysed and where suspended salt has been measured (Hagen et al., 2005). In these data a significant portion of the suspended PM_{10} was found to be salt (~25%). In an analysis using the receptor model COPREM of the same filter samples (Denby et al. 2009) it was found that ~15% of the traffic related PM_{10} was salt. Some days showed roughly equal contributions from both dust and salt (Figure 5.8). In addition to the observed ambient salt concentrations salting activity data from a nearby road is also available for RV4. Using these salting data the model is run to try to recreate the observed level of salt. Two parameters are adjustable to influence this, the drainage and spray efficiency of the salt and the total suspension rate (which has been fixed at $f_{0,suspension} = 2 \times 10^{-6} \text{ veh}^{-1}$ in Section 5.3).

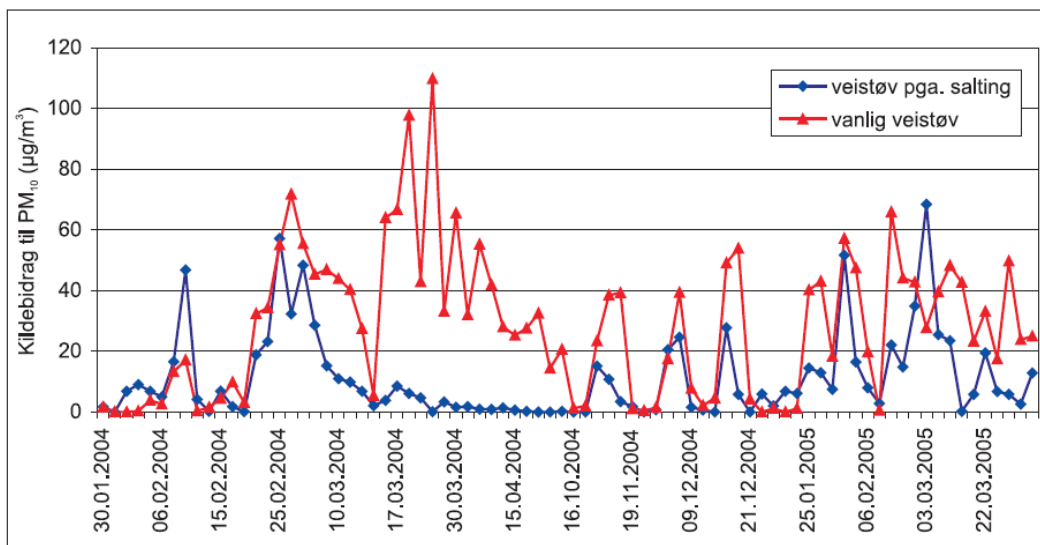


Figure 5.8. Taken from Hagen et al. (2004) showing the salt (blue) and dust (red) contribution to PM_{10} for 80 half day filter samples in the winter periods of 2004 and 2005 at the RV4 site in Oslo.

The results indicate that drainage efficiency rates cannot be greater than around 0.4 to achieve the levels of salt observed. We choose a value of 0.3 for both the drainage and the spray efficiencies ($h_{drainage-eff}$ and $h_{spray-eff}$) that provides a salt contribution for the RV4 data of around 10%. Note that the filter data and the model data cover a longer period of time and there are far less filter samples available for the analysis than modelled days. The average contribution of the various sources, including salt, is shown in Figure 5.9 for the two years (2004 and

2005) of data from RV4. These are compared with the results from the receptor model COPREM, using the measured filter chemical analysis. A more thorough analysis of the RV4 datasets, salting and speed dependence will be carried out in a separate study.

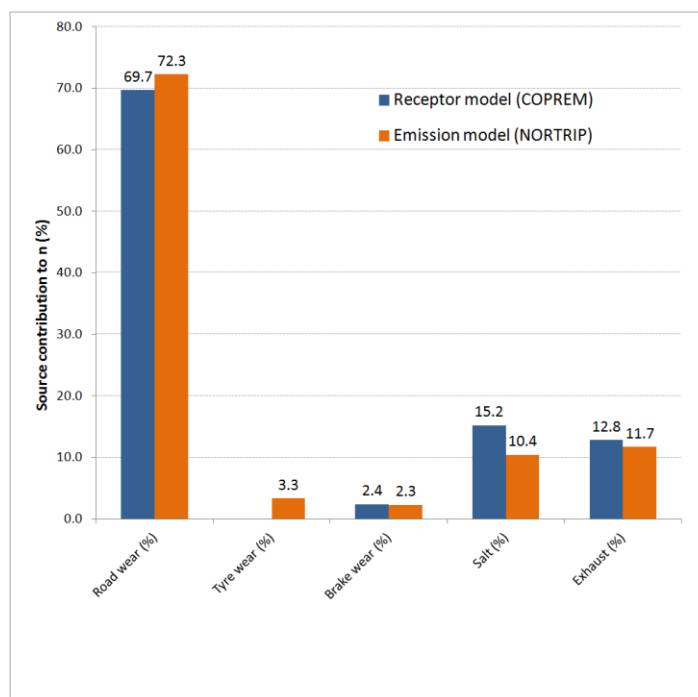


Figure 5.9. Comparison of the average source contribution to road dust at RV4 for the two winter periods in 2004 and 2005. Calculated using the NORTRIP emission model and observed using the COPREM receptor model. The periods and hours sampled are similar but not coincident.

5.6 Drainage parameters

The major drainage parameter is the threshold level for drainage ($g_{drainable}$). This is expected to be different for different surface textures and for other properties of the road such as slope. The drainage threshold impacts in two ways. Firstly, it affects the road surface moisture directly by removing all the water above the threshold level and secondly it impacts on the drainage of dust and salt. The smaller the threshold value then the larger the proportion of ‘well mixed’ salt and dust that is removed, Equation 2.29.

To assess the impact of the drainage threshold parameter on the results, the model is run for a number of the datasets using the moisture sub-model to predict surface moisture. From this the correlation is determined and optimum values for the drainage threshold are determined, Figure 5.10. Though the drainage threshold is not the only important factor for determining the suspension we adjust this parameter to assess its impact on the moisture model.

For most datasets the optimal value for the drainage threshold is between 0.2 - 0.8 mm. Though this drainage parameter may vary from road to road there is insufficient evidence to adapt it specifically. For example, Runeberg in Helsinki has a much higher concentration correlation when the drainage threshold is higher

(around 1 mm), indicating a wetter street. HCAB in Copenhagen has the highest correlation when the drainage threshold value is low, indicating a drier street. For consistency a value of $g_{drainable} = 0.6$ mm is adopted as default for the model.

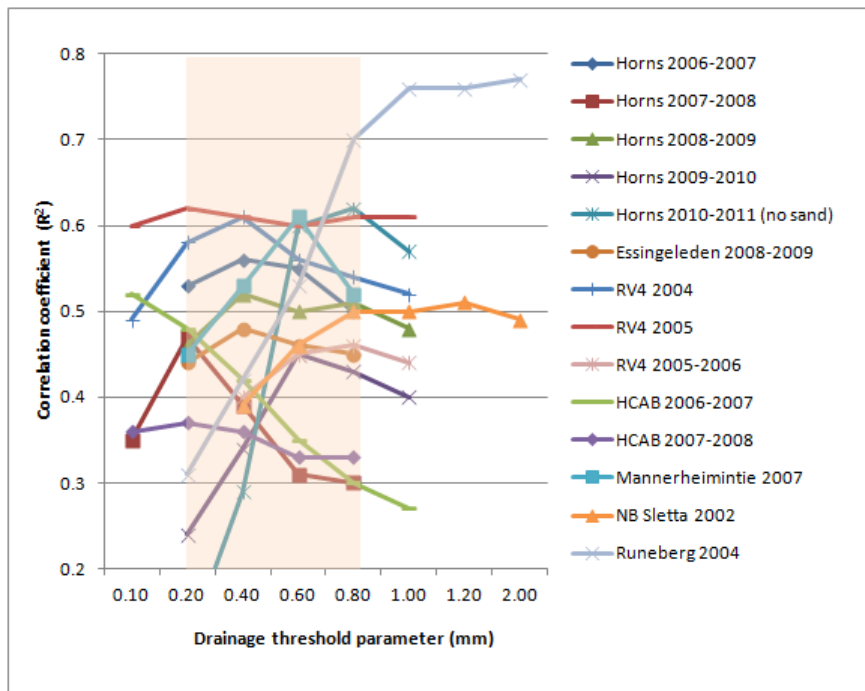


Figure 5.10. Sensitivity study of the daily mean model correlation for various datasets to the model drainage threshold.

5.7 Spray parameters

Based on the report from Möller concerning winter road condition modelling (Möller, 2006) the spray rate parameters given in Equation 3.13 would be:

$$f_{0,spray}^{li} = 5 \times 10^{-3} \text{ veh}^{-1}, \text{ for heavy duty this is } f_{0,spray}^{he} = 6f_{0,spray}^{li}$$

$$V_{ref,spray} = 70 \text{ km/hr}$$

For a traffic volume of 1000 veh/hr travelling at the reference speed this gives a removal time scale of around 10 minutes, which is fast compared to other processes. This fast removal rate is because the assessment from Möller is focused on the wheel tracks only and assumes that the rate of decay was due to spray only. If we consider the removal process to be relevant for the entire road surface, and not just the wheel tracks, then these factors should be significantly lower. A value for $f_{0,spray}$ of around $1 \times 10^{-4} \text{ veh}^{-1}$ (1/50 the indicated value) would suggest spray removal time scales of around 10 hours for the given traffic volume and speed. These are similar to ‘normal’ evaporation rates.

Currently there is not enough information available concerning spray for it to be effectively included in the model based on external experiments. Nor is information available on the speed dependence though this is assumed to be quadratic, Equation 3.13. We adopt the value of $f_{0,spray}^{di} = 1 \times 10^{-4} \text{ veh}^{-1}$.

5.8 Surface retention parameters

The surface retention is dependent on the surface moisture and is simply described as a function of this in Section 3.10. Sensitivity of the model to this parameterisation is investigated for a number of datasets and an optimal parameter value is determined, Figure 5.11. A value of $g_{retention-thresh} = 0.1$ mm and $g_{retention-min} = 0.04$ mm was chosen. The model is fairly insensitive to these parameters, except in two cases, within the range investigated. It should be noted that the adopted values are also dependent on the surface humidity description, Section 3.7.2.2, and the optimal value chosen is linked to this.

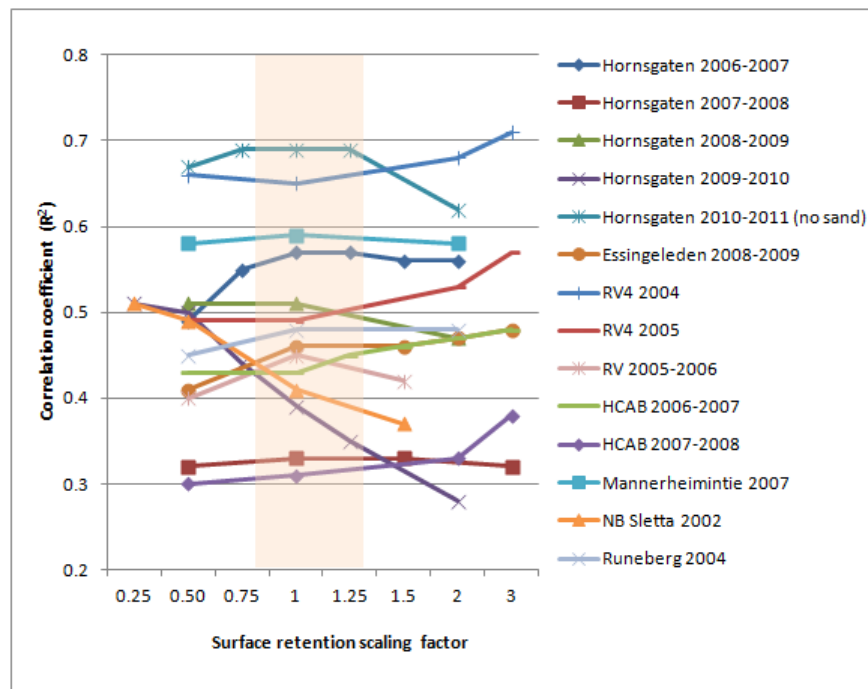


Figure 5.11. Sensitivity study of the model for various datasets to the model retention factor. Scaling factor of 1 refers to the parameter set of $g_{retention-thresh} = 0.1$ mm and $g_{retention-min} = 0.04$ mm. Scaling increases or decreases both these values.

5.9 Energy balance parameters

There are a number of parameters used in the energy balance calculation need to be defined. These may include:

- the surface roughness length that controls the turbulent exchange rate without traffic
- the traffic enhancement exchange coefficient that determines the enhanced exchange due to traffic
- the surface slab depth that controls the surface heat flux and surface temperature
- the traffic heat flux that adds to the surface heat
- the surface albedo that controls the absorbed shortwave radiation

Of these parameters only the sensitivity of the model to the turbulent exchange coefficients has been explored. Further assessment of these parameters will be carried out at a later date.

5.9.1 Sensitivity to surface roughness and traffic induced turbulence

The moisture sub-model shows a degree of sensitivity to the surface roughness parameter, that determines the turbulent exchange rate, Section 3.7.2. However, this parameter is not unique as the traffic induced exchange rate also impacts in a similar way on the turbulent fluxes. Sensitivity tests with both of these parameters have been carried out for a limited number of datasets and are presented in Figure 5.12. It is clear that the model correlation can be very sensitive to the choice of these parameters. E.g. there is a large change in correlation in the Hornsgatan 2010-2011 results due to a change in the surface roughness. Such large differences result when the modelled surface moisture is close to being dry on certain days and slight changes in the energy balance parameters can lead to large modelled emissions for these days.

The result of the sensitivity study is an optimal choice for these parameters of $z_0 = 2$ mm and $a_{traffic}^{li} = 1 \times 10^{-3}$ s/veh.

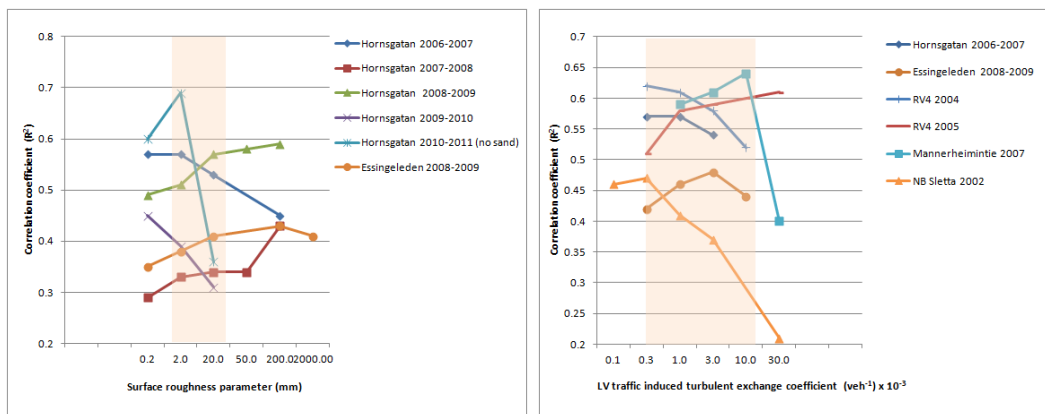


Figure 5.12. Model PM_{10} correlation sensitivity to surface roughness (left) and traffic induced turbulent exchange coefficient (right) for a selection of the datasets.

5.10 Impact of salt on surface moisture

The addition of salt has the general tendency of keeping the surface moist. At the moment it is included in all model runs as it has been seen to be very important in determining the surface wetness. An assessment is shown, Figure 5.13, for two examples in Hornsgatan (2008-2009 and 2010-2011) where the model was applied in the following way:

1. Without salt
2. With salt (estimated) but no humidity impact
3. With salt (estimated) and with humidity impact
4. With salt (reported) and with humidity impact (2010-2011 only)
5. Using observed moisture for retention

Results show a clear improvement, particularly in correlation, with the inclusion of the salt humidity impact. The impact on the mean values is generally small but there can be significant differences in the percentile concentrations as a result of the salting and its impact on surface humidity.

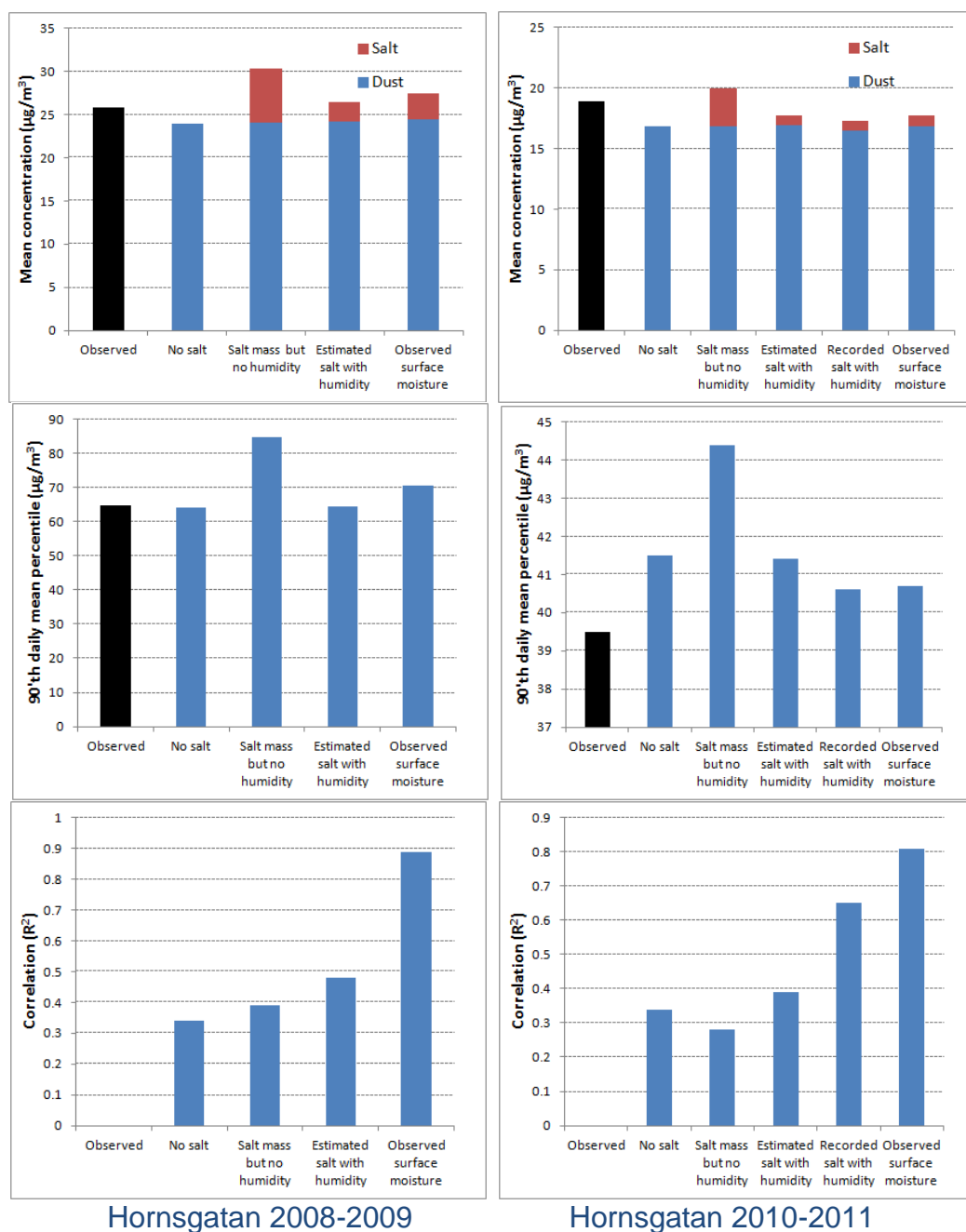


Figure 5.13. Summary of the model application to Hornsgatan 2008-2009 (left) and Hornsgatan 2010-2011 (right) where different salting applications are assessed. Shown in each plot are the results for no salting, estimated salt (using salting model) but no humidity impact, estimated salting (salting model) including humidity impact, reported salting including humidity impact (2010-2011 only) and use of the observed surface moisture. Top: Mean concentrations of dust and salt. Middle: 90'th percentile of the daily mean concentrations. Bottom: Correlation coefficient (R^2) of the daily mean concentrations.

5.11 Conversion of emissions to concentrations

The use of NO_x as a tracer is sometime problematic. This is particularly the case when background levels of NO_x are high. If the background station is not in the vicinity of the traffic station then the temporal changes in background NO_x may not match those at the traffic site. In addition the subtraction of large numbers to determine a smaller one is always prone to error.

The assumption that NO_x can be used as a tracer requires that the emission of NO_x is reflected in the concentration of NO_x . During periods when there is a build up of NO_x in the street canyon then this assumption is no longer valid and high NO_x concentrations may be measured with low NO_x emissions, or visa versa.

The use of dispersion models can relieve some of these problems but generally the accuracy of the dispersion model is considered to be less than the use of measured NO_x as a tracer.

6 Steady state solution to the road dust model under dry conditions

A steady state under dry conditions will be approached when $t \gg R^{-1}$, resulting in a steady state road dust loading given by

$$M_{road,steadystate} = \frac{P}{R} \quad (6.1)$$

If we consider only production through road wear (no sandpaper) and only the sink through suspension then the steady state solution for a road surface occurs when

$$P_{retention-roadwear} = S_{sus-road}$$

$$\sum_{t=st,wi,su}^{tyre} \sum_{v=he,li}^{vehicle} N^{t,v} \cdot W_{roadwear}^{t,v} \cdot f_{retained} = M_{road} \cdot \sum_{t=st,wi,su}^{tyre} \sum_{v=he,li}^{vehicle} \frac{N^{t,v}}{n_{lanes}} \cdot f_{sus-road}^{t,v} \quad (6.2)$$

Where the term $f_{retained}$ indicates the fraction of the wear retained on the surface. This may reflect the fraction of time the surface is wet or may reflect the model parameter $(1 - f_{0,direct})$, indicating the amount of wear directly emitted.

6.1 Simplified steady state equation for road dust loading

If we further simplify that the studded tyres dominate the road wear and write the ratio of light and heavy duty vehicles with studded tyres as $r_{st,li}$ and $r_{st,he}$ respectively (also the ratio of total light and heavy duty vehicles as r_{li} and r_{he}) then we can rewrite the above equation to give the steady state dry road dust loading as

$$M_{road,steadystate} = \frac{(r_{st,li} \cdot W_{roadwear}^{st,li} + r_{st,he} \cdot W_{roadwear}^{st,he})}{(r_{li} \cdot f_{sus-road}^{li} + r_{he} \cdot f_{sus-road}^{he})} \cdot n_{lanes} \cdot f_{retained} \quad (6.3)$$

This equation indicates that the steady state dust loading is the same no matter the traffic volume, though the road dust will increase linearly with the studded tyre percentage. If the vehicle speed dependence of both the wear and the suspension is the same, i.e. linear, then the steady state mass loading will also be independent of vehicle speed.

The time scale on which this steady state is reached is given by:

$$\tau_{road} = \frac{n_{lanes}}{N \cdot (r_{li} \cdot f_{sus-road}^{li} + r_{he} \cdot f_{sus-road}^{he})} \quad (6.4)$$

For a 2 lane road with 10 000 veh/day, 90% light duty vehicles, a 50% proportion of cars with studded tyres, wear rates of 2.5 g/km/veh, a retainment fraction of 50% and a suspension rate of 2×10^{-6} veh⁻¹ (as used in the model) would result in time scales of approximately 100 days and mass loadings of around 100 g/m². Increasing the suspension rate by a factor of 100 (similar to those found for dry sanding) would reduce the time scale and the mass loading by a factor of 100. These results indicate that measurements of mass loading can provide important information concerning the suspension rates.

6.2 Ratio of direct to suspended emissions

In addition, under the steady state assumptions given above, we can also find the ratio of direct emissions to suspended emissions. If we assume, for simplicity, only light vehicle contributions and that the suspension rate ($f_{sus-road}$) as well as the size distribution ($f_{PM,sus-road}$) is the same for both studded and winter tyres, then the ratio of direct to suspended emissions is given by:

$$\frac{E_{dir-roadwear}^x}{E_{sus-road}^x} = \frac{(1 - f_{retained})}{f_{retained}} \cdot \frac{f_{PM,dir-roadwear}^{x,st,li}}{f_{PM,sus-road}^{x,li}} \quad (6.5)$$

This indicates that the ratio of direct and suspended emissions under steady state conditions is determined by the factor $f_{retained}$, which indicates the fraction of road wear mass that is retained on the road surface, as well as by the size distributions of the emitted particles from both direct and suspended sources. Given a value of $f_{retained} = 0.5$ we see that these two emissions should have a ratio of 1.

7 Datasets and NORTRIP model results

The model has been extensively applied and tested on a number of datasets. Several aspects of this have already been described in Section 5. A summary of these datasets and some standard statistical results are presented in this section. Summary graphical results for each dataset is provided in Appendix D and a detailed presentation for one of the datasets (Hornsgatan 2010-2011) is presented in Appendix E.

A total of seven different sites covering from 3 months to 5 years provided 14 different datasets for application of the model. These are listed in the Table 7.1 below, indicating the availability and type of input data provided for each dataset.

Table 7.1. Summary of the available datasets and the available input parameters. '?' indicates unknown information.

| Dataset name | Period | Traffic | | Meteorology | | | | Surface conditions | | |
|--------------------------------------|-----------------------|----------|----------|----------------|----------------|----------------|----------------|------------------------|-------------|--------------|
| | | Volume | Speed | Radiation | Temperature | Humidity | Precip | Cloud cover | Temperature | Moisture |
| Hornsgatan 2006-2007 (Stockholm) | Jul 2006 - Jun 2007 | Measured | Measured | Roof | Street | Street | Roof | None | 3 sensors | conductivity |
| Hornsgatan 2007-2008 (Stockholm) | Jul 2007 - Jun 2008 | Measured | Measured | Roof | Street | Street | Roof | None | 3 sensors | conductivity |
| Hornsgatan 2008-2009 (Stockholm) | Jul 2008 - Jun 2009 | Measured | Measured | Roof | Street | Street | Roof | None | 3 sensors | conductivity |
| Hornsgatan 2009-2010 (Stockholm) | Jul 2009 - Jun 2010 | Measured | Measured | Roof | Street | Street | Roof | None | 3 sensors | conductivity |
| Hornsgatan 2010-2011 (Stockholm) | Jul 2010 - Jun 2011 | Measured | Measured | Roof | Street | Street | Roof | None | 3 sensors | conductivity |
| Essingeleden 2008-2009 (Stockholm) | Jul 2008 - Dec 2009 | Measured | Measured | Roof | Roof | Roof | Roof | None | None | None |
| RV4 2004 | Jan 2004 - April 2004 | Measured | Measured | Mast 3 km away | Mast 3 km away | Mast 3 km away | Mast 3 km | Synops 4 km (not used) | None | None |
| RV4 2005 (Oslo) | Jan 2005 - April 2005 | Measured | Measured | Mast 3 km away | Synops 4 km (not used) | None | None |
| RV4 2005-2006 (Oslo) | Nov 2005 - April 2006 | Measured | Measured | Mast 3 km away | Synops 4 km (not used) | None | None |
| HCAB 2006-2007 (Copenhagen) | Nov 2006 - May 2007 | Modelled | Modelled | Synops station | Synops station | Synops station | Synops station | None | 1 sensor | Depth |
| HCAB 2007-2008 (Copenhagen) | Nov 2007 - May 2008 | Modelled | Modelled | Synops station | Synops station | Synops station | Synops station | None | 1 sensor | Depth |
| Mannerheimintie 2007-2008 (Helsinki) | Jan 2007 - Dec 2008 | Modelled | Modelled | ? | ? | ? | ? | None | None | None |
| NB Sletta 2002 (Oslo) | Jan 2002 - April 2002 | Measured | Measured | Synops 12 km | Local | Local | Local | None | None | None |
| Runeberg 2004 (Helsinki) | Jan 2004 - Apr 2004 | Modelled | Measured | ? | ? | ? | ? | None | None | None |

| Activity | Concentrations | | | | | | Emission Quality | |
|---|----------------|-------------------------|---------------|---------------------|---------------|---------------------|------------------|-----------------------------------|
| | PM10 Traffic | PM10 Background | PM2.5 Traffic | PM2.5 Background | NOX Traffic | NOX Background | Ex/NOX | Usefulness and quality of dataset |
| Modelled salt | Street canyon | Roof top | Street canyon | Roof top | Street canyon | Roof top | Yes | Very good |
| Modelled salt | Street canyon | Roof top | Street canyon | Roof top | Street canyon | Roof top | Yes | Very good |
| Modelled salt | Street canyon | Roof top | Street canyon | Roof top | Street canyon | Roof top | Yes | Very good |
| Modelled salt | Street canyon | Roof top | Street canyon | Roof top | Street canyon | Roof top | Yes | Very good |
| Sanding and salting, day and | Street canyon | Roof top | Street canyon | Roof top | Street canyon | Roof top | Yes | Very good |
| Modelled salt | Road side | Average urban/rural | Road side | Average urban/rural | Road side | Average urban/rural | Yes | Good |
| Salting (from nearby road) | Kerb side | Nearby background | Kerb side | Nearby background | Kerb side | Nearby background | Yes | Fair |
| Salting (from nearby road) | Kerb side | Nearby background | Kerb side | Nearby background | Kerb side | Nearby background | Yes | Fair |
| Modelled salt | Kerb side | Nearby background | Kerb side | Nearby background | Kerb side | Nearby background | Yes | Good |
| Salting | Kerb side | ? | Kerb side | ? | Kerb side | ? | Yes | Good |
| Salting | Kerb side | ? | Kerb side | ? | Kerb side | Kerb side | Yes | Good |
| Salting/sanding (modelled by FMI) | Kerb side | ? | Kerb side | ? | Kerb side | Kerb side | Yes | Good |
| Modelled salt | Near kerb | Nearby daily means only | None | none | Near kerb | Upwind (120 m) | Yes | Poor |
| Sanding (modelled by FMI)/ Salting modelled | Street canyon | ? | Street canyon | ? | Street canyon | ? | Yes | Poor |

Statistical results of the modelling are summarised in Table 7.2 and Figures 7.1 – 7.4. In these figures the means, percentiles, correlation and relative root mean square error (RMSE) are presented. In Sections 7.1 – 7.7 each of the sites and related datasets are described in summary.

In general the model can be seen to consistently predict the means and percentiles of sites with more than one year of data, indicating the robustness of the model over many years. However, due to a lack of information concerning road surface wear parameters in Helsinki and Copenhagen the model wear rates have been adjusted at these sites to approach the observed mean values. For datasets in Oslo and Stockholm the model, based on calculated road wear, has been applied without adjustment. See the set of model parameters for the pavement type scaling factors (h_{pave}), Appendix C.1, for these scaling factors.

Table 7.2. Summary of input data and statistical modelling results for the 14 datasets.

| Dataset name | Period | Number of days | Traffic | | | | Meteorology | | | | | | | |
|--|-----------------------|----------------|---------------------|-------------|----------------------------|-----------------------|----------------------|-------------------|------------------------------|-----------------|--------------------|------------------------|------------------------|--|
| | | | Total ADT (veh/day) | HDV ADT (%) | Mean vehicle speed (km/hr) | Mean studded tyre (%) | Mean temperature (C) | Mean humidity (%) | Mean global radiation (W/m2) | Cloud cover (%) | Total precip. (mm) | Frequency wet road (%) | Mean dispersion factor | |
| * indicates use of observed surface moisture | | | | | | | | | | | | | | |
| Hornsgatan 2006-2007 * | Jul 2006 - Jun 2007 | 365 | 28472 | 7.1 | 43.3 | 31.7 | 10.2 | 72 | 117.4 | 51.2 | 346.6 | 36 | 0.166 | |
| Hornsgatan 2007-2008 * | Jul 2007- Jun 2008 | 366 | 27999 | 6.8 | 44.2 | 30.2 | 9 | 72.8 | 118.5 | 51.4 | 284.9 | 36 | 0.158 | |
| Hornsgatan 2008-2009 * | Jul 2008 - Jun 2009 | 365 | 27404 | 6.5 | 44.3 | 29.6 | 8.3 | 74.2 | 114.9 | 52.2 | 361.6 | 39 | 0.17 | |
| Hornsgatan 2009-2010 * | Jul 2009 - Jun 2010 | 351 | 24638 | 6.7 | 44.3 | 18.6 | 6.8 | 74.8 | 118 | 49.6 | 318.9 | 43 | 0.174 | |
| Hornsgatan 2010-2011 * (with sand) | Jul 2010 - Jun 2011 | 365 | 22490 | 6.8 | 43 | 12.6 | 7.5 | 73.7 | 124.6 | 45.2 | 372.1 | 45 | 0.166 | |
| Hornsgatan 2006-2007 | Jul 2006 - Jun 2007 | 365 | 28472 | 7.1 | 43.3 | 31.7 | 10.2 | 72 | 117.4 | 51.2 | 346.6 | 32 | 0.166 | |
| Hornsgatan 2007-2008 | Jul 2007- Jun 2008 | 366 | 27999 | 6.8 | 44.2 | 30.2 | 9 | 72.8 | 118.5 | 51.4 | 284.9 | 36 | 0.158 | |
| Hornsgatan 2008-2009 | Jul 2008 - Jun 2009 | 365 | 27404 | 6.5 | 44.3 | 29.6 | 8.3 | 74.2 | 114.9 | 52.2 | 361.6 | 42 | 0.17 | |
| Hornsgatan 2009-2010 | Jul 2009 - Jun 2010 | 351 | 24638 | 6.7 | 44.3 | 18.6 | 6.8 | 74.8 | 118 | 49.6 | 318.9 | 52 | 0.174 | |
| Hornsgatan 2010-2011 (with sand) | Jul 2010 - Jun 2011 | 365 | 22490 | 6.8 | 43 | 12.6 | 7.5 | 73.7 | 124.6 | 45.2 | 372.1 | 52 | 0.166 | |
| Essingeleden 2008-2009 | Jul 2008 - Dec 2009 | 549 | 134265 | 7 | 71.6 | 24.6 | 8.3 | 79 | 112 | 52.5 | 618.6 | 31 | 0.019 | |
| RV4 2004 | Jan 2004 - April 2004 | 100 | 43859 | 7 | 74.9 | 25.8 | 1.2 | 75.4 | 72.4 | 53.9 | 122.9 | 50 | 0.04 | |
| RV4 2005 | Jan 2005 - April 2005 | 108 | 41027 | 6.3 | 64.5 | 19.5 | 1.5 | 69.8 | 61 | 69.9 | 56.5 | 35 | 0.04 | |
| RV4 2006 | Jan 2006 - April 2006 | 105 | 41453 | 4.2 | 68.2 | 20 | -0.95 | 76.8 | 96.4 | 40.8 | 109.8 | 79 | 0.041 | |
| HCAB 2006-2007 * (road wear x 5) | Nov 2006 - May 2007 | 212 | 58474 | 3.4 | 43.7 | 0 | 8.6 | 77.6 | 56.1 | 62 | 501 | 46 | 0.051 | |
| HCAB 2007-2008 * (road wear x 5) | Nov 2007 - May 2008 | 213 | 57911 | 3.4 | 43.8 | 0 | 6.7 | 75.4 | 52.6 | 64.2 | 371.8 | 37 | 0.06 | |
| Mannerheimintie 2007-2008 (road wear x 2) | Jan 2007 - Dec 2008 | 731 | 18890 | 4.2 | 36.5 | 33.4 | 7.3 | 79 | 110.4 | 58.6 | 1512.4 | 50 | 0.144 | |
| NB Sletta 2002 | Jan 2002 - April 2002 | 105 | 35330 | 5.9 | 92 | 32 | -0.6 | 81.3 | 53.6 | 61.6 | 831.6 | 59 | 0.115 | |
| Runeberg 2004 | Jan 2004 - Apr 2004 | 123 | 21122 | 10.4 | 48.2 | 68.5 | -1.1 | 80.1 | 88.7 | 65.9 | 112.1 | 71 | 0.078 | |

| Activity | | Net concentrations | | | | Statistics | | | | | Source contributions | | | | | |
|--------------------|--------------------|---|---|--|--|---------------------|---------------------------|-----------------------------------|---------------|------------------|----------------------|---------------|----------------|----------|----------|-------------|
| Salting events (#) | Sanding events (#) | Mean observed net PM10 ($\mu\text{g}/\text{m}^3$) | Mean modelled net PM10 ($\mu\text{g}/\text{m}^3$) | 90 th per. observed net PM10 ($\mu\text{g}/\text{m}^3$) | 90 th per. modelled net PM10 ($\mu\text{g}/\text{m}^3$) | Fractional Bias (%) | Fractional percentile (%) | RMSE ($\mu\text{g}/\text{m}^3$) | Relative RMSE | Correlation (R2) | Road wear (%) | Tyre wear (%) | Brake wear (%) | Sand (%) | Salt (%) | Exhaust (%) |
| 40 | 0 | 31 | 29 | 75 | 70 | -9.0 | 7.7 | 15.3 | 0.49 | 0.83 | 67.1 | 7.0 | 7.0 | 0.0 | 5.9 | 13.3 |
| 36 | 0 | 26 | 26 | 62 | 67 | 1.6 | -7.1 | 12.3 | 0.48 | 0.76 | 68.0 | 6.9 | 6.9 | 0.0 | 4.6 | 13.5 |
| 51 | 0 | 26 | 27 | 65 | 68 | 3.8 | -4.5 | 10 | 0.39 | 0.9 | 63.8 | 6.7 | 6.7 | 0.0 | 9.7 | 13.4 |
| 70 | 0 | 19 | 19 | 41 | 44 | 2.7 | -6.3 | 6.2 | 0.34 | 0.91 | 59.5 | 8.4 | 8.9 | 0.0 | 5.8 | 17.9 |
| 88 | 29 | 19 | 17 | 40 | 40 | -8.3 | -1.3 | 9 | 0.48 | 0.81 | 44.8 | 7.5 | 9.2 | 15.5 | 5.2 | 17.2 |
| 40 | 0 | 31 | 28 | 75 | 70 | -11.1 | 7.4 | 22.5 | 0.72 | 0.62 | 66.4 | 6.8 | 7.1 | 0.0 | 6.1 | 13.6 |
| 36 | 0 | 26 | 25 | 62 | 61 | -4.0 | 1.9 | 16.7 | 0.65 | 0.55 | 66.5 | 6.9 | 7.3 | 0.0 | 4.9 | 14.3 |
| 51 | 0 | 26 | 26 | 65 | 67 | 1.2 | -2.7 | 20.8 | 0.81 | 0.58 | 64.8 | 6.9 | 6.9 | 0.0 | 7.7 | 13.8 |
| 70 | 0 | 19 | 18 | 41 | 43 | -2.2 | -5.0 | 17.8 | 0.96 | 0.43 | 58.0 | 8.3 | 9.4 | 0.0 | 5.5 | 18.8 |
| 88 | 29 | 19 | 16 | 40 | 39 | -14.8 | 1.5 | 13.3 | 0.70 | 0.61 | 44.2 | 7.4 | 9.8 | 15.3 | 4.9 | 18.4 |
| 93 | 0 | 20 | 18 | 49 | 47 | -11.7 | 4.8 | 18.5 | 0.93 | 0.47 | 73.4 | 7.3 | 4.5 | 0.0 | 4.5 | 9.6 |
| 75 | 0 | 32 | 28 | 86 | 80 | -13.6 | 7.6 | 21.7 | 0.69 | 0.52 | 74.9 | 3.3 | 2.2 | 0.0 | 8.7 | 10.9 |
| 38 | 0 | 22 | 21 | 55 | 55 | -8.9 | 0.7 | 12.6 | 0.56 | 0.58 | 68.8 | 3.4 | 2.4 | 0.0 | 12.7 | 12.7 |
| 50 | 0 | 12 | 12 | 32 | 36 | 3.4 | -11.2 | 10 | 0.86 | 0.46 | 64.2 | 4.2 | 4.2 | 0.0 | 5.0 | 22.5 |
| 28 | 0 | 12 | 10 | 25 | 23 | -22.6 | 10.9 | 6.1 | 0.50 | 0.39 | 55.1 | 7.1 | 9.2 | 0.0 | 1.0 | 27.6 |
| 40 | 0 | 20 | 15 | 48 | 37 | -26.6 | 26.4 | 9.7 | 0.49 | 0.47 | 55.3 | 6.7 | 8.0 | 0.0 | 8.0 | 22.0 |
| 44 | 20 | 17 | 13 | 36 | 36 | -22.2 | 2.0 | 12.5 | 0.76 | 0.42 | 77.3 | 4.5 | 6.1 | 0.8 | 0.8 | 11.4 |
| 63 | 0 | 32 | 49 | 84 | 142 | 41.7 | -51.6 | 51.7 | 1.60 | 0.33 | 79.9 | 6.1 | 2.4 | 0.0 | 6.1 | 5.5 |
| 83 | 20 | 21 | 20 | 64 | 68 | -4.3 | -5.9 | 14.9 | 0.70 | 0.71 | 54.9 | 2.9 | 3.9 | 7.8 | 13.7 | 16.2 |

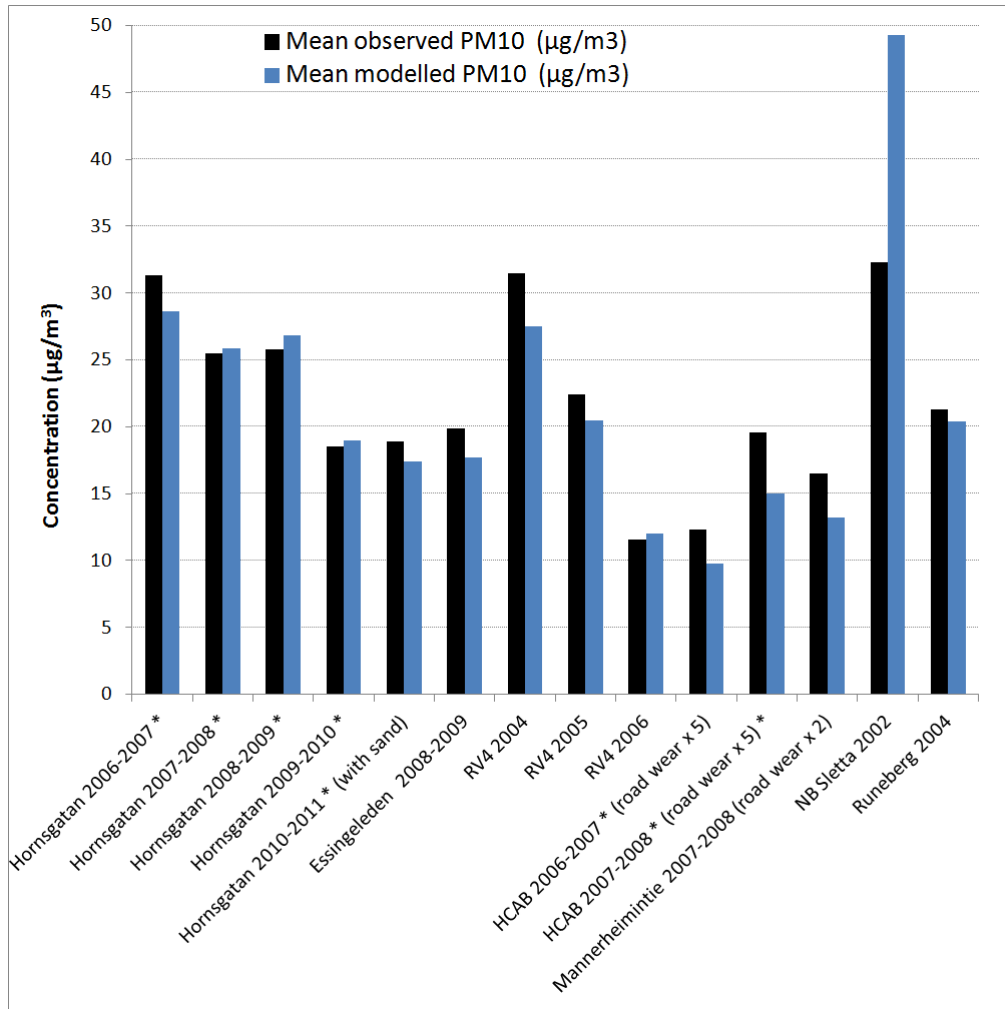


Figure 7.1. Observed (black) and predicted (blue) mean PM₁₀ concentrations for the 14 data sets.

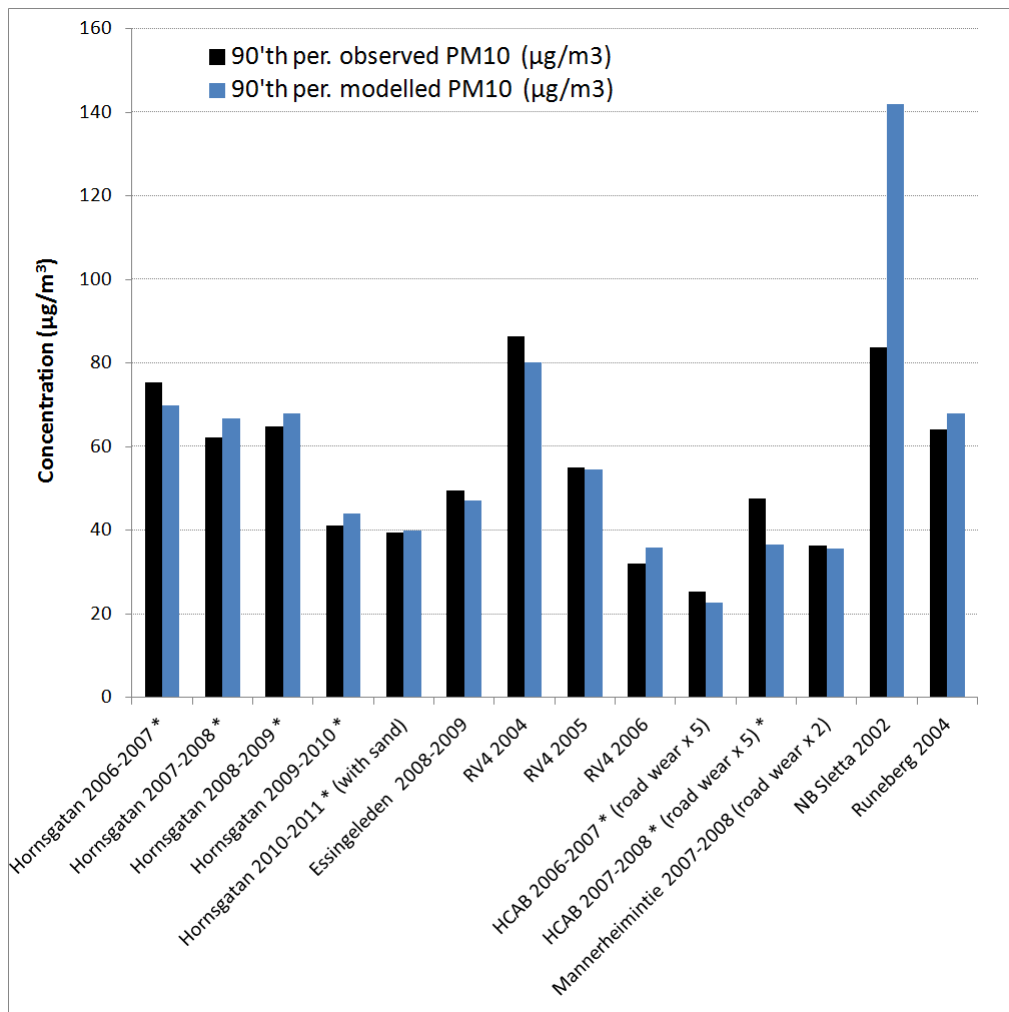


Figure 7.2. Observed (black) and predicted (blue) 90'th percentile PM₁₀ concentrations for the 14 data sets.

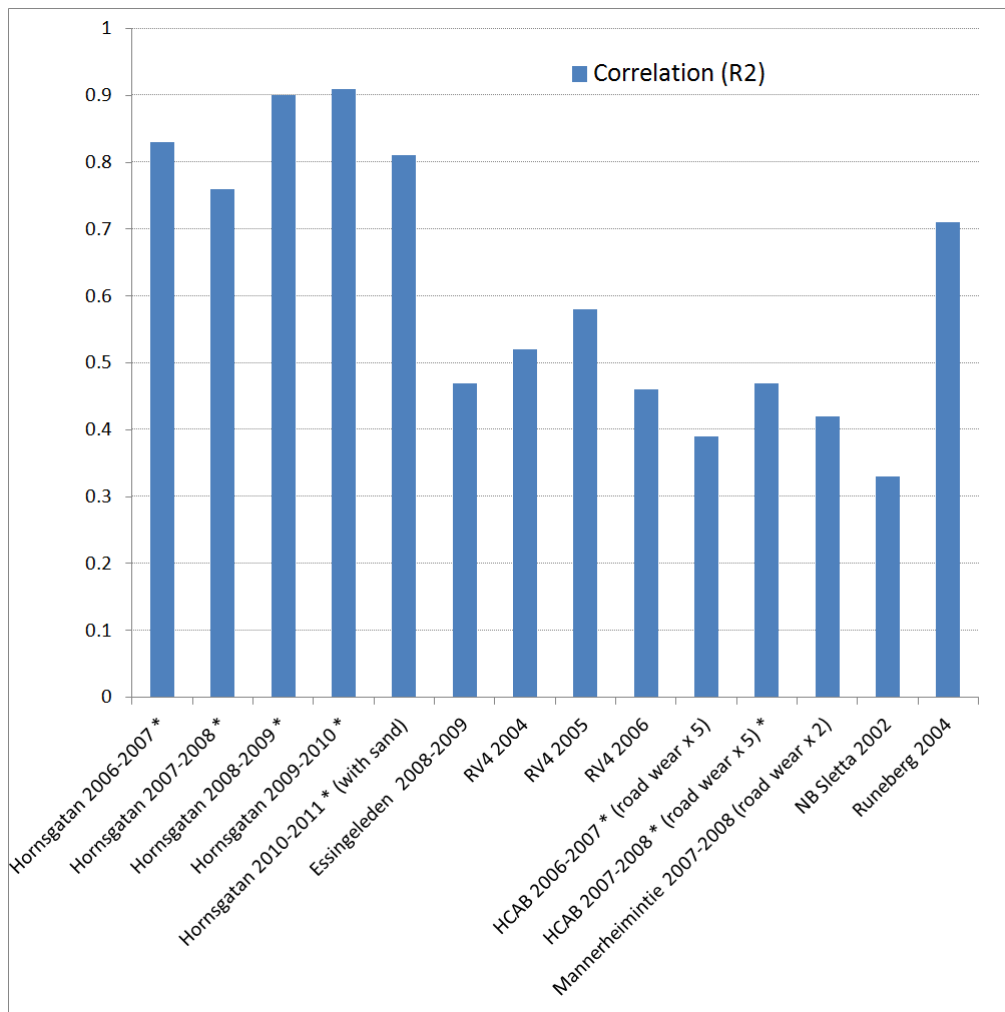


Figure 7.3. Correlation (R^2) of the daily mean modelled and observed PM_{10} concentrations for the 14 datasets. (* Using observed surface moisture for surface retention).

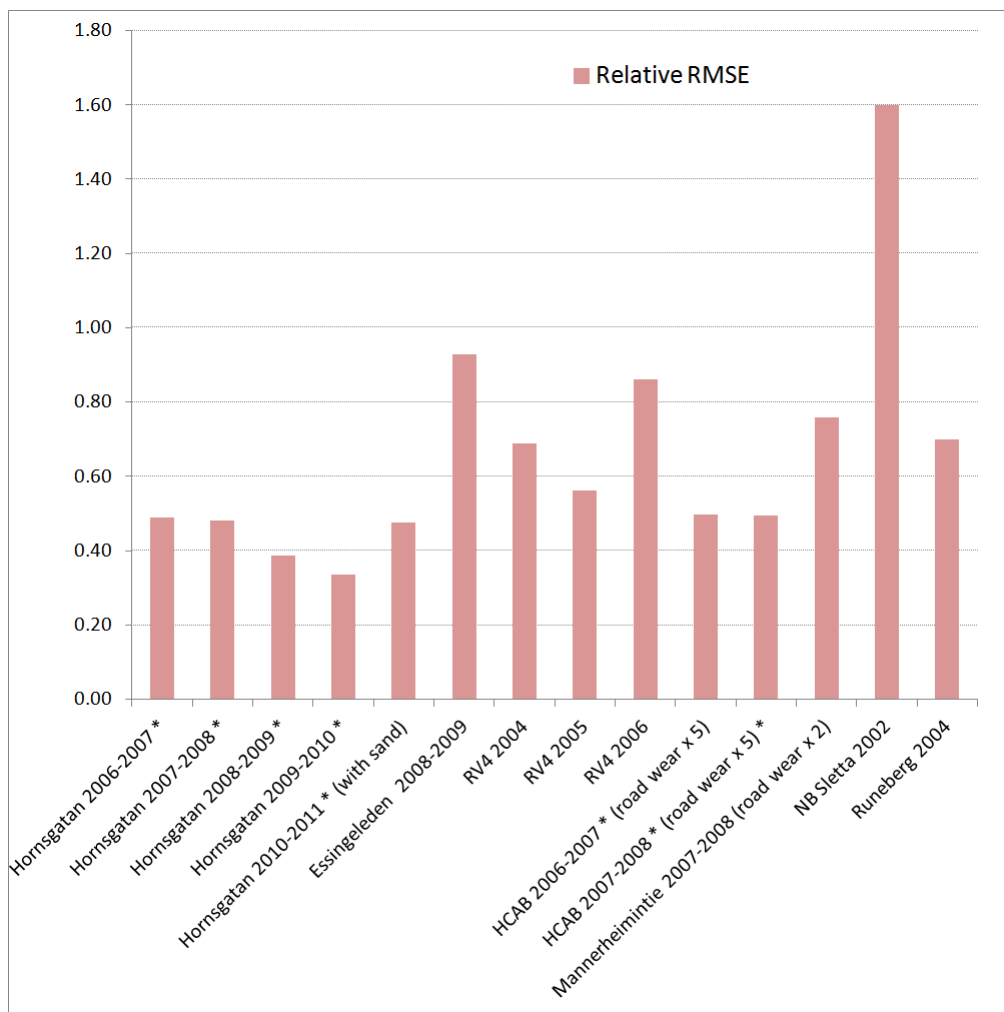


Figure 7.4. Relative RMSE (RMSE normalised with mean observed concentration) for the daily mean modelled and observed PM_{10} concentrations for the 14 datasets.

7.1 Hornsgatan, Stockholm

Hornsgatan is the most complete and best dataset of all the data collected. This is due to the availability of surface moisture and temperature measurements, the large difference between traffic and background concentrations due to its confinement in the street canyon and the availability of important meteorological parameters such as temperature and humidity at the street level, supported by roof station measurements. In addition it has both traffic and studded tyre counts.

Since surface moisture measurements are available for Hornsgatan results are shown in Figures 7.1-7.4 when using observed moisture. In Appendix D.1 results using both measured and modelled surface moisture are shown. Salting and sanding information is available only for the period 2010-2011. For the other years a salting model was implemented to estimate the salting events but no sand was implemented.

The results for Hornsgatan, when observed surface wetness is applied to control the surface retention, show remarkably high correlation, explaining 76% - 92% of the variability of the daily mean PM₁₀ concentrations. When modelled surface moisture is used (see Appendix D, Figure D.1) then the correlation is reduced to 43% - 61%. This emphasizes the importance of the surface moisture in controlling the suspended emissions and the need for high quality surface moisture modelling if the temporal evolution of the emissions is to be well represented.

From the year 2010 onwards a ban on studded tyres in Hornsgatan reduced the percentage of studded tyres from 70% to 40% during the winter season. This management strategy is well represented by the model, where both the mean and the percentile concentrations closely follow those observed.

7.2 Essingeleden, Stockholm

In Essingeleden, a highway site with a high traffic volume, no surface moisture measurements or salting (no sanding applied) data were available. In addition there was no locally placed background site so an average was taken of the nearest urban and regional background stations. There are some large discrepancies during the winter but the decay during spring and the build up in the following year is well modelled. Improved results can be achieved by reducing the suspension rates, as discussed in Section 5.3. The model predicts well both the mean and the percentiles, with a correlation of 0.47. Graphical results are presented in Appendix D.2.

7.3 Riksvei 4 (RV4), Oslo

Three years of data are available at RV4. As in the Hornsgatan case a management strategy of reducing the signed vehicle speed was introduced in the last two years. In the last year the addition of dust binding salt (MgCl₂) was used. The model follows the changes of these impacts along with the impact of different meteorology for the different years. Between 45% and 60% of the variability is explained by the model for these three years. No surface moisture measurements were available at this site. Further studies concerning this site will be carried out to provide a more detailed assessment of the model processes including the

impacts of changes in vehicle speed, in meteorology and in the contribution of salt to the total emitted PM₁₀, see Section 5.5. Graphical results are presented in Appendix D.3.

7.4 H. C. Andersen Boulevard (HCAB), Copenhagen

For HCAB, an open street canyon site, surface moisture measurements and salting (no sanding was undertaken) data were available. This dataset is unique in that there are no studded tyres during the winter period. HCAB has been shown to show significantly higher PM₁₀ concentrations when compared to other streets in Copenhagen. The model underestimates the PM₁₀ concentrations by a factor of 2 in this street. To achieve the appropriate average the road wear would need to be increased by a factor of 5. In addition the model would appear to overestimate surface wetness, even though it agreed well with the observed moisture observations. Graphical results are presented in Appendix D.4 using both observed and modelled surface moisture. A more detailed assessment of these data and other streets in Copenhagen is required to understand these differences.

7.5 Mannerheimintie, Helsinki

Mannerheimintie in Helsinki is paved with cobbled stones and as such is different to all the other datasets. Modelling at this site spanned a two year period. The model performs reasonably well ($R^2=0.42$) and shows the decay of dust loading continues until the following winter season. Since no information concerning road wear parameters were available for this site the Hornsgatan wear rates were applied and enhanced by a factor of 2 to approximate the observed mean concentrations. Graphical results are presented in Appendix D.5.

7.6 Nordby Sletta (NB), Oslo

Nordby Sletta near Oslo has the highest vehicle speeds of all the datasets (90 km/hr). Only a three month period is available. Using the default suspension rates and the same wear rates as for RV4 in Oslo, the model overestimates the concentrations during the winter but performs well during the spring but provides better results with lower suspension rates. In general this was the worst performing site of all the data sets, overestimating the mean and percentiles significantly and providing the lowest correlation coefficient of $R^2=0.33$. Graphical results are presented in Appendix D.6 for both the default model settings and with a reduced suspension rate.

7.7 Runeberg, Helsinki

Runeberg is a street canyon site in Helsinki. Results from this site are very sensitive to the surface moisture model parameters. Despite this a relatively high correlation of $R^2=0.71$ is obtained with the default model settings. Means and percentiles are well estimated. Wear rates are the same as for Hornsgatan in Stockholm. Graphical results are presented in Appendix D.7.

8 Conclusions and future development

The NORTRIP model is the most comprehensive non-exhaust model currently developed. This is the result of a strong co-operation between the Nordic partners involved in the NORTRIP project. The consolidation of expertise in this area and the collection of a range of datasets has made significant improvements in non-exhaust modelling possible.

The Hornsgatan data set has provided the most useful source of data and the model performs very well in this situation. What has become clear from this modelling application is that if PM concentrations are to be well modelled then the surface moisture must also be well represented. The model successfully follows the hour to hour, day to day and year to year variation in Hornsgatan, correctly representing the sensitivity of the model to changes in studded tyre fractions that have occurred as a result of a ban in the street. The relatively successful application of the model to a highway site outside of Stockholm, Essingeleden, with significantly different speeds and traffic volumes also indicates the ability of the model to represent the impact of these aspects on the emissions.

On the other hand the application of the model to HCAB in Copenhagen shows a distinct underestimate of the concentrations without a fivefold increase in the wear rates. This point has been noted already in Ketzler et al. (2007) where HCAB has been shown to have consistently higher emission factors compared to other similar roads in Copenhagen. Though the model provides higher correlation with observed concentrations when salting is included, there is little improvement with the inclusion of surface retention and suspension. If this is to be improved then a more specific study over more years and other streets in Copenhagen is required to resolve these differences. This is particularly important as Copenhagen, which does not use studded tyres, is more representative of most cities in Europe.

The application to RV4 in Oslo shows that the model can represent several different years of data, with different meteorological situations and traffic flows, with an appropriate dynamic sensitivity. In this case speed reductions were implemented on this stretch of road whilst road wetness conditions varied significantly between years. A thorough analysis of these data will be undertaken to assess the model validity and the impact of the management strategy.

The moisture sub-model developed has not been extensively analysed beyond its implementation here and a few sensitivity tests. In general its ability to provide the correct temporal variation of the concentrations, rather than surface wetness itself, has been the focus of the assessment. It is interesting to note that this sub-model fulfils a similar role to other road weather models available for traffic safety applications. A more comprehensive assessment of this sub-model should be carried out as this may provide significant improvements in the future.

The NORTRIP model has been developed with the main aim of improving our understanding of non-exhaust emissions for air quality management applications. The procedure was to identify a number of important processes, even if these cannot be well defined with current knowledge, and implement these in a

conceptual and mathematical modelling tool. As such there are some poorly defined processes, e.g. crushing and abrasion, which are not currently included in the model applications but are described within the model structure. Other processes such as suspension rates did not show the expected dependence on vehicle speed. If these are to be improved upon then additional existing databases, particularly outside of Nordic countries, need to be acquired and the model applied and tested on these to assess the robustness of the model concept and its implementation.

In addition there are a number of measurements that would greatly help improve the model and its process descriptions. In the field simultaneous measurements over a winter season of the following parameters would be invaluable to improve the model. These include:

- Collection of ambient air filter samples, size fraction and chemical analysis to establish the source contributions of road, tyre, brake, salt and sand particles
- Collection of surface dust mass loading with an analysis of size distribution and chemical analysis to establish the surface mass loading, its size distribution and its source contributions
- Collection of surface dust mass loading before and after precipitation events to establish the impact of drainage
- Measurement of surface wetness, temperature and salt content
- Collection of spray water and analysis of dust and salt concentrations to establish the impact of spray
- In situ measurement of surface macro-structure and road wear properties
- In situ measurement of actual road surface depletion to determine total road wear
- Combination of road dust loading measurements with behind vehicle dust emissions, e.g. Sniffer.
- Collection of road maintenance activity data

In addition to these field measurements, laboratory experiments can also be carried out to improve the model. These would include:

- Further refinement of the PM fraction from wear and its dependency on speed
- The role of surface macro-structure, surface moisture history and salt in determining suspension rates

There are also a number of processes not described in the model that can be considered for further implementation. These include:

- The impact of dust loading on surface moisture retention.
- The migration/deposition of coarse sand and gravel from down road and cross road sources, and the impact on the sandpaper and crushing processes by these.

9 Acknowledgments

This work has been carried out within the Nordic Council of Ministers Project NORTRIP (BLS- 306-00064) with substantial financial support provided by the Norwegian Climate and Pollution Agency (KLIF 4011009).

10 References

- Berger, J., Denby, B. (2011) A generalised model for traffic induced road dust emissions. Model description and evaluation. *Atmos. Environ.*, 45, 3692-3703. doi:10.1016/j.atmosenv.2011.04.021.
- Blomqvist, G., Gustafsson, M., Eram M., Ünver, K. (2012) Prediction of salt on road surface. *Transport Res. Rec.*, 2258, 131-138. doi:10.3141/2258-16.
- Blomqvist, G., Gustafsson, M., Bennet, C., Halldin, T. (2011) PM₁₀ suspension of road dust is depending on the road surface macro texture. In: *Proceedings of the European Aerosol Conference*, September 2011, Manchester.
URL: <http://ww.eac2011.com> [05.10.2012]
- Boulter, P. G. (2005) A review of emission factors and models for road vehicle non-exhaust particulate matter. Wokingham, UK, TRL Limited (TRL Report PPR065).
- Boulter, P.G. Thorpe, A.J., Harrison, R.M., Allen, A.G. (2006) Road vehicle non-exhaust particulate matter: final report on emission modelling. Wokingham, UK, TRL Limited (TRL Report PPR110).
- Denby, B., Karl, M., Laupsa, H., Johansson, C., Pohjola, M., Karppinen, A., Kukkonen, J., Ketzel, M., Wählin, P. (2009) Source-receptor and inverse modelling to quantify urban PARTICULATE emissions (SRIMPART). Copenhagen, Nordic Council of Ministers (TemaNord, 2009:552).
- Denby, B. R. (2012) NORTRIP emission model user guide. Kjeller, Norwegian Institute for Air Research (NILU TR 02/2012).
- EEA (2010) The European environment state and outlook 2010: Air pollution. Copenhagen, European Environment Agency.
- Garratt, J. R. (1992) The atmospheric boundary layer. Cambridge, UK, Cambridge University Press.
- Gustafsson, M., Blomqvist, G., Gudmundsson, A., Dahl, A., Jonsson, P., Swietlicki, E. (2008) Factors influencing PM₁₀ emissions from road pavement wear. *Atmos. Environ.*, 43, 4699-4702. doi:10.1016/j.atmosenv.2008.04.028.
- Hagen, L.O., Larssen, S., Schaug, J. (2005) Speed limit in Oslo. Effect on air quality of reduced speed on RV4. Kjeller, Norwegian Institute for Air Research (NILU OR 41/2005) (in Norwegian).

- Iqbal, M. (1983) An introduction to solar radiation. Toronto, Canada, Academic Press.
- Jacobson T., Wågberg, L.G. (2007) Developing and upgrading of a prediction model of wear caused by studded tyres and an overview of the knowledge of the factors influencing the wear – Version 3.2.03. Linköping, The Swedish National Road and Transport Research Institute (VTI notat 7-2007) (in Swedish).
- Johansson, C., Denby, B.R., Sundvor, I., Kauhaniemi, M., Härkönen, J., Kukkonen, J., Karppinen, A., Kangas, L., Omstedt, G., Ketznel, M., Massling, A., Pirjola, L., Norman, M., Gustafsson, M., Blomqvist, G., Bennet, C., Kupiainen, K., Karvosenoja, N. (2012) NORTRIP: NOn-exhaust Road TRaffic Induced Particle emissions. Development of a model for assessing the effect on air quality and exposure. Stockholm, Department of Applied Environmental Science, Stockholm university (ITM-report 212).
- Karlsson, M. (2001) Prediction of hoar-frost by use of a Road Weather Information System. *Meteorol. Appl.*, 8, 95-105.
- Konzelmann, T., van deWal, R.S.W., Greuell, W., Bintanja, R., Henneken, E.A.C., Abe-Ouchi, A. (1994) Parameterization of global and longwave incoming radiation for the Greenland ice sheet. *Global Planet. Change*, 9, 143-164. doi:10.1016/0921-8181(94)90013-2.
- Kupiainen, K.J., Tervahattu, H., Räisänen, M., Mäkelä, T., Aurela, M., Hillamo, R. (2005) Size and composition of airborne particles from pavement wear, tires, and traction sanding. *Environ. Sci. Technol.*, 39, 699-706. doi: 10.1021/es035419e.
- Kupiainen, K., Pirjola, L. (2011) Vehicle non-exhaust emissions from the tyre-road interface - Effect of stud properties, traction sanding and resuspension. *Atmos. Environ.* 45, 4141-4146. doi:10.1016/j.atmosenv.2011.05.027.
- Langston, R., Merle Jr., R. S., Etyemezian, V., Kuhns, H., Gillies, J., Zhu, D., Fitz, D., Bumiller, K., James, D.E., Teng, H. (2008) Clark County (Nevada) paved road dust emission studies in support of mobile monitoring technologies. Las Vegas, NV, Clark County Department of Air Quality and Environmental Management.
- Lysbakken, K.R., Norem, H. (2012) Processes that control development of quantity of salt on road surfaces after salt application. *Transport Res. Rec.*, 2258, 139-146. doi:10.3141/2258-17.
- Möller, S. (2006) Winter model. Road condition model. Linköping, The Swedish National Road and Transport Research Institute (VTI Report 529) (in Swedish).
- Morillon, V., Debeaufort, F., Jose, J., Tharrault, J.F., Capelle, M., Blond, G., Voilley, A. (1999) Water vapour pressure above saturated salt solutions at low

- temperatures. *Fluid Phase Equil.*, 155, 297-309. doi:10.1016/S0378-3812(99)00009-6.
- Nicholson, K. W. (1993) Wind tunnel experiments on the resuspension of particulate material. *Atmos. Environ.*, 27, 181-188. doi:10.1016/0960-1686(93)90349-4.
- Omstedt, G., Bringfelt, B., Johansson, C. (2005) A model for vehicle-induced non-tailpipe emissions of particles along Swedish roads. *Atmos. Environ.*, 39, 6088-6097. doi:10.1016/j.atmosenv.2005.06.037.
- Patra, A., Colvile, R., Arnold, S., Bowen, E., Shallcross, D., Martin, D., Price, C., Tate, J., ApSimon, H., Robins, A. (2008) On street observations of particulate matter movement and dispersion due to traffic on an urban road. *Atmos. Environ.*, 42, 3911-3926. doi:10.1016/j.atmosenv.2006.10.070.
- Pirjola, L., Kupiainen, K.J., Perhoniemi, P., Tervahattu, H., Vesala, H. (2009) Non-exhaust emission measurement system of the mobile laboratory SNIFFER. *Atmos. Environ.*, 43, 4703-4713. doi:10.1016/j.atmosenv.2008.08.024.
- Sass B.H. (1997). A numerical forecasting system for the prediction of slippery roads. *Journal of Applied Meteorology*, 36, pp. 801-817. doi: 10.1175/1520-0450(1997)036<0801:ANFSFT>2.0.CO;2.
- Snilsberg, B., Myran, T., Uthus, N. (2008) The influence of driving speed and tires on road dust properties. In: *B. Snilsberg: Pavement wear and airborne dust pollution in Norway. Characterization of the physical and chemical properties of dust particles*. Doctoral Thesis. Trondheim, Norwegian University of Science and Technology (Doctoral theses at NTNU, 2008:133).
- Vaze, J. and F.H.S. Chiew (2002) Experimental study of pollutant accumulation on an urban road surface. *Urban Water*, 4, 379-389. doi:10.1016/S1462-0758(02)00027-4.

Appendix A

Physical constants and equations used in the NORTRIP model

A.1 Physical constants

The following physical constants are used in the model.

| | |
|--|--|
| Latent heat of condensation (vapour-water) | $\lambda_s = 2.5 \times 10^6 \text{ J kg}^{-1}$ |
| Latent heat of sublimation (vapour-ice) | $\lambda_{ice} = 2.8 \times 10^6 \text{ J kg}^{-1}$ |
| Latent heat of fusion (water-ice) | $\lambda_m = 3.3 \times 10^6 \text{ J kg}^{-1}$ |
| Heat capacity of dry air | $C_p = 1005 \text{ J kg}^{-1} \text{ K}^{-1}$ |
| Specific gas constant for dry air | $R_d = 287 \text{ J kg}^{-1} \text{ K}^{-1}$ |
| Stefan-Boltzmann constant | $\sigma = 5.67 \times 10^{-8} \text{ W m}^{-2} \text{ K}^{-4}$ |
| von Karman constant | $\kappa = 0.4$ |
| Angular velocity of the Earth | $\Omega = 7.3 \times 10^{-5} \text{ rad.s}^{-1}$ |

A.2 Physical equations

The relative humidity in air, RH_a , is specified by the ratio of the water vapour partial pressure and the saturated partial pressure

$$RH_a = \frac{e_a}{e_a^*} \cdot 100 \quad (\text{A.1})$$

Calculation of the specific humidity, saturated or unsaturated, is carried out using

$$q_a = \frac{0.622 \cdot e_a}{(p_a - 0.378 \cdot e_a)} \quad (\text{A.2})$$

Where the Bolton equation fit to the saturated water vapour pressure is given by

$$e_a^* = 6.112 \cdot \exp \left[\frac{17.67 \cdot T_a}{T_a + 243.5} \right] \quad (\text{A.3})$$

The temperature derivative is usually given by Clasius-Clapeyron equation but we use the direct derivative of the Bolton equation

$$\frac{de_a^*}{dT} = e_a^* \cdot \frac{17.67 \cdot 243.5}{(T_a + 243.5)^2} \quad (\text{A.4})$$

Similarly the temperature derivative of the specific humidity is given by

$$\frac{dq_a^*}{dT} = \left[\frac{0.622 \cdot p_a}{(p_a - 0.378 \cdot e_a^*)^2} \right] \frac{de_a^*}{dT} \quad (\text{A.5})$$

Calculation of air density from pressure and temperature

$$\rho_a = \frac{p_a}{R_d T K_a} \quad (\text{A.6})$$

Appendix B
NORTRIP model variables

Table B.1. Variables principally related the road dust emission sub-model.
 *Variable types are defined as prognostic (P), diagnostic (D), model input parameter (IP), site specific input metadata (IM) or site specific input time series (IT).

| Variable | Units | Variable type * | Description |
|--------------------------|---|-----------------|--|
| Δt | hr | IP | Model time step |
| M_{road}^m | g.km ⁻¹ or g.m ⁻² | P | Road surface mass (dust or salt) loading for the mass type m |
| $M_{road(total)}$ | g.km ⁻¹ or g.m ⁻² | D | Total road surface mass loading for all mass types |
| P_{road}^m | g.km ⁻¹ .hr ⁻¹ | D | Production of road surface dust or salt for the mass type m |
| S_{road}^m | g.km ⁻¹ .hr ⁻¹ | D | Sink (removal) of road surface dust or salt for the mass type m |
| $WR_{source}^{t,v}$ | g.km ⁻¹ .hr ⁻¹ | D | Wear rate for different tyre types (t), vehicle types (v) and wear sources ($source = roadwear, tyrewear, brakewear$) |
| $f_{0,dir-source}^{t,v}$ | 0 - 1 | IP | Fraction of wear that is directly emitted to the air and not retained on the surface |
| $f_{q,source}$ | 0 - 1 | D | Surface retainment factor based on the surface moisture. Wear and dust loading is retained on the surface when this has a value of zero. ($source = road-tyrewear, brakewear$ and $suspension$). |
| $N^{t,v}$ | veh.hr ⁻¹ | IT | Number of vehicles per hour with the specified tyre types (t) and vehicle type (v) |
| $W_{0,source}^{t,v}$ | g.km ⁻¹ .veh ⁻¹ | IP | Basis wear factor for different tyre types (t), vehicle types (v) and wear ($source = roadwear, tyrewear, brakewear$) |
| h_{pave}^p | | IM, IP | Pavement type factor, used to adjust the basic wear factor for road wear only ($W_{0,roadwear}^{t,v}$) |
| $h_{drivingcycle}^d$ | | IM, IP | Driving cycle factor, used to adjust the basic wear factor for brake wear only ($W_{0,brakewear}^{t,v}$) |
| V_{veh}^v | km.hr ⁻¹ | IT | Vehicle speed for the different vehicle types (v) |
| $V_{ref,sus}$ | km.hr ⁻¹ | IP | Reference vehicle speed at which the suspension factor ($f_{0,suspension}^{t,v}$) is valid |
| $V_{ref,sandpaper}$ | km.hr ⁻¹ | IP | Reference vehicle speed at which the sandpaper factor ($f_{0,sandpaper}^{t,v}$) is valid |

| | | | |
|--------------------------|---------------------|---------|--|
| $V_{ref,crushing}$ | km.hr ⁻¹ | IP | Reference vehicle speed at which the sand crushing factor ($f_{0,crushing}^{t,v}$) is valid |
| $V_{ref,roadwear}$ | km.hr ⁻¹ | IP | Reference vehicle speed for which the road wear parameter ($W_{0,roadwear}^{t,v}$) is valid |
| $V_{ref,tyrewear}$ | km.hr ⁻¹ | IP | Reference vehicle speed for which the reference PM fraction ($W_{0,tyrewear}^{t,v}$) is valid |
| $V_{ref,PM-fraction}$ | km.hr ⁻¹ | IP | Reference vehicle speed for which the reference PM fractions ($f_{PM,ref,dir-source}^{x,t}$ and $f_{PM,ref,sus-road}^{x,t}$) are valid |
| a^{wear} | - | IP | Power law index for the vehicle speed dependence of road and tyre wear. |
| a^{sus} | - | IP | Power law index for the vehicle speed dependence of road suspension. |
| w_{dep}^{TSP} | m.s ⁻¹ | IP | Dry deposition velocity for total suspended particles (TSP). |
| $PM_{TSP,background}$ | m.s ⁻¹ | IT | Background concentrations of total suspended particles (TSP). |
| $M_{sanding}$ | g.m ⁻² | P | Mass of sand applied to the road during a traction sanding event at time $t_{sanding}$ |
| b_{lane} | m | IM | Width of a single traffic lane on the road |
| n_{lanes} | | IM | Number of lanes on the road |
| $f_{sanding}^{sus}$ | 0 - 1 | IP | Fraction of traction sanding mass that is classified in the model as suspendable (< 200 µm) |
| $f_{0,sandpaper}^{t,v}$ | veh ⁻¹ | IP | Basis rate of abrasion per vehicle for the generation of suspendable dust through the sandpaper effect. |
| $f_{0,crushing}^{t,v}$ | veh ⁻¹ | IP | Basis rate of abrasion per vehicle for the generation of suspendable dust through the crushing. |
| $M_{salting}^{salt(i)}$ | g.m ⁻² | D or IT | Mass of salt applied to the road during a road salting event for salt type i |
| $t_{salting}$ | hr | D or IT | Timing of the salting event. Input or derived by salting rules |
| $f_{0,suspension}^{t,v}$ | veh ⁻¹ | IP | Basis rate of suspension per vehicle for the given tyre (t) and vehicle (v) type |
| $h_{0,suspension}^m$ | - | IP | Scaling factor to adjust the basic suspension rates for the different mass types m |
| h_{sus} | - | IM | Scaling factor to adjust the basic suspension rate that can be specified per site. Default is unity. |

| | | | |
|-------------------------------|---------------------|---------|--|
| FF_{thresh} | $m.s^{-1}$ | IP | Threshold wind speed for windblown suspension |
| τ_{wind} | hr | IP | Time scale for windblown suspension |
| $h_{drain-eff}^m$ | 0 - 1 | IP | Drainage efficiency factor for dust and salt |
| $h_{cleaning-eff}^m$ | 0 - 1 | IP | Efficiency factor for the removal of road mass type (m) by cleaning |
| $h_{ploughing-eff}^m$ | 0 - 1 | IP | Efficiency factor for the removal of road mass type (m) by snow ploughing |
| $t_{ploughing}$ | hr | D or IT | Timing of ploughing events. Input or derived by ploughing rules |
| $t_{cleaning}$ | hr | IT | Timing of cleaning events |
| $t_{sanding}$ | hr | D or IT | Timing of sanding events. Input or derived by sanding rules |
| $h_{spray-eff}^m$ | 0 - 1 | IP | Efficiency factor for the removal of road mass type (m) by spray processes |
| E^x | $g.km^{-1}.hr^{-1}$ | D | Total non-exhaust emissions in the size fraction x |
| $E_{dir-source}^x$ | $g.km^{-1}.hr^{-1}$ | D | Total non-exhaust direct wear emissions in the size fraction x ($source = roadwear, tyrewear, brakewear$) |
| $E_{suspension}^x$ | $g.km^{-1}.hr^{-1}$ | D | Total non-exhaust suspended emissions in the size fraction x |
| $E_{sus-road}^x$ | $g.km^{-1}.hr^{-1}$ | D | Total non-exhaust traffic induced suspension emissions in the size fraction x |
| $E_{wind-road}^x$ | $g.km^{-1}.hr^{-1}$ | D | Total non-exhaust windblown emissions in the size fraction x |
| $f_{PM,ref,dir-source}^{x,t}$ | 0 - 1 | IP | Reference value for the proportion of the direct wear mass in the size fraction x . |
| $f_{PM,ref,sus-road}^{x,t}$ | 0 - 1 | IP | Reference value for the proportion of the suspended mass in the size fraction x . |
| $C_{PM-fraction}^x$ | $(km.hr^{-1})^{-1}$ | IP | Slope of the vehicle speed dependence for the proportion of the suspended mass in the size fraction x . |
| $FF(z)$ | $m.s^{-1}$ | IT | Wind speed as height z . |
| $S_{roadweathresh}$ | mm | IP | Snow/ice depth threshold value above which road and tyre wear does not occur |
| $S_{drain-limit}$ | mm | IP | Snow/ice depth limit value above which dust is not drained from the road |
| m | | | Index for dust types used in the model. Suspendable dust from wear $dust(sus)$, suspendable sand $dust(sus-sand)$, non-suspendable sand $dust(non-sus)$ and the two salt types $salt(na)$ and $salt(mg)$. |

| | |
|-----|---|
| t | Index for tyre types: Studded (st), winter non-studded (wi) and summer (su) |
| v | Index for vehicle types: Light (li) and heavy (li) |

*Table B.2. Variables principally related the road moisture sub-model. *Variable types are defined as prognostic (P), diagnostic (D), model input parameter (IP), site specific input metadata (IM) or site specific input time series (IT).*

| Variable | Units | Variable type * | Description |
|--------------------------|---------------------|------------------------|--|
| g_{road} | mm | P | Water mass on the road surface |
| S_{road} | mm w.e. | P | Snow/ice mass on the road surface. Units for ice/snow are in mm w.e. (water equivalent) |
| $g_{road,drainable}$ | mm | D | Amount of water that may be drained from the road |
| $g_{road,drainable-min}$ | mm | IP | Non-drainable road water mass |
| P_g | mm.hr ⁻¹ | D | Production rate of liquid water on the road surface |
| P_s | mm.hr ⁻¹ | D | Production rate of frozen water (ice/snow) on the road surface. |
| S_g | mm.hr ⁻¹ | D | Sink rate of liquid water on the road surface |
| S_s | mm.hr ⁻¹ | D | Sink rate of frozen water (ice/snow) on the road surface. |
| $Rain$ | mm | IT | Amount of liquid precipitation within the model time step Δt |
| $Snow$ | mm w.e. | IT | Amount of solid precipitation within the model time step Δt |
| $g_{road-wetting}$ | mm | IT or D | Amount of water applied when wet salting/sanding or during cleaning. |
| $t_{wetting}$ | hr | IT or D | Timing of the wetting event. Input or derived by salting rules |
| $g_{road,sprayable-min}$ | mm | IP | Minimum surface moisture level for spray to occur |
| $R_{g,spray}$ | hr ⁻¹ | D | Rate of road water removal by spray processes |
| $f_{0,spray}^v$ | veh ⁻¹ | IP | Basic factor defining the proportion of surface moisture removed with the passage of one vehicle due to spray processes at the reference speed |

| | | | | |
|----------------------------|---------------------|---------|---|--|
| | | | $V_{ref,spray}$ | |
| $V_{ref,sprasy}$ | km.hr ⁻¹ | IP | Reference vehicle speed at which $f_{0,spray}^v$ is valid | |
| $h_{ploughing-eff}^{snow}$ | 0 - 1 | IP | Efficiency factor for removal of snow due to snow ploughing | |
| T_{melt} | °C | D | Melt/freezing temperature of the surface moisture | |
| T_a | °C | IT | Atmospheric temperature, usually at 2 m. | |
| TK_a | K | IT | Atmospheric temperature in Kelvin, usually at 2 m. | |
| T_s | °C | P | Road surface temperature | |
| TK_s | K | P | Road surface temperature in Kelvin | |
| G_s | W.m ⁻² | D | Surface energy flux | |
| G_{sub} | W.m ⁻² | D | Sub-surface energy flux | |
| $R_{net,s}$ | W.m ⁻² | IT or D | Surface net radiation flux | |
| RS_{in} | W.m ⁻² | IT | Incoming short wave radiation | |
| α_{road} | 0 - 1 | IM | Road surface albedo | |
| α_{snow} | 0 - 1 | IP | Road surface snow albedo | |
| RL_{in} | W.m ⁻² | D | Incoming long wave radiation | |
| RL_{out} | W.m ⁻² | D | Outgoing long wave radiation | |
| H_s | W.m ⁻² | D | Surface sensible heat flux | |
| L_s | W.m ⁻² | D | Surface latent heat flux | |
| $H_{traffic}$ | W.m ⁻² | D | Traffic heat flux to the surface | |
| $RS_{in,0}$ | W.m ⁻² | D | Short wave radiation at the top of the atmosphere | |
| $RS_{in,obs}$ | W.m ⁻² | IT | Observed short wave radiation | |
| $RS_{clear,s}$ | W.m ⁻² | D | Clear sky short wave radiation | |
| τ_{clear} | 0 - 1 | D | Clear sky radiation attenuation factor | |
| τ_{cloud} | 0 - 1 | D | Cloudy sky radiation attenuation factor | |
| n_c | 0 - 1 | D or IT | Cloud cover fraction | |
| $f_{road-shadow}$ | 0 - 1 | D | Fraction of the road surface in shadow due to street canyon walls | |
| $\tau_{diffuse}$ | 0 - 1 | IP | Fraction of clear sky global radiation that is diffuse | |
| $RS_{in,road-shadow}$ | W.m ⁻² | D | Average short wave radiation on the road surface accounting for shadowing | |

| | | | |
|--------------------------------|------------|----|--|
| $RS_{in,diffuse}$ | $W.m^{-2}$ | D | Clear sky global radiation that is diffuse |
| $RS_{in,direct}$ | $W.m^{-2}$ | D | Clear sky global radiation that is direct (non-diffuse) |
| ϵ_{eff} | 0 - 1 | D | Effective long wave emissivity of the atmosphere |
| ϵ_{cs} | 0 - 1 | D | Clear sky long wave emissivity of the atmosphere |
| ϵ_{cl} | 0 - 1 | IP | Cloudy sky long wave emissivity of the atmosphere |
| ϵ_s | 0 - 1 | IP | Long wave emissivity of the surface |
| $f_{RL,canyon}$ | 0 - 1 | D | Fraction of sky area covered by the street canyon facade |
| b_{road} | m | IM | Total width of the road, from kerb to kerb |
| b_{canyon} | m | IM | Width of the street canyon |
| h_{canyon} | m | IM | Height of the street canyon. Two values, one for north and one for south. |
| TK_{facade} | K | D | Street canyon facade temperature in Kelvin |
| e_w, e_a^* | Pa | D | Water vapour partial and saturated* pressure in the atmosphere. |
| e_s, e_s^* | Pa | D | Water vapour partial and saturated* pressure on the surface. |
| e_{salt}, e_{salt}^* | Pa | D | Water vapour partial and saturated* pressure on the surface for a salt solution. |
| e_{ice} | Pa | D | Vapour pressure for water and ice. |
| q_w, q_a^* | | D | Water vapour specific humidity and saturated* specific humidity in the atmosphere. |
| q_s, q_s^* | | D | Water vapour specific humidity and saturated* specific humidity on the surface. |
| RH_w, RH_s and $RH_{s,salt}$ | | D | Relative humidity of the atmosphere, on the surface and of the salt solution on the surface. |
| $r^{traffic}$ and r^{wind} | $s.m^{-1}$ | D | Aerodynamic resistance for traffic induced turbulence and wind shear induced turbulence |
| r_T and r_q | $s.m^{-1}$ | D | Aerodynamic resistance for temperature and water vapour |
| $z_0, z_T,$ and z_q | m | IP | Roughness lengths for momentum, |

| | | | |
|--------------------------------|--------------------------------------|---------|---|
| | | | temperature and water vapour |
| $a_{traffic}^v$ | s.veh ⁻¹ | IP | Aerodynamic traffic coefficient |
| l_{veh}^v | m | IP | Length of vehicle type v |
| H_{veh}^v | W.m ⁻² .veh ⁻¹ | IP | Surface heat flux from vehicle type v |
| $g_{road, evap-thresh}$ | mm | IP | Threshold value for surface moisture below which evaporation is reduced by reduction of relative humidity |
| p_a | Pa | IM | Atmospheric pressure |
| ρ_a | kg.m ⁻³ | D | Atmospheric density |
| ρ_s | kg.m ⁻³ | IP | Road surface density |
| c_s | J.kg ⁻¹ .K ⁻¹ | IP | Road surface specific heat |
| k_s | W.m ⁻¹ .K ⁻¹ | IP | Road surface thermal conductivity |
| Δz_s | m | D or IP | Sub-surface layer slab depth |
| $evap_{road}$ | kg.m ⁻² .hr ⁻¹ | D | Evaporation/condensation rate from/to the road surface |
| $N_{moles, salt/water}$ | mol.m ⁻² | D | Moles of salt/water on the road surface |
| $Solution_{salt}$ | | D | Molar fraction of salt solution on the road surface |
| $Saturated_{salt}$ | | IP | Molar fraction of saturated salt solution |
| $g_{retention-thresh, source}$ | mm | IP | Threshold value defining the upper limit for retention, above which full surface retention is achieved |
| $g_{retention-min, source}$ | mm | IP | Threshold value defining the lower limit for retention, below which no surface retention is achieved |

Appendix C

NORTRIP model parameters and input data requirements

The following input data is provided in two Excel sheets for the model.

Model parameter file: This includes all the model parameters, model control flags and the parameters for the salting and sanding model. This file is intended to be generic and not specific to any one site, though the salting and sanding model parameters may be site specific. Also included in this file is a calculator for the road wear, based on the Swedish road wear model.

Input data file: This contains all the site specific meta- and temporal data for running the model for a specific site.

C.1 Default set of model parameters

ROAD DUST SUB-MODEL PARAMETERS

Road wear

| $W_{0,roadwear}$ (g km ⁻¹ veh ⁻¹) | Studded tyres (<i>st</i>) | Winter tyres (<i>wi</i>) | Summer tyres (<i>su</i>) |
|--|-----------------------------|--|----------------------------|
| Heavy (<i>he</i>) | 28.8 | 1.5 | 1.5 |
| Light (<i>li</i>) | 2.88 | 0.15 | 0.15 |
| Reference speed $V_{ref,roadwear}$ (km/hr) | 70 | Set to 0 if no speed dependence required | |
| Power law factor for road wear a_{wear} | 1 | | |

Tyre wear

| $W_{0,tyrewear}$ (g km ⁻¹ veh ⁻¹) | Studded tyres (<i>st</i>) | Winter tyres (<i>wi</i>) | Summer tyres (<i>su</i>) |
|--|-----------------------------|----------------------------|----------------------------|
| Heavy (<i>he</i>) | 0.5 | 0.5 | 0.5 |
| Light (<i>li</i>) | 0.1 | 0.1 | 0.1 |
| Reference speed $V_{ref,tyrewear}$ (km/hr) | 70 | | |

Brake wear

| $W_{0,brakewear}$ (g km ⁻¹ veh ⁻¹) | Studded tyres (<i>st</i>) | Winter tyres (<i>wi</i>) | Summer tyres (<i>su</i>) |
|---|-----------------------------|----------------------------|----------------------------|
| Heavy (<i>he</i>) | 0.05 | 0.05 | 0.05 |
| Light (<i>li</i>) | 0.01 | 0.01 | 0.01 |
| Reference speed $V_{ref,brakewear}$ (km/hr) | 70 | | |

Snow depth wear threshold

| Parameter | Value |
|---------------------------------|-------|
| $S_{roadwear,thresh}$ (mm w.e.) | 3 |

Pavement type scaling factor

| Number of pavement types | 7 | |
|--------------------------|-----------------|---------------|
| Index(<i>p</i>) | Name | $h_{pave}(p)$ |
| 1 | Hornsgatan | 0.83 |
| 2 | Mannerheimintie | 1.7 |
| 3 | Essingeleden | 0.83 |
| 4 | RV4 | 1.32 |
| 5 | NBS | 0.83 |
| 6 | HCAB | 4.12 |

| | | |
|---|----------|------|
| 7 | Runeberg | 0.83 |
|---|----------|------|

Driving cycle scaling factor

| | | |
|-------------------------------|-----------|-----------------------|
| Number of driving cycle types | 4 | |
| Index(<i>d</i>) | Name | $h_{drivingcycle}(d)$ |
| 1 | Reference | 1 |
| 2 | Urban | 1.5 |
| 3 | Highway | 0.5 |
| 4 | Congested | 2 |

Road suspension

| | | | |
|---|-----------------------------|--|----------------------------|
| $f_{0,suspension}(veh^{-1})$ | Studded tyres (<i>st</i>) | Winter tyres (<i>wi</i>) | Summer tyres (<i>su</i>) |
| Heavy (<i>he</i>) | 2.00E-05 | 2.00E-05 | 2.00E-05 |
| Light (<i>li</i>) | 2.00E-06 | 2.00E-06 | 2.00E-06 |
| Reference speed $V_{ref,sus}$ (km/hr) | 50 | Set to 0 if no speed dependence required | |
| Power law factor for suspension a_{sus} | 1 | | |

Suspension scaling factors for sand and salt

| | |
|------------------|-----|
| $h_{0,sand}$ | 100 |
| $h_{0,sus-sand}$ | 1 |
| $h_{0,salt}$ | 1 |

Sand paper factor

| | | | |
|---|-----------------------------|----------------------------|----------------------------|
| $f_{sandpaper}(veh^{-1})$ | Studded tyres (<i>st</i>) | Winter tyres (<i>wi</i>) | Summer tyres (<i>su</i>) |
| Heavy (<i>he</i>) | 1.00E-05 | 1.00E-05 | 1.00E-05 |
| Light (<i>li</i>) | 1.00E-06 | 1.00E-06 | 1.00E-06 |
| Reference speed $V_{ref,sandpaper}$ (km/hr) | 60 | | |

Crushing factor

| | | | |
|--|-----------------------------|----------------------------|----------------------------|
| $f_{0,crushing}(veh^{-1})$ | Studded tyres (<i>st</i>) | Winter tyres (<i>wi</i>) | Summer tyres (<i>su</i>) |
| Heavy (<i>he</i>) | 5.00E-05 | 5.00E-05 | 5.00E-05 |
| Light (<i>li</i>) | 5.00E-06 | 5.00E-06 | 5.00E-06 |
| Reference speed $V_{ref,crushing}$ (km/hr) | 60 | | |

Suspendable fraction for sanding

| | |
|-------------------|-------|
| Parameter | Value |
| $f_{sus-sanding}$ | 0.01 |

Direct emission factor

| | |
|-----------------------|-----------|
| Wear parameter | All types |
| $f_{0,dir-roadwear}$ | 1 |
| $f_{0,dir-tirewear}$ | 1 |
| $f_{0,dir-brakewear}$ | 1 |
| $f_{0,dir-crushing}$ | 1 |
| $f_{0,dir-sandpaper}$ | 1 |

Fractional size distribution emissions (no tyre or vehicle dependence)

| | | | |
|----------------|-------------------|------------------|-------------------|
| Wear parameter | PM _{TSP} | PM ₁₀ | PM _{2.5} |
|----------------|-------------------|------------------|-------------------|

| | | | |
|---|-------|--|-------|
| $f_{PM,ref,roadwear}$ | 0.5 | 0.18 | 0.008 |
| $f_{PM,dir,tirewear}$ | 0.5 | 0.1 | 0.01 |
| $f_{PM,dir,brakewear}$ | 1 | 0.8 | 0.5 |
| $f_{PM,ref,sus-road}$ | 0.5 | 0.18 | 0.008 |
| Reference speed $V_{ref,PM-fraction}$ (km/hr) | 50 | Set to 0 if no speed dependence required | |
| $c_{PM-fraction}$ (km/hr) ⁻¹ | 0.012 | | |

Wind blown dust emission factors

| Parameter | Value |
|---------------------|-------|
| τ_{wind} (hr) | 12 |
| FF_{thresh} (m/s) | 10 |

Activity efficiency factors for dust and salt

| Efficiency parameter | Suspendable dust | Non-suspendable dust | Salt |
|----------------------|------------------|----------------------|------|
| $h_{ploughing-eff}$ | 0.001 | 0.01 | 0.01 |
| $h_{cleaning-eff}$ | 0.1 | 0.3 | 0.2 |
| $h_{drainage-eff}$ | 0.0001 | 0.001 | 0.3 |
| $h_{spraying-eff}$ | 0.0001 | 0.001 | 0.3 |

Deposition velocity

| | PM _{TSP} | PM ₁₀ | PM _{2.5} |
|-------------|-------------------|------------------|-------------------|
| w_x (m/s) | 0.003 | 0.001 | 0.0005 |

Concentration conversion limit values

| Parameter | Value |
|---|-------|
| $NO_x,concentration-min$ ($\mu\text{g}/\text{m}^3$) | 5 |
| $NO_x,emission-min$ (g/km/hr) | 50 |

MOISTURE SUB-MODEL PARAMETERS

Spray and splash factors

| Parameter | Heavy (he) | Light (li) |
|------------------------------------|------------|------------|
| $f_{0,spray}$ (veh ⁻¹) | 6.00E-04 | 1.00E-04 |
| $V_{ref,spray}$ (km/hr) | 70 | |
| $g_{road,sprayable-min}$ (mm) | 0.1 | |

Drainage parameters

| Parameter | Value |
|----------------------------|-------|
| $g_{drainable}$ (mm) | 0.6 |
| Snow retainment limit (mm) | 5 |

Ploughing parameters

| Parameter | Value |
|---------------------------------------|-------|
| Ploughing efficiency for snow removal | 0.8 |
| Ploughing threshold (mm) | 2 |

Energy balance parameters

| Parameter | Value |
|-----------|-------|
|-----------|-------|

| | | | |
|--|-------------------------------|--|---------------|
| $g_{road, evap-thresh}$ (mm) | 0.02 | Road albedo defined in local metadata Automatically defined when set to 0 | |
| Roughness length (mm) | 2 | | |
| Snow albedo | 0.6 | | |
| Subsurface slab depth (m) | 0 | | |
| Subsurface parameters | ρ_s (kg/m ³) | c_s (J/kg/K) | k_s (W/m/K) |
| | 2400 | 800 | 2 |
| Traffic turbulent exchange and heat flux | Heavy (he) | Light (li) | |
| $a_{traffic}$ (veh ⁻¹) | 1.00E-02 | 1.00E-03 | |
| H_{veh} (W m ⁻² veh ⁻¹) | 1.50E+02 | 5.00E+01 | |

Retention parameters

| Parameter | Road | Brake |
|-----------------------------|------|-------|
| $g_{retention-thresh}$ (mm) | 0.1 | 1 |
| $g_{retention-min}$ (mm) | 0.04 | 0.7 |

Included in the input excel sheet is also the possibility to calculate road wear, based on the Swedish road wear model. An example is provide below.

| ROAD WEAR MODEL INPUT | | | | OUTPUT ($W_0=2.88$, $V_{ref}=70$) | OUTPUT | OUTPUT |
|-------------------------|------------|----------------|-------|--------------------------------------|-----------------|---------------|
| NBM | Stone size | Stone % > 4 mm | Speed | h_{pave} | ROAD WEAR W_0 | PM10 fraction |
| 5.00 | 16.00 | 75.00 | 70.00 | 0.83 | 2.40 | 7.7 |
| Recommended wear values | | | | h_{pave} | | |
| 2.40 | 0.13 | 0.13 | 0.83 | | | |

C.2 Control flags for model processes

The following table is used in the model to activate the various model processes.

| DUST | 0 | Keep this line and number here |
|----------------------|---|--|
| road_wear_flag | 1 | Allows road wear |
| tyre_wear_flag | 1 | Allows tyre wear |
| brake_wear_flag | 1 | Allows brake wear |
| road_suspension_flag | 1 | Allow road suspension |
| dust_drainage_flag | 1 | Allows dust and salt to be drained from the road |
| dust_spray_flag | 1 | Allows dust and salt to be sprayed from the road |
| dust_ploughing_flag | 1 | Allows dust and salt to be ploughed from the road |
| sandpaper_flag | 0 | Allows the sand paper effect |
| crushing_flag | 0 | Allows crushing of non-suspendable sand to suspendable sand to occur |
| dust_deposition_flag | 0 | Allows deposition of background PM |
| wind_suspension_flag | 0 | Allows wind blown dust suspension |
| MOISTURE | | |
| retention_flag | 1 | Allows retention of particles due to surface wetness. 1 is linear, 2 is exponential, 0 is none |

| | | |
|-------------------------|---|---|
| use_obs_retention_flag | 1 | Uses the observed moisture to determine the surface retention, if available |
| water_spray_flag | 1 | Allows spray from the road surface. Must be 1 for dust and salt to be sprayed |
| surface_humidity_flag | 1 | Sets the method for describing the surface humidity. 1 is linear, 2 is exponential |
| use_salt_humidity_flag | 1 | Allows road salt concentrations to influence the surface humidity and melt temperature |
| ENERGY BALANCE | | |
| evaporation_flag | 2 | 1 = Penman modified, 2 = energy balance with ice and sub-surface |
| canyon_shadow_flag | 1 | Use the street canyon dimensions to shadow the road |
| canyon_long_rad_flag | 1 | Use the street canyon dimensions to produce long wave radiation |
| use_subsurface_flag | 1 | Use the underlying subsurface in the energy balance calculations |
| ACTIVITY | | |
| use_salting_data_flag | 1 | Allows salting, either from the input data or by rule |
| use_sanding_data_flag | 1 | Allows sanding, either from the input data or by rule |
| use_ploughing_data_flag | 1 | Allows ploughing, either from the input data or by rule |
| use_wetting_data_flag | 1 | Allows wetting to occur, either from the input data or by rule |
| use_cleaning_data_flag | 0 | Allows cleaning, either from the input data or by rule |
| auto_salting_flag | 0 | Allows salting by rule (over rides the input data values) |
| auto_sanding_flag | 0 | Allows sanding by rule (over rides the input data values) |
| auto_ploughing_flag | 1 | Allows ploughing by rule (over rides the input data values) |
| OUTPUT | | |
| plot_type_flag | 2 | 1 = hourly means, 2 = daily means, 3 = daily cycle, 4 = 1/2 daily means , 5 = weekday means |
| save_type_flag | 0 | 1 = save data, 2 = save plots, 3 = save both, 0 = none |

C.3 Input data for the sand and salt model

The following rule table is used for the application of salt and sand.

| Salting | Value | Comment |
|-------------------------------|-------|--|
| salting_hour(1) (hour) | 5 | First time of day when salting can occur |
| salting_hour(2) (hour) | 20 | Second time of day when salting can occur |
| delay_salting_day (day) | 0.2 | Minimum allowable time between saltings events in days |
| check_salting_day (day) | 0.5 | Time window checked ahead (temperature, RH) and behind (precip) |
| min_temp_salt (C) | -6 | Minimum temperature for salting in the forward time window |
| max_temp_salt (C) | 0 | Maximum temperature for salting in the forward time window |
| precip_rule_salt (mm/hr) | 0.1 | Salt if precipitation occurs above this level in the forward and behind time window or RH_rule |
| RH_rule_salt (%) | 95 | Salt if the relative humidity is above this level in the forward time window or precip rule |
| g_salting_rule (mm) | 0.1 | Dry salt if the surface moisture is above this value at time of salting |
| salt_mass (g/m ²) | 20 | Salt applied at each application |
| salt_dilution | 0.2 | Salt solution, if 0 then always dry salting |
| salt_type | 1 | $M(\text{salt}) = M(\text{NaCl}) * \text{salt_type} + M(\text{MgCl}_2) * (1 - \text{salt_type})$ |

| Sanding | Value | Comment |
|------------------------|-------|---|
| sanding_hour(1) (hour) | 5 | First time of day when sanding can occur |
| sanding_hour(2) (hour) | 5 | Second time of day when sanding can occur |

| | | |
|--------------------------|-----|--|
| delay_sanding_day (day) | 0.9 | Minimum allowable time between sanding events in days |
| check_sanding_day (day) | 0.5 | Time window checked ahead (temperature, RH) and behind (precip) |
| min_temp_sand (C) | -12 | Minimum temperature for sanding in the forward time window |
| max_temp_sand (C) | -4 | Maximum temperature for sanding in the forward time window |
| precip_rule_sand (mm/hr) | 0.1 | Sand if precipitation occurs above this level in the forward and behind time window or RH_rule |
| RH_rule_sand(%) | 95 | Sand if the relative humidity is above this level in the forward time window or precip_rule |
| g_sanding_rule (mm) | 0.1 | Dry sand if the surface moisture is above this value at time of sanding |
| sand_mass (g/m2) | 250 | Sand applied at each application |
| sand_dilution | 0 | Sand in solution, if 0 then always dry sanding |

C.4 Dataset input

The following input data is required to run the model for any particular street. It consists of

- **Metadata** describing the street configuration and other street specific parameters (static)
- **Initial conditions** for the model (static)
- **Traffic** data regarding traffic volume, category and tyre type (temporal)
- **Meteorological** data required for the model (temporal)
- **Activity** data concerning road maintenance (temporal)
- **Air quality** data for direct comparison with observations (temporal)

C.4.1 Metadata

The following data is used by the model. Many are optional and can be excluded from the list. Non-optional parameters are given in bold and do not have a default value. The 'key word' is searched for and the value provided is allocated (if found). The parameters can be placed in any order in the excel sheet.

| Key word | Example value | Default value | Comments |
|--|---------------|---------------|---|
| Driving cycle index (d) | 1 | 1 | Specifies the lookup for driving cycle index in the parameter table |
| Pavement type index (p) | 1 | 1 | Specifies the lookup for pavement type index in the parameter table |
| Number of lanes | 4 | 2 | Needed to calculate road surface area and to distribute traffic |
| Width of lane (m) | 3.5 | 3.5 | Combined with the number of lanes specifies the surface area of the road |
| Road width (b_road) (m) | 12 | - | Width of the road from one side to the other. Used for radiation calculations |
| Street canyon width (m) | 23 | b_road | |
| Street canyon height (m) | 25 | 0 | Same on both sides of the canyon |
| Street canyon height north (m) | 25 | h_canyon | Optional if street canyon facade is different on each side of the canyon |
| Street canyon height south (m) | 2 | h_canyon | Optional if street canyon facade is different on each side of the canyon |
| Street orientation (degrees) | 76 | 0 | Clockwise from North (0 – 180) |
| Latitude (decimal degrees) | 59.17 | - | Used in radiation calculations |
| Longitude (decimal degrees) | 18.3 | - | Used in radiation calculations |
| Elevation (m) | 0 | 0 | Used for radiation calculations |
| Height obs wind (m) | 20 | - | Height of the wind speed measurements |
| Height obs temperature and RH (m) | 2 | - | Height of temperature and humidity measurements. Assumed to be the same |

| | | | |
|------------------------------------|-----------|------|---|
| Surface albedo (0-1) | 0.3 | 0.3 | Albedo of the road surface |
| Time difference (UTC) (hr) | -1 | - | Decreasing westward |
| Surface pressure (mbar) | 1000 | 1000 | Used in radiation calculations |
| Missing data value | -9900 | -99 | Indicates missing data in the input data |
| Wind speed correction factor (0-1) | 1 | 1 | Scales wind speed by this factor. Can be used to represent lower wind speeds in street canyons |
| Observed moisture cut off | 2 | 2 | Cut off value for observed moisture wet/dry in mV. 0 uses automatic value = half way between max and min |
| Suspension rate scaling factor | 1 | 1 | Site specific scaling of suspension scaling factor (h_{sus}). Can be used for sensitivity runs or for specifying site specific suspension factors |

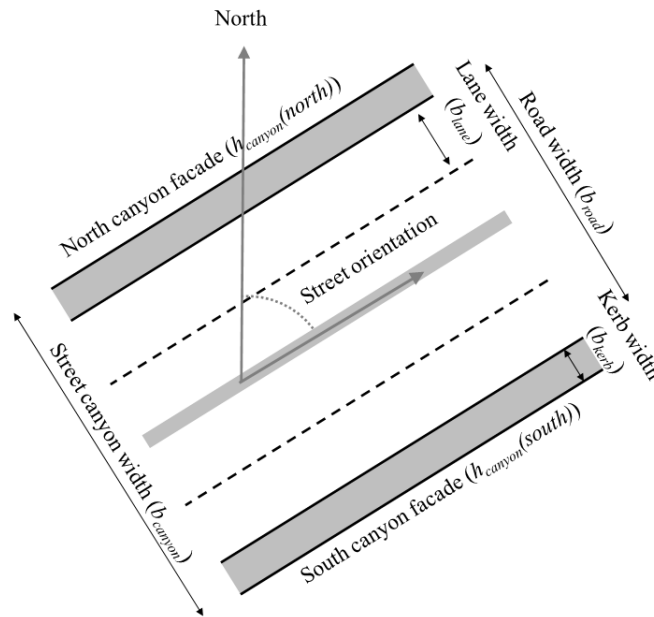


Figure C.1 Road configuration parameters used in defining the street metadata. In this case there are 4 lanes.

C.4.2 Initial conditions

The following are a list of initial conditions and offsets that can be used to assess model sensitivity. All of these parameters are optional.

| Key word | Example value | Default value | Comments |
|--|---------------|---------------|--|
| M_dust_road (g/km) | 1.20E+05 | 0 | Initial suspendable dust loading |
| M_salt_road(na) (g/km) | 0 | 0 | Initial NaCl salt loading |
| M_salt_road(mg) (g/km) | 0 | 0 | Initial MgCl2 salt loading |
| g_road (mm) | 0.1 | 0 | Initial surface wetness |
| s_road (mm) | 0.1 | 0 | Initial surface ice depth |
| long_rad_in_offset (W/m ²) | 0 | 0 | Offset for incoming long wave radiation |
| RH_offset (%) | 0 | 0 | Offset for Relative humidity |
| T_a_offset (degrees C) | 0 | 0 | Offset for air temperature |
| P_sand_fugitive (g/km/hr) | 0 | 0 | Continuous fugitive rate of sand application |
| P_sus_fugitive (g/km/hr) | 0 | 0 | Continuous fugitive rate of suspended dust application |

C.4.3 Traffic data

The following is a list of required traffic data. This is arranged in columns with each hour of data placed per row. Columns of data can be placed in any order but all columns must be present and all rows must contain data! It is the traffic data date stamps that are used in the model. No gap filling is employed in the traffic data.

| Key word | Comments |
|-------------------|--|
| Year | |
| Month | |
| Day | |
| Hour | |
| N(total) | Total traffic volume |
| N(he) | Total heavy duty vehicle traffic volume |
| N(li) | Total light duty vehicle traffic volume |
| N(st,he) | Studded tyre heavy duty vehicle traffic volume |
| N(st,li) | Studded tyre light duty vehicle traffic volume |
| N(wi,he) | Winter friction tyre heavy duty vehicle traffic volume |
| N(wi,li) | Winter friction tyre light duty vehicle traffic volume |
| N(su,he) | Summer tyre heavy duty vehicle traffic volume |
| N(su,li) | Summer tyre light duty vehicle traffic volume |
| V_veh(he) (km/hr) | Heavy duty vehicle speed |
| V_veh(li) (km/hr) | Light duty vehicle speed |

C.4.4 Meteorological data

The following is a list of required meteorological data. This is arranged in columns with each hour of data placed per row. Columns of data can be placed in any order but all columns must be present and all rows must contain data! Gap filling is employed in the meteorological data where the next valid measurement is used to fill in previous missing data.

| Key word | Comments |
|--------------------------------------|---|
| Year | |
| Month | |
| Day | |
| Hour | |
| T2m (deg C) | Atmospheric temperature |
| FF (m/s) | Wind speed |
| RH (%) | Relative humidity |
| Rain (mm/hr) | Liquid precipitation |
| Snow (mm/hr) | Solid precipitation |
| Global radiation (W/m ²) | Incoming global radiation |
| Cloud cover (fraction) | If not available then is calculated from the global radiation |
| Road wetness (mV) | Measurement of road wetness. Units of mV for conductivity measurements, units of mm for film thickness. Need to specify the units. Optional column. |
| Road surface temperature (deg C) | Measured road surface temperature. Optional column |

C.4.5 Activity data

The following is a list of required road maintenance activity data. This is arranged in columns with each hour of data placed per row. Columns of data can be placed in any order but all columns must be present and all rows must contain data! No gap filling is employed in the activity data and only the wetting is optional. If no activities occur this should be filled with 0's.

| Key word | Comments |
|-----------------------------------|---|
| Year | |
| Month | |
| Day | |
| Hour | |
| M_sanding (g/m ²) | Total mass of sanding |
| M_salting(na) (g/m ²) | Total mass of NaCl salting |
| M_salting(mg) (g/m ²) | Total mass of MgCl ₂ salting |
| Ploughing_road (0/1) | Flag if snow ploughing occurs on the hour |
| Cleaning_road (0/1) | Flag if road cleaning occurs on the hour |
| Wetting (mm) | mm of water applied during wetting, e.g. salt solution or wet cleaning. Input is optional |

C.4.6 Air quality data

The following is a list of required air quality data if the model is to be compared with observations. This is arranged in columns with each hour of data placed per row. Columns of data can be placed in any order but all columns must be present and all rows must contain data! No gap filling is employed in the air quality data and only the exhaust and NO_x emissions are optional. The model uses the NO_x concentrations and NO_x emissions to calculate the conversion of emissions to concentrations. If a dispersion model has been employed then the output of NO_x (or any other tracer for that matter) can be put here instead of observations

| Key word | Comments |
|--------------------------------------|--|
| Year | |
| Month | |
| Day | |
| Hour | |
| PM10_obs(ug/m ³) | Traffic station observations of PM10. Fill with missing data value if not available |
| PM10_background (ug/m ³) | Background station observations of PM10. Fill with missing data value if not available |
| PM25_obs (ug/m ³) | Traffic station observations of PM2.5. Fill with missing data value if not available |
| PM25_background (ug/m ³) | Background station observations of PM2.5. Fill with missing data value if not available |
| NOX_obs (ug/m ³) | Traffic station observations of NO _x . Fill with missing data value if not available |
| NOX_background (ug/m ³) | Background station observations of NO _x . Fill with missing data value if not available |
| NOX_emis (g/km/hr) | NO _x emissions. This is optional |
| EP_emis (g/km/hr) | Exhaust emissions. This is optional. |

Appendix D

Graphical summary presentation of model results

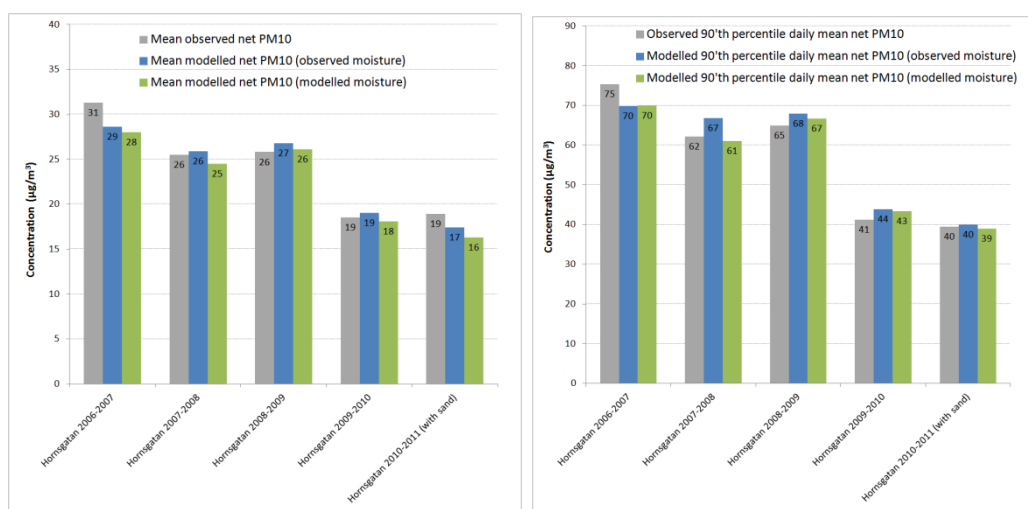
For each dataset a summary graphical presentation of the modelling results is given. In some cases two summary graphs are provided, e.g. when observed surface moisture is available both the modelled and the observed moisture have been used and the results are shown. In each graphical representation the following information is provided:

- Time series plot of net observed and modelled daily mean PM₁₀ concentrations. Included in the plot is the contribution from salt, from dust, from sand and the total modelled concentrations including the exhaust particulates (EP).
- Time series plot of the daily mean suspendable surface mass balance including dust, suspendable sand and salt loadings.
- Scatter plot of the net observed and the total modelled daily mean PM₁₀ concentrations.
- Bar chart showing the mean PM₁₀ emission factors for direct, suspended and exhaust emissions (based on hourly data).
- Bar chart showing the net mean contribution of the different sources (road wear, tyre wear, brake wear, sand, salt and exhaust) to the modelled PM₁₀ concentrations. Also includes the observed mean concentration.

In all cases, comparative statistics of the model with observations is only carried out for hours when both observed and modelled concentrations are. Daily means are calculated when more than 6 hours of data are available for that day.

D.1 Hornsgatan, Stockholm

Surface moisture measurements are available for Hornsgatan and results are shown when using both modelled and observed moisture for the surface retention. The results for all five years are summarized in Figure D.1 in order to compare the model results when using observed surface moisture.



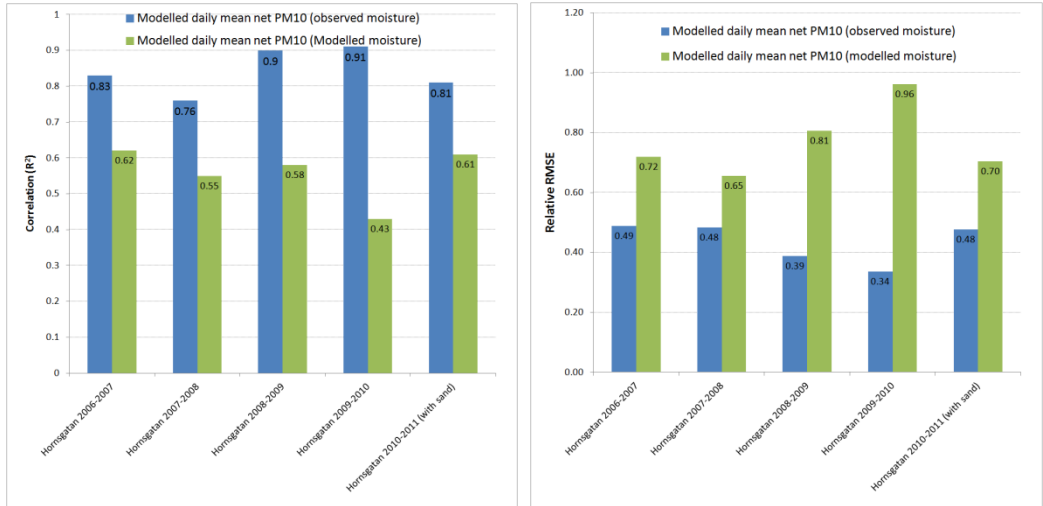
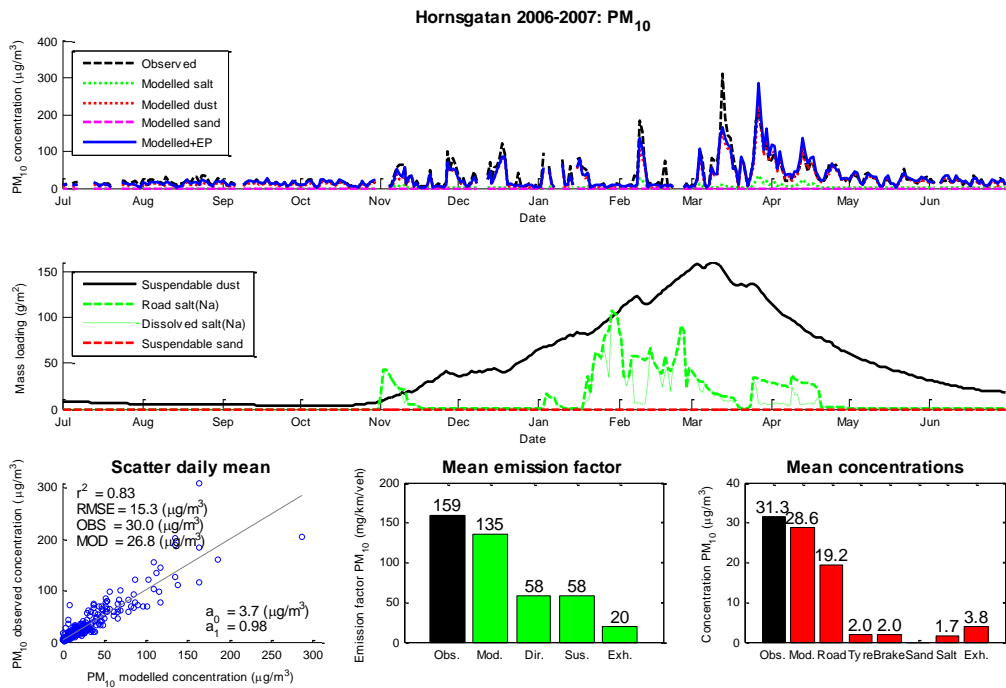


Figure D.1. Model results for Hornsgatan for all years where model results are compared to observations (grey bars) when using observed surface moisture (blue bars) and using the moisture model (green bars).



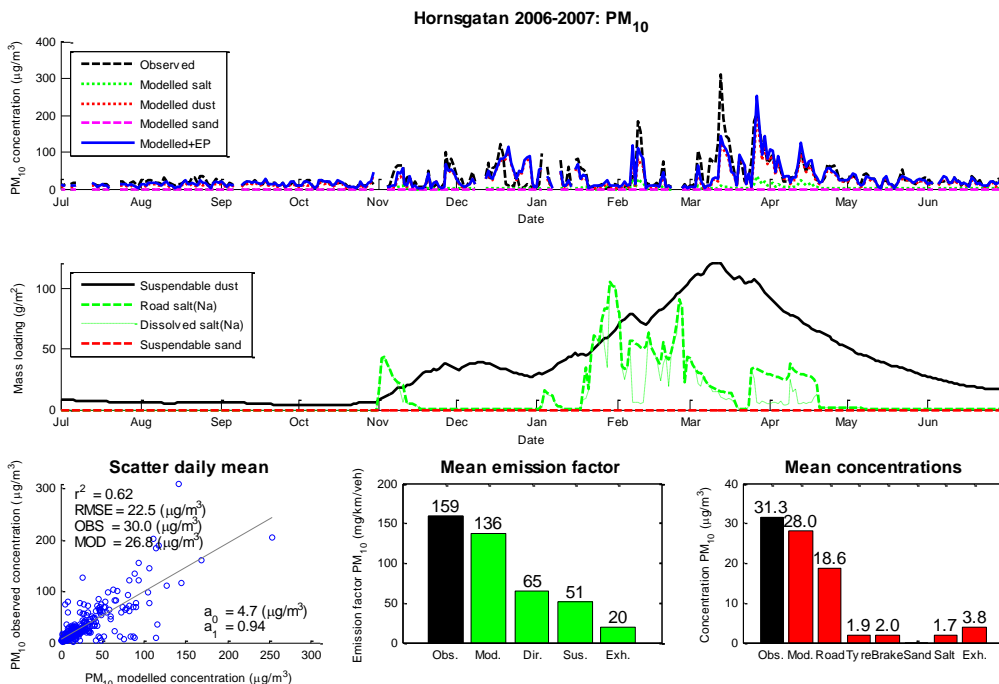
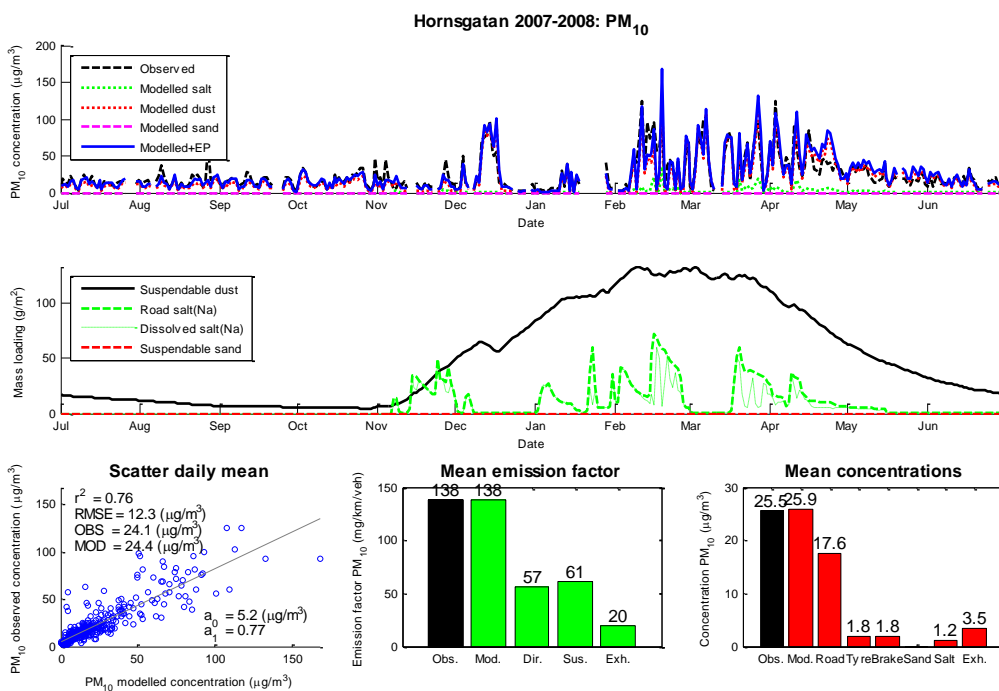


Figure D.2. Model results for Hornsgatan (Jul 2006 – Jun 2007) using *observed* (top) and *modelled* (bottom) surface moisture for surface retention



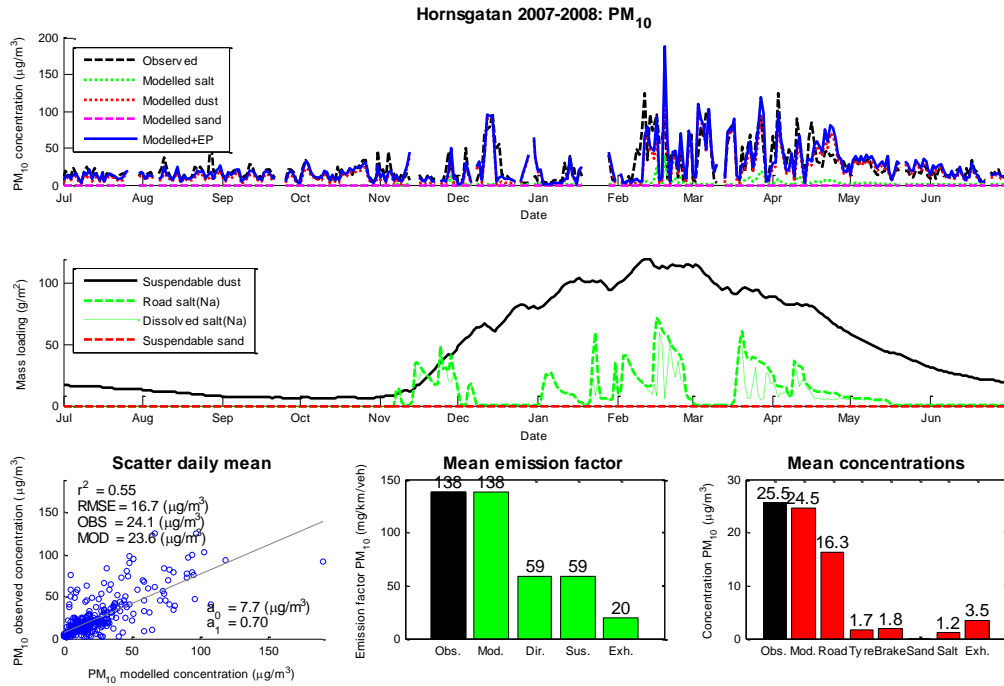
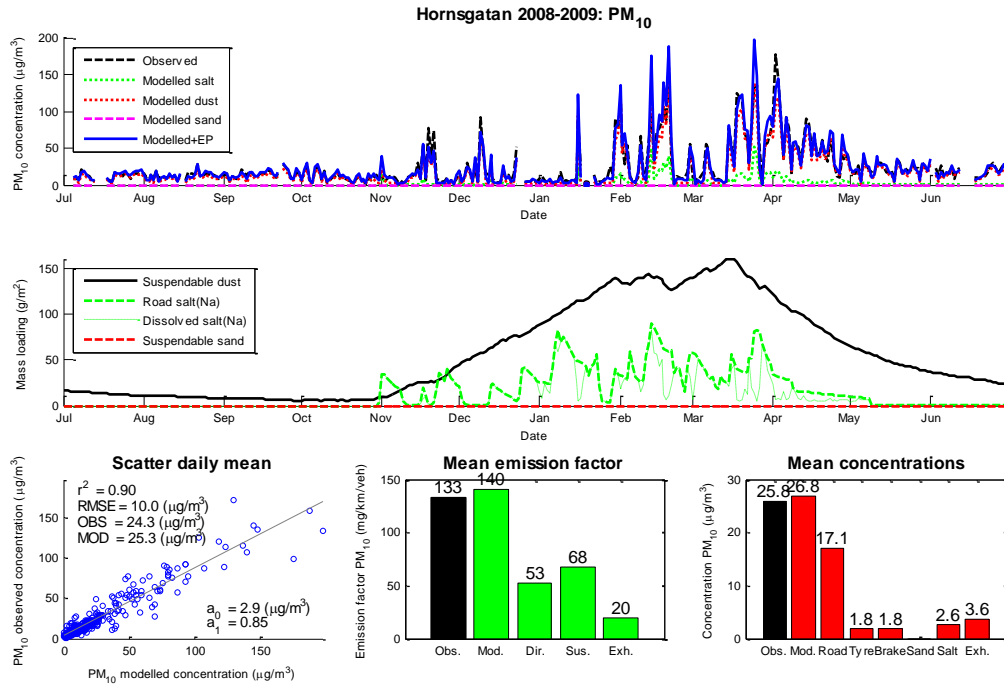


Figure D.3. Model results for Hornsgatan (Jul 2007 – Jun 2008) using **observed** (top) and **modelled** (bottom) surface moisture for surface retention



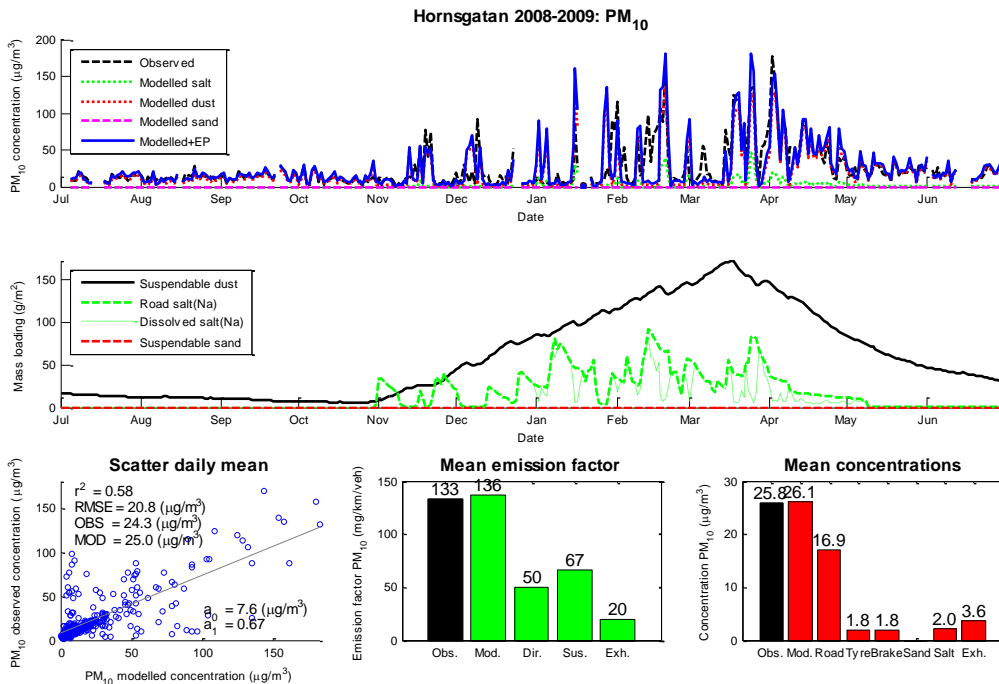
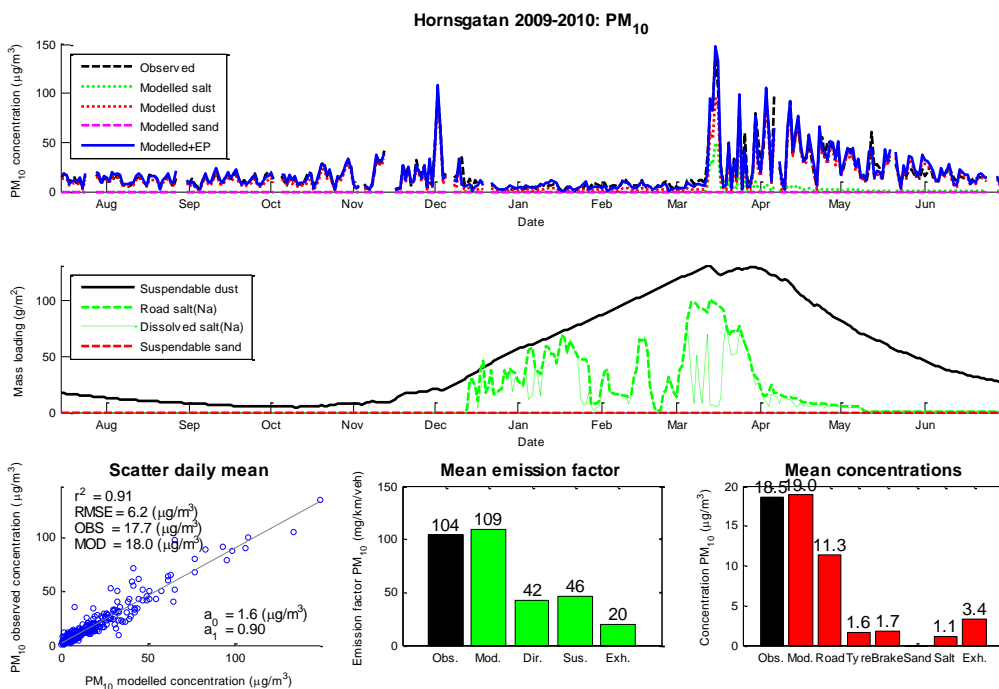


Figure D.4. Model results for Hornsgatan (Jul 2008 – Jun 2009) using **observed** (top) and **modelled** (bottom) surface moisture for surface retention



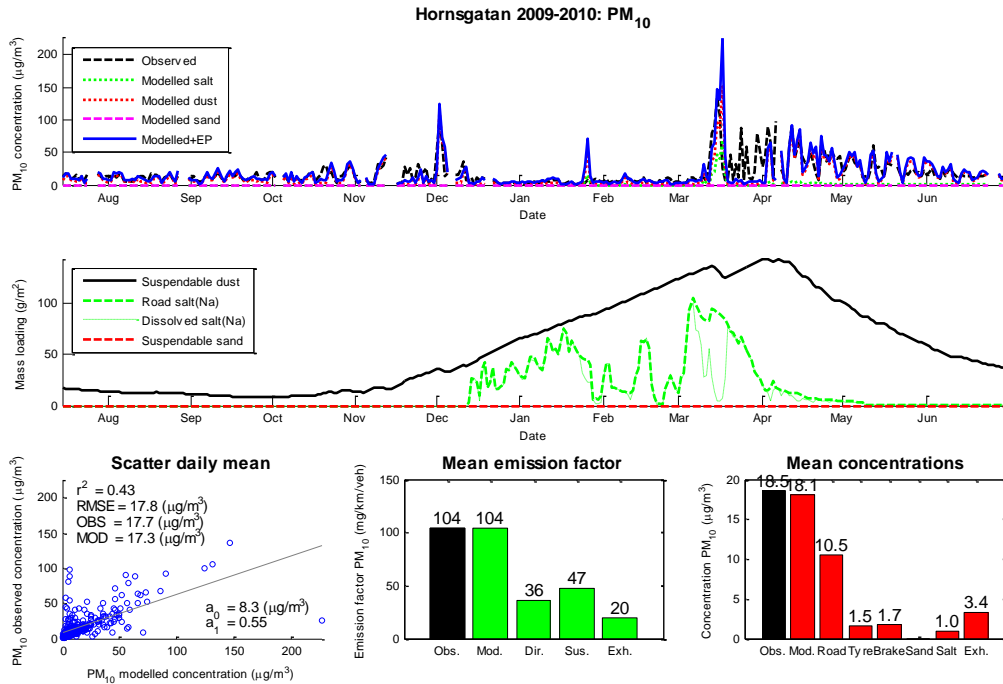
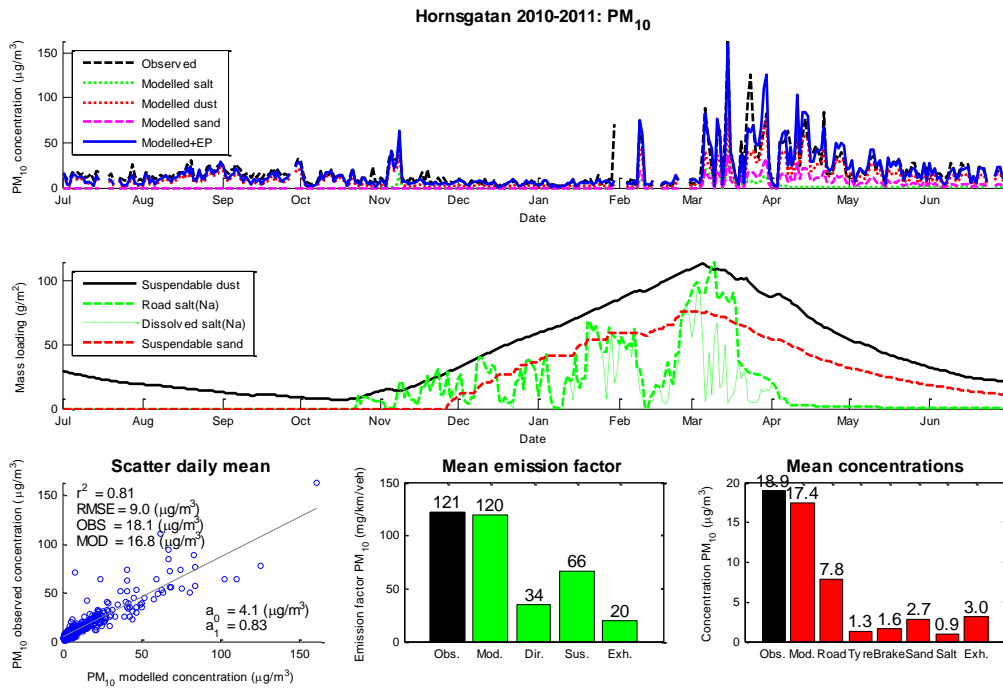


Figure D.5. Model results for Hornsgatan (Jul 2009 – Jun 2010) using **observed** (top) and **modelled** (bottom) surface moisture for surface retention



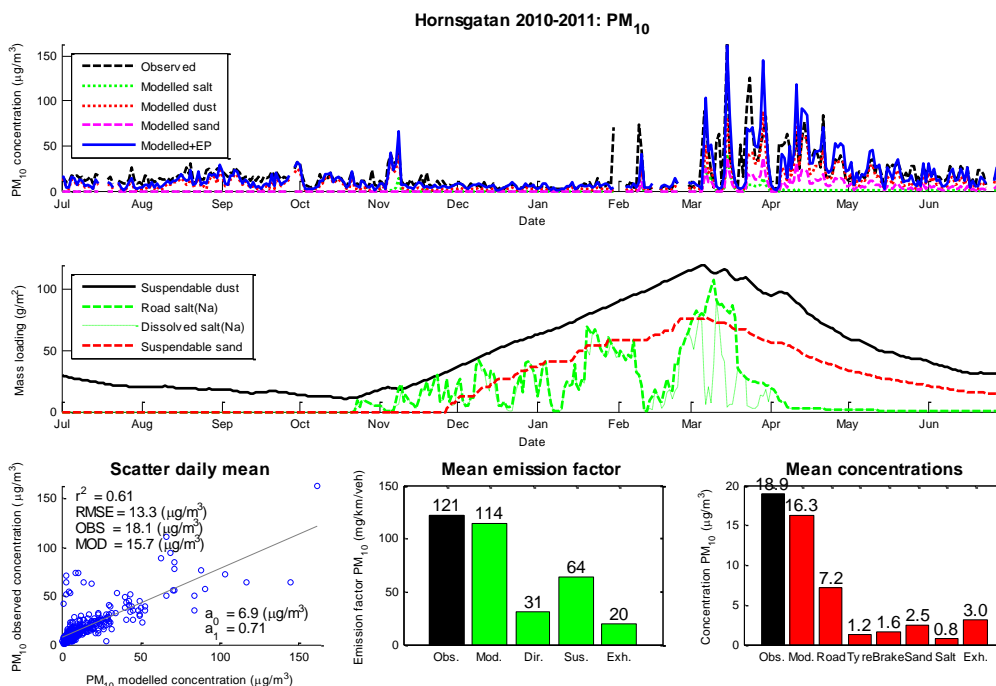


Figure D.6. Model results for Hornsgatan (Jul 2010 – Jun 2011) using **observed** (top) and **modelled** (bottom) surface moisture for surface retention.

D.2 Essingeleden, Stockholm

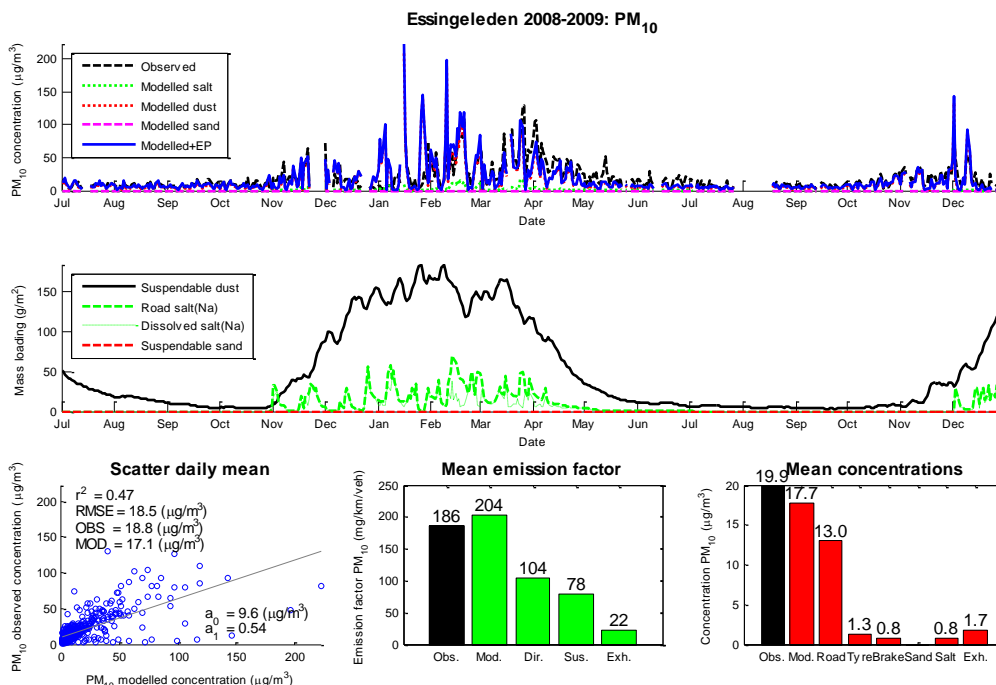


Figure D.7. Model results for Essingeleden (Jul 2008 – Dec 2009) using **modelled** surface moisture for surface retention

D.3 Riksvei 4 (RV4), Oslo

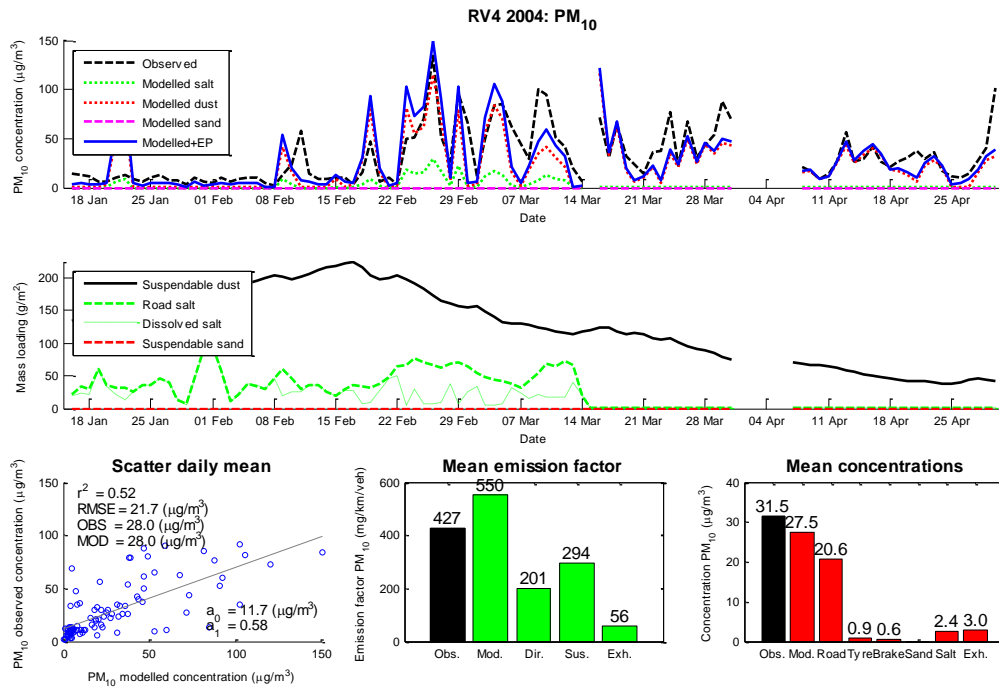


Figure D.8. Model results for RV4 (Jan 2004 – Apr 2004) using *modelled* surface moisture for surface retention

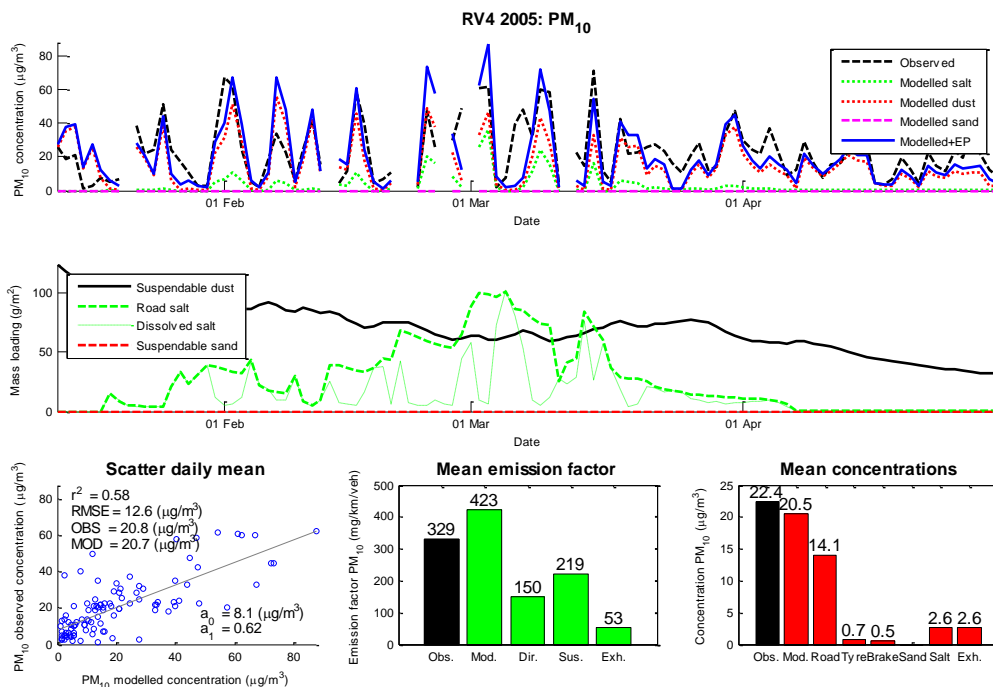


Figure D.9. Model results for RV4 (Jan 2005 – Apr 2005) using *modelled* surface moisture for surface retention

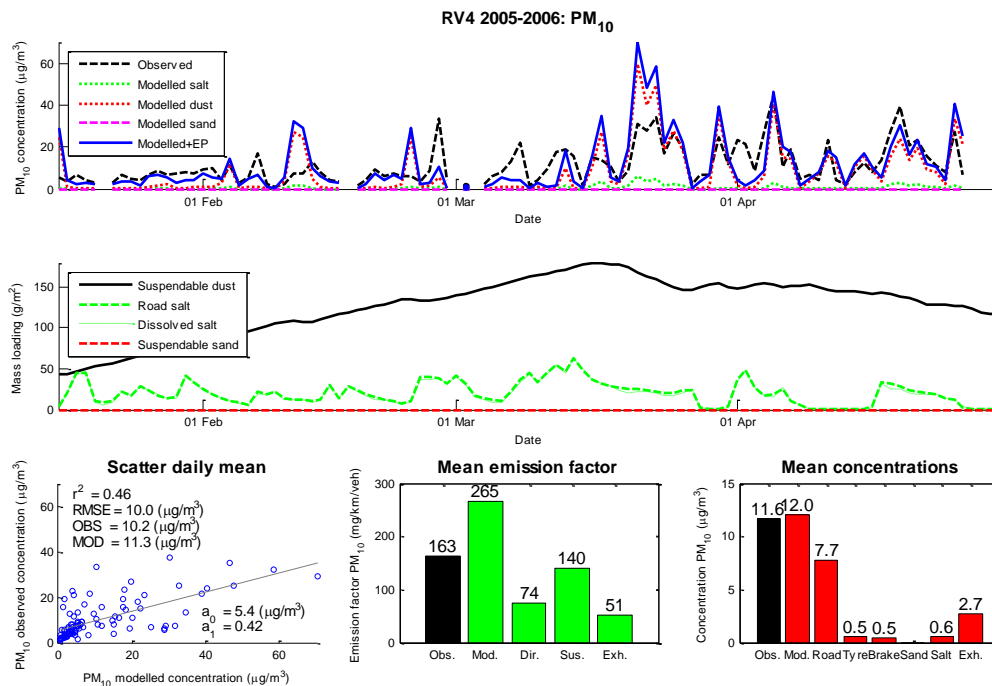
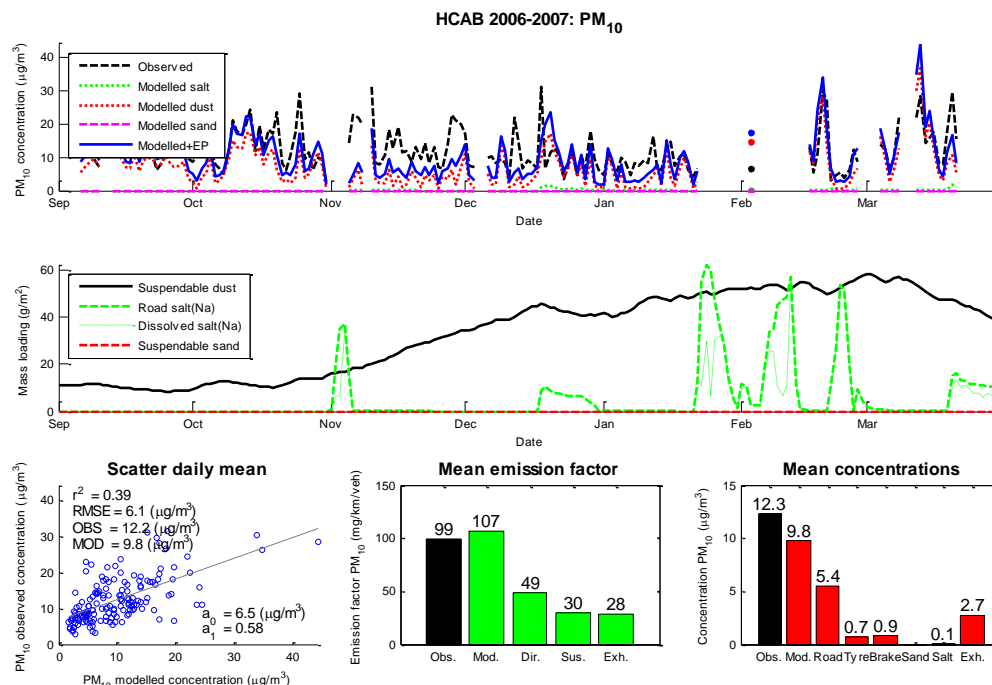


Figure D.10. Model results for RV4 (Jan 2006 – Apr 2006) using modelled surface moisture for surface retention

D.4 H. C. Andersen Boulevard (HCAB), Copenhagen



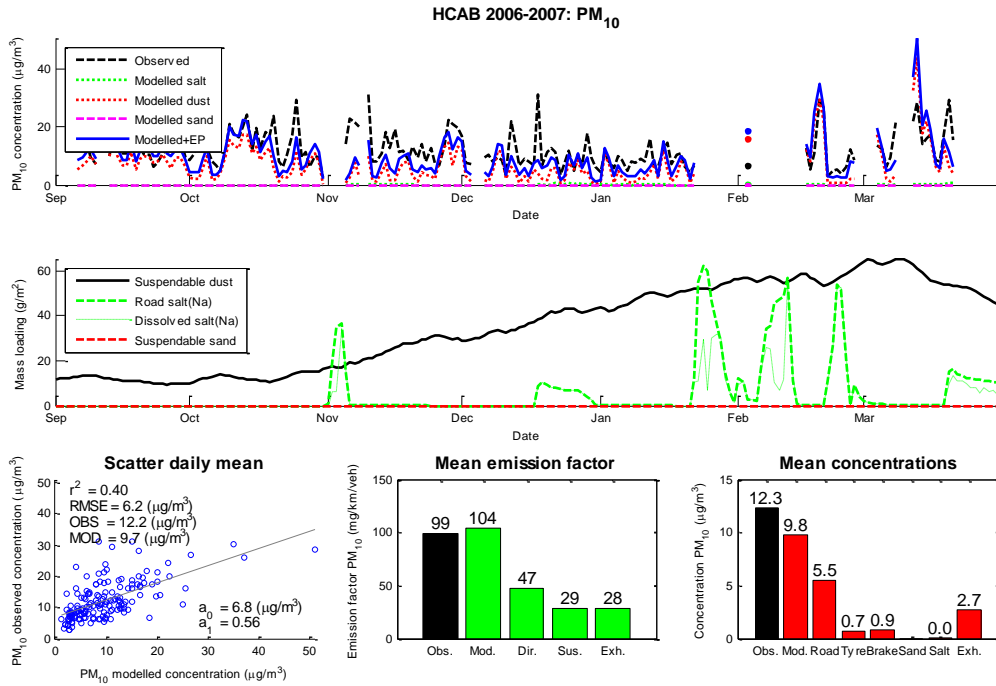
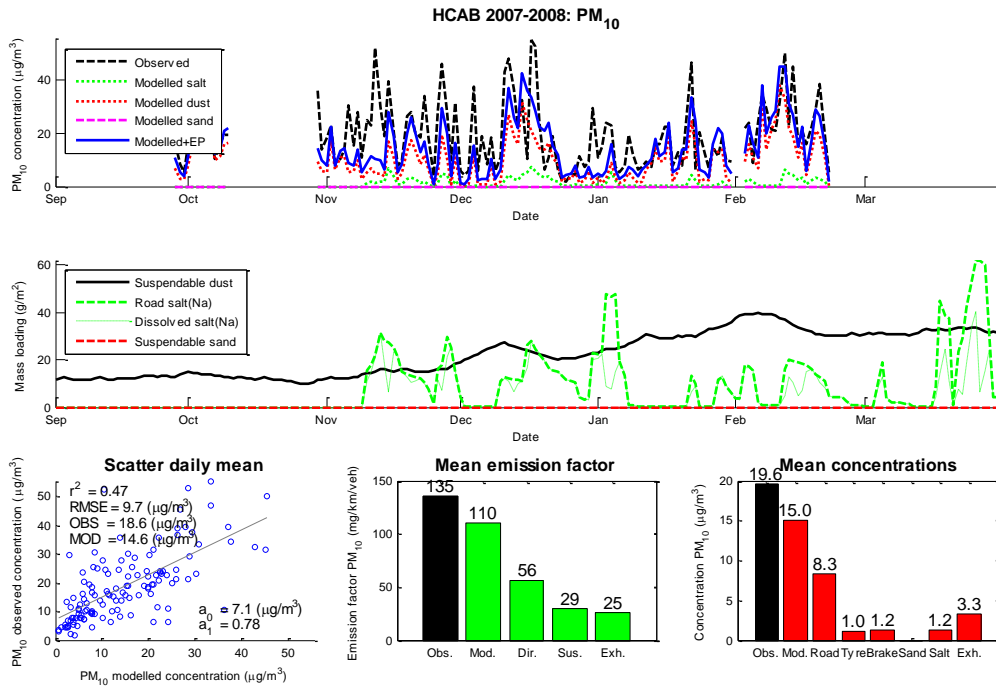


Figure D.11. Model results for HCAB (Nov 2006 – Mar 2007) using **observed** (top) and **modelled** (bottom) surface moisture for surface retention (road wear x5).



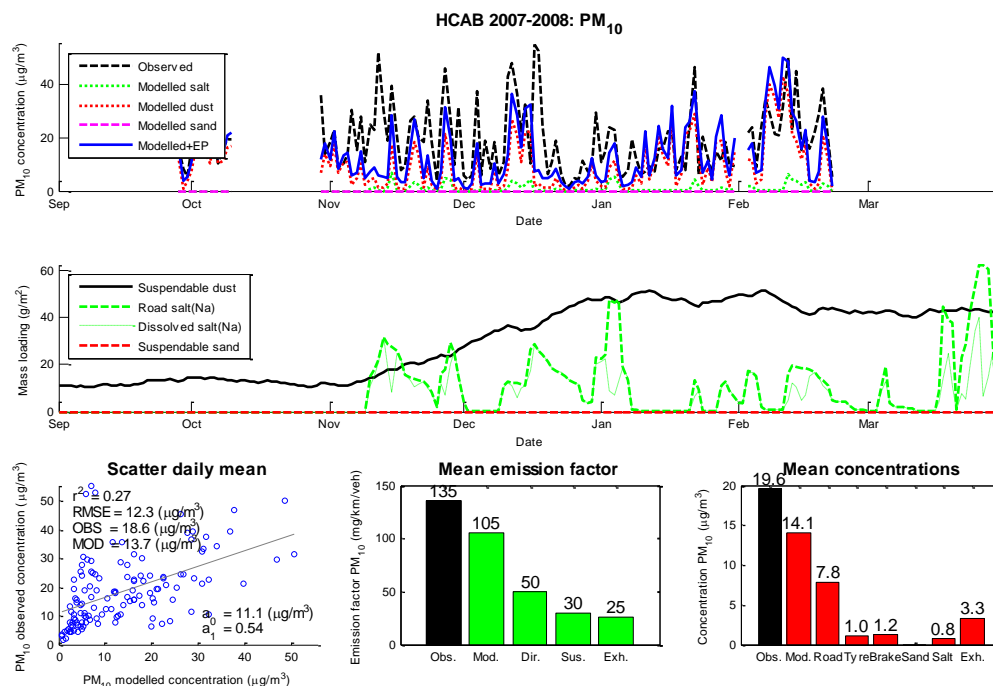


Figure D.12. Model results for HCAB (Nov 2007 – Mar 2008) using **observed** (top) and **modelled** (bottom) surface moisture for surface retention (road wear x5).

D.5 Mannerheimintie, Helsinki

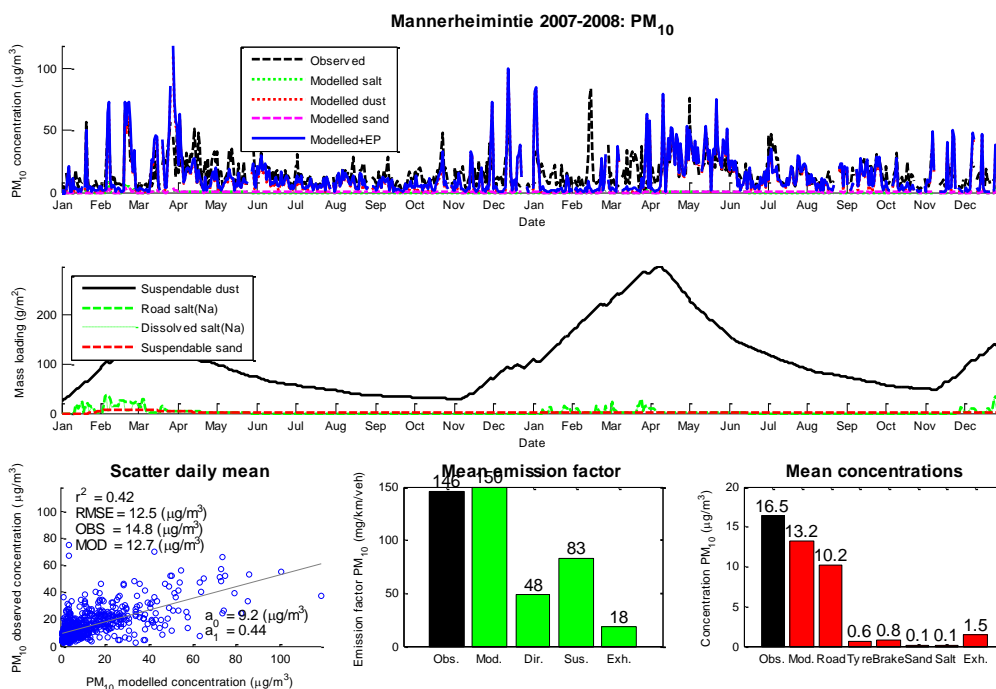


Figure D.13. Model results for Mannerheimintie (Jan 2007 – Dec 2008) using **modelled** surface moisture for surface retention.

D.6 Nordby Sletta (NB), Oslo

In this case we present two results, the first using the default setting of the model and the second using reduced suspension rates (factor of 4). Reduced suspension rates can have a significant impact on the mean concentrations.

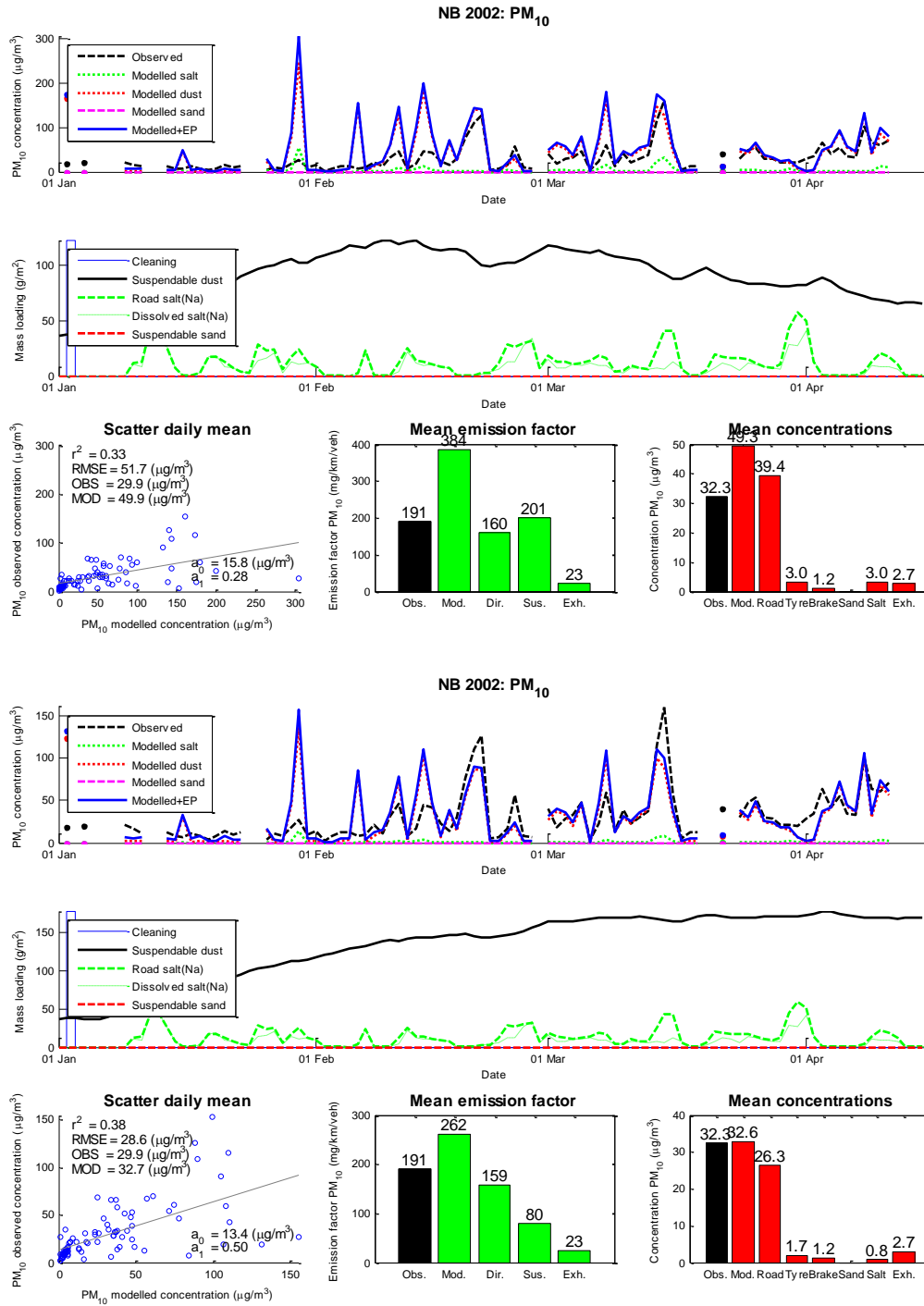


Figure D.14. Model results for NB (Nov 2002 – Apr 2002) using *default* (top) model suspension rates and *reduced* (bottom), factor of 4, suspension rates.

D.7 Runeberg, Helsinki

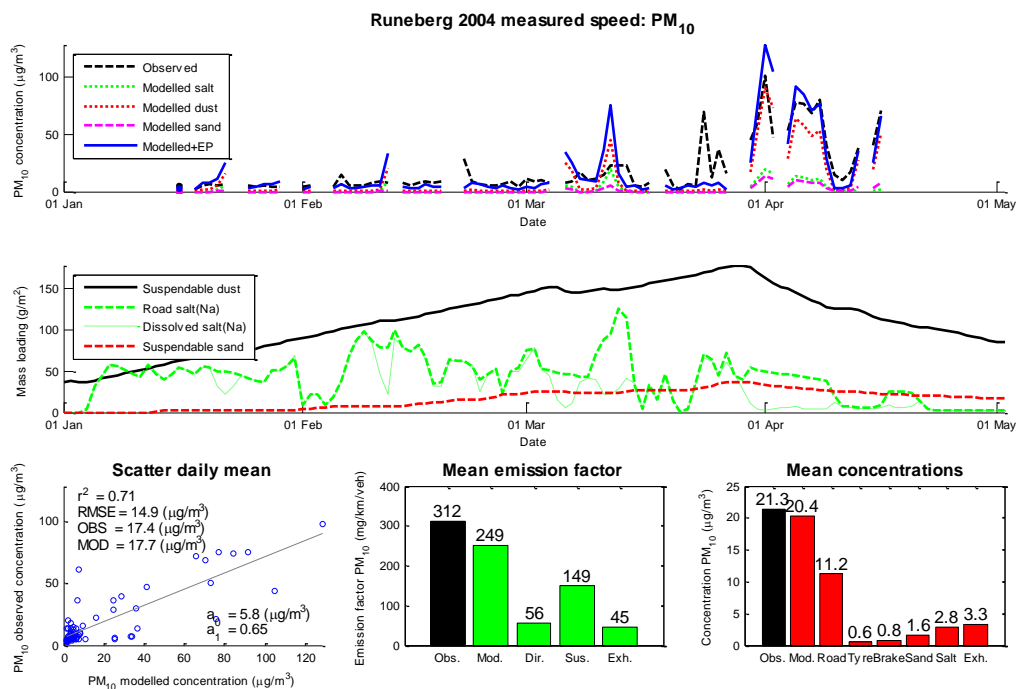


Figure D.15. Model results for Runeberg (Jan 2004– may 2004) using *modelled* surface moisture for surface retention.

Appendix E

Example of a complete set of model output plots, Hornsgatan 2010-2011

To provide an overview of typical model input, results and analysis the complete set of model graphics are shown here for the dataset Hornsgatan 2010-2011.

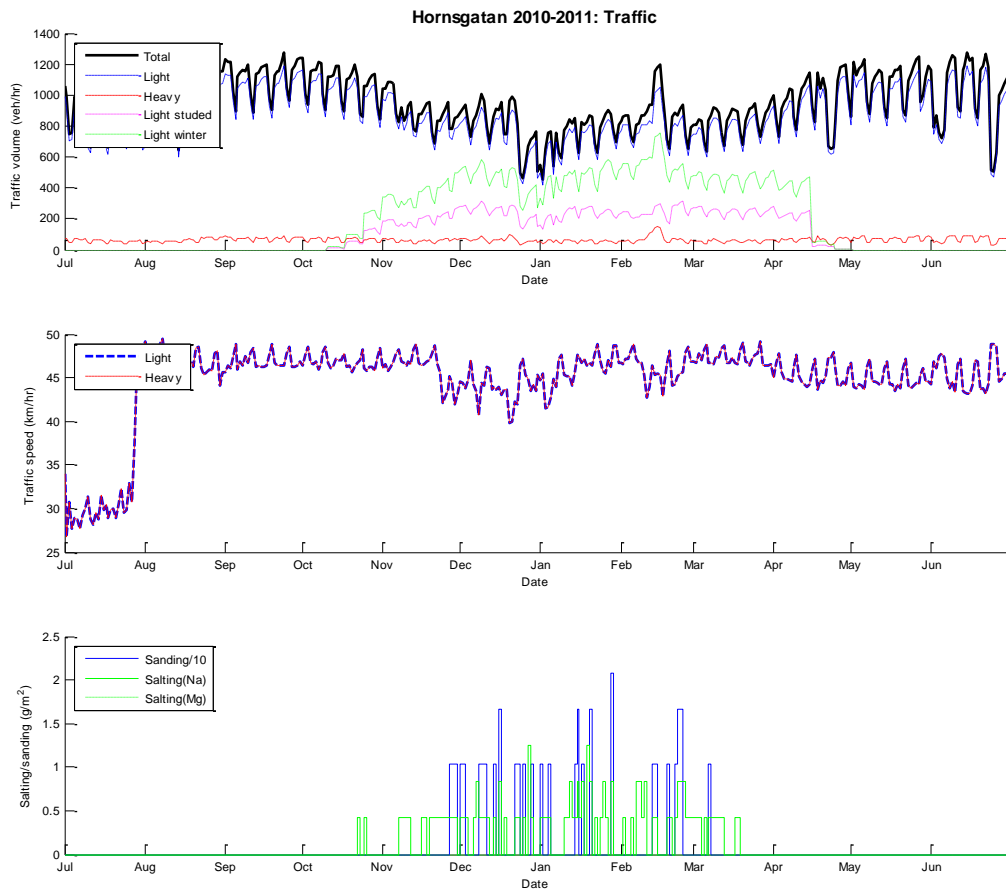


Figure E.1. Daily mean traffic and road maintenance activity data for Hornsgatan 2010-2011.

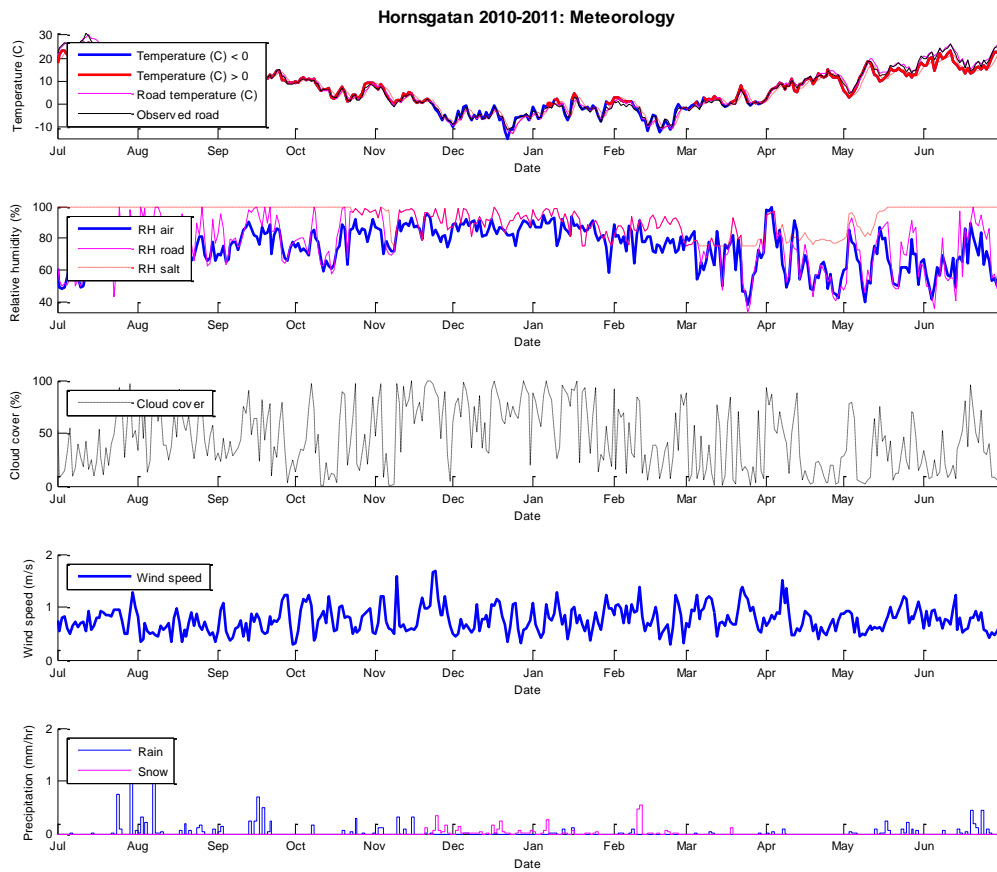


Figure E.2. Daily mean meteorological data for Hornsgatan 2010-2011.

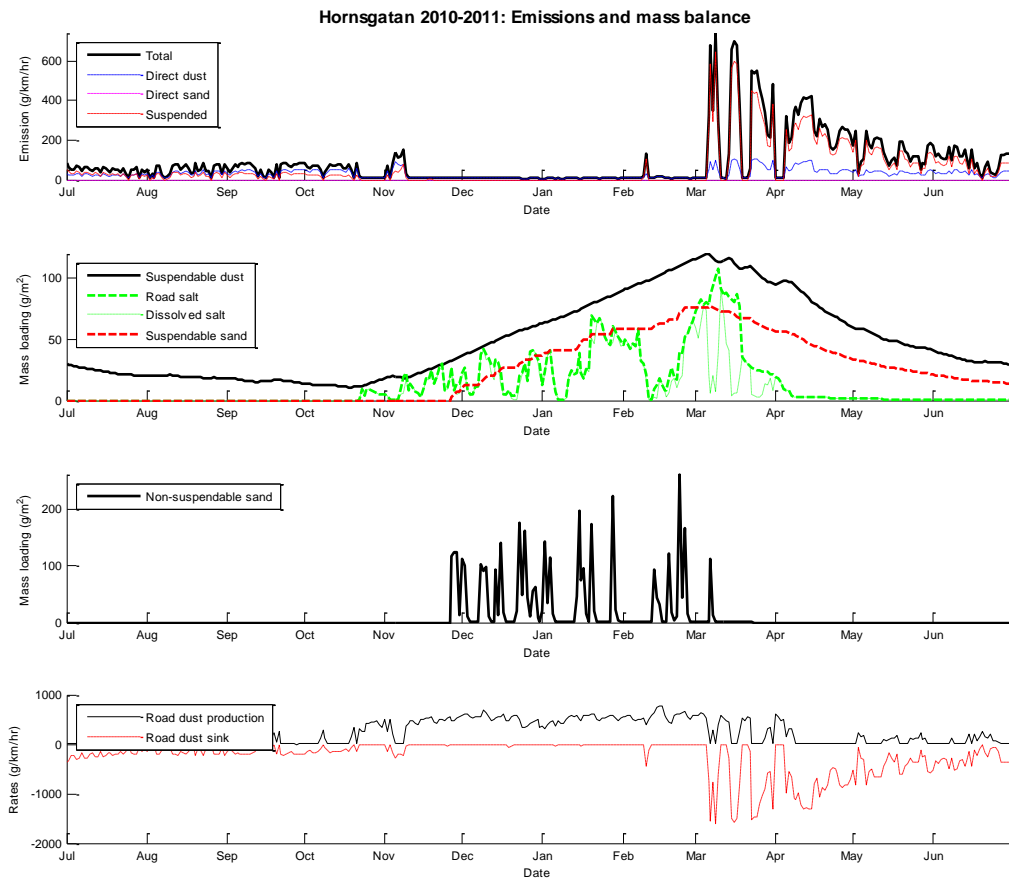


Figure E.3. Daily mean emissions and mass balance data for Hornsgatan 2010-2011.

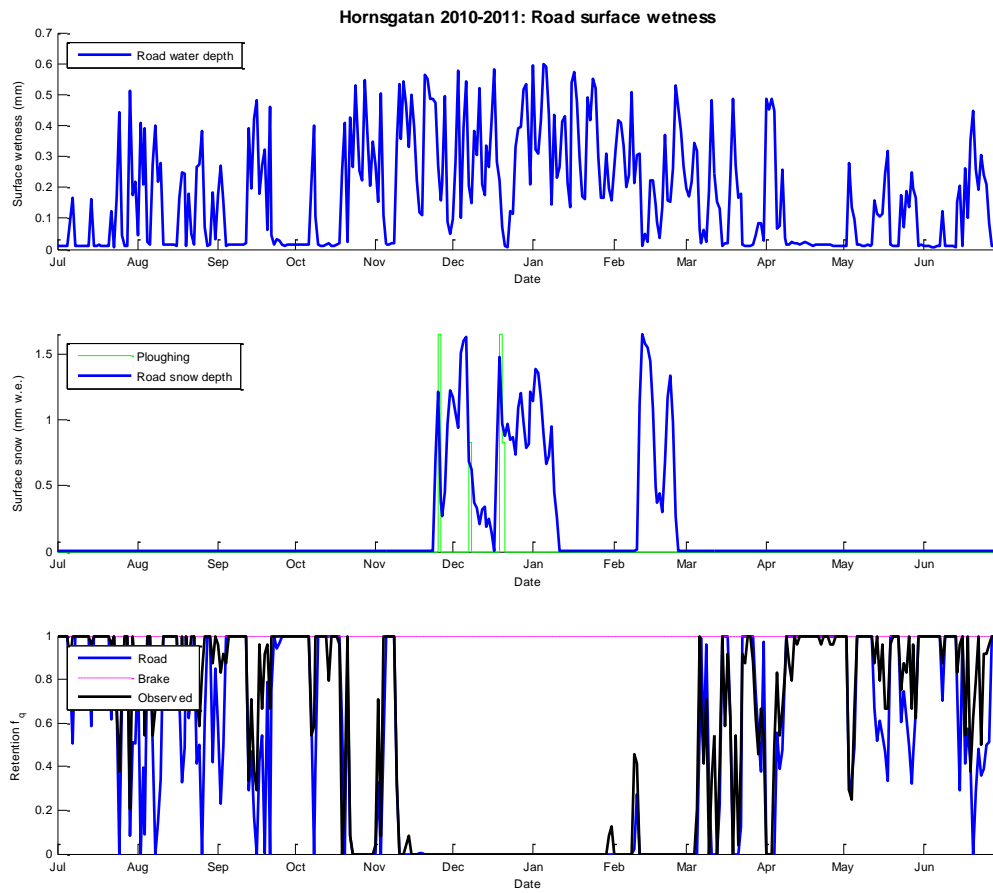


Figure E.4. Daily mean surface moisture and retention factor data for Hornsgatan 2010-2011.

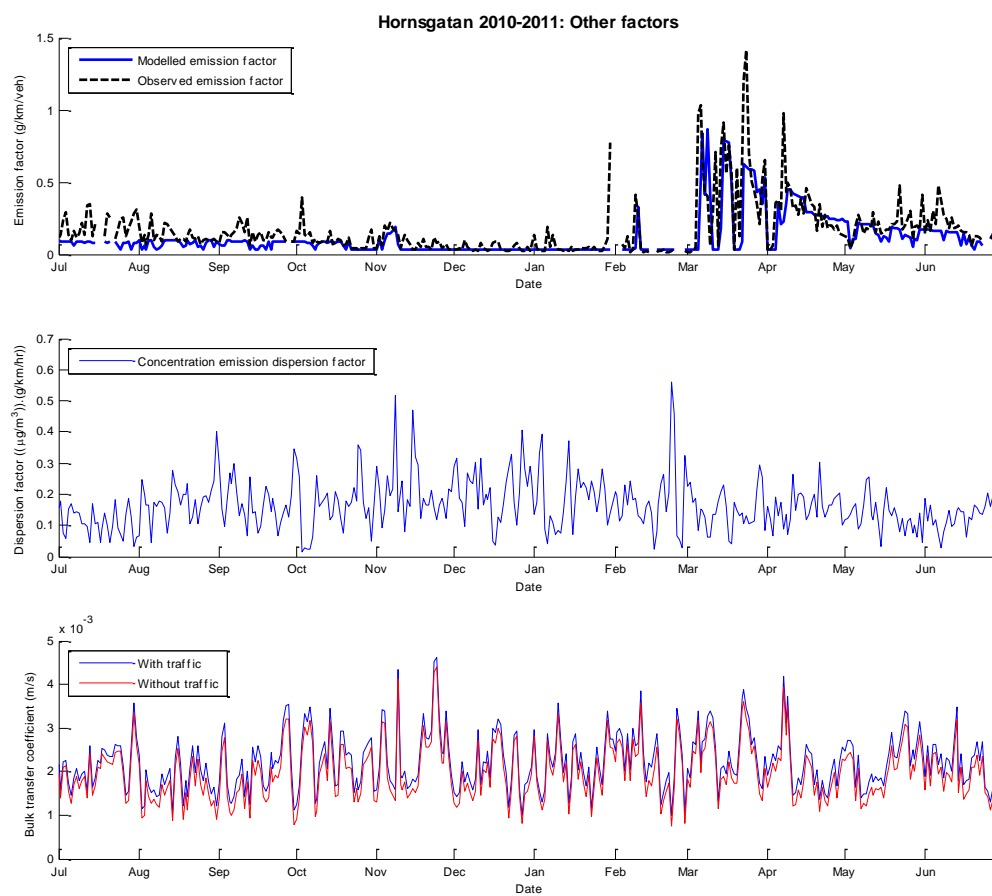


Figure E.5. Daily mean emission factor, concentration-emission dispersion factor and bulk transfer coefficients for Hornsgatan 2010-2011.

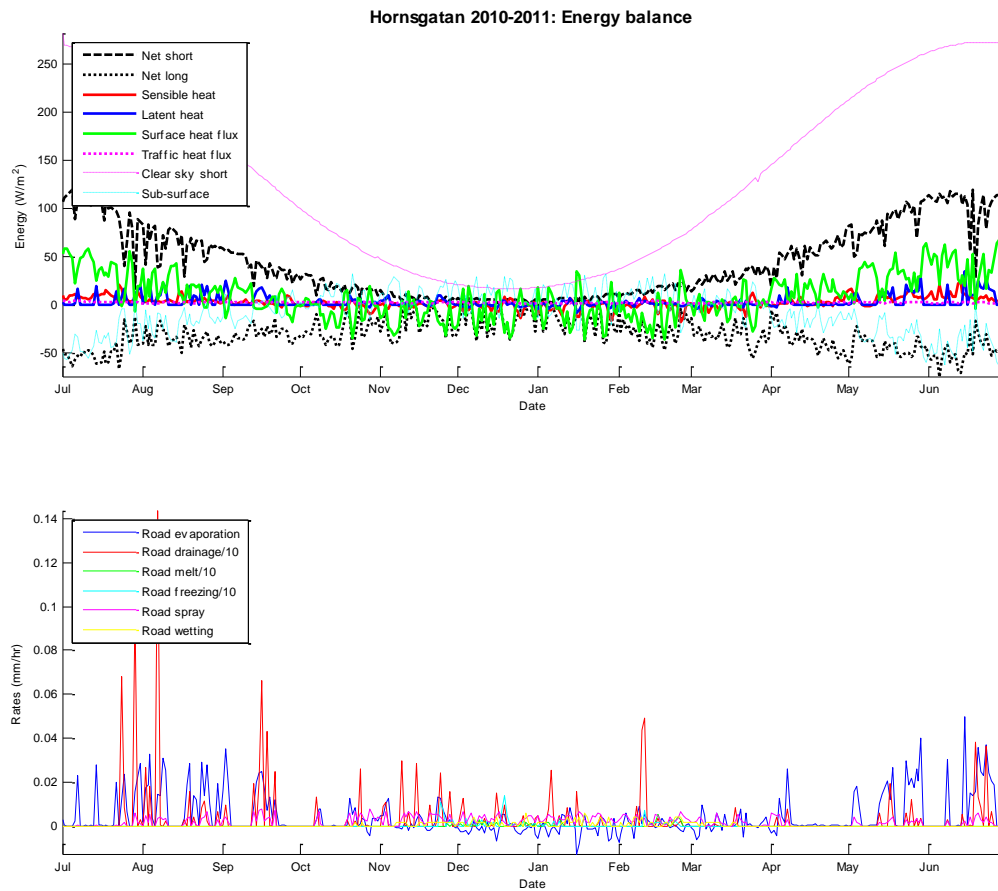


Figure E.6. Daily mean energy balance and moisture mass balance rates for Hornsgatan 2010-2011.

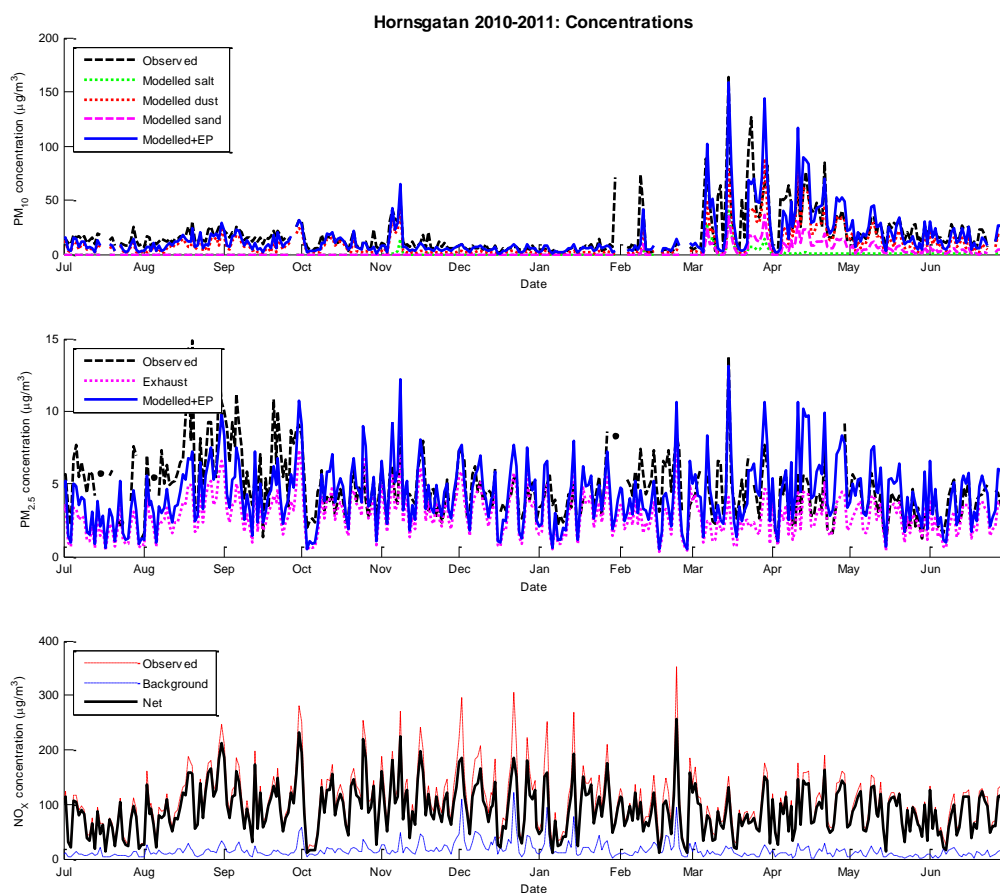


Figure E.7. Daily mean time series of observed and modelled concentrations for PM_{10} , $PM_{2.5}$ and NO_x for Hornsgatan 2010-2011.

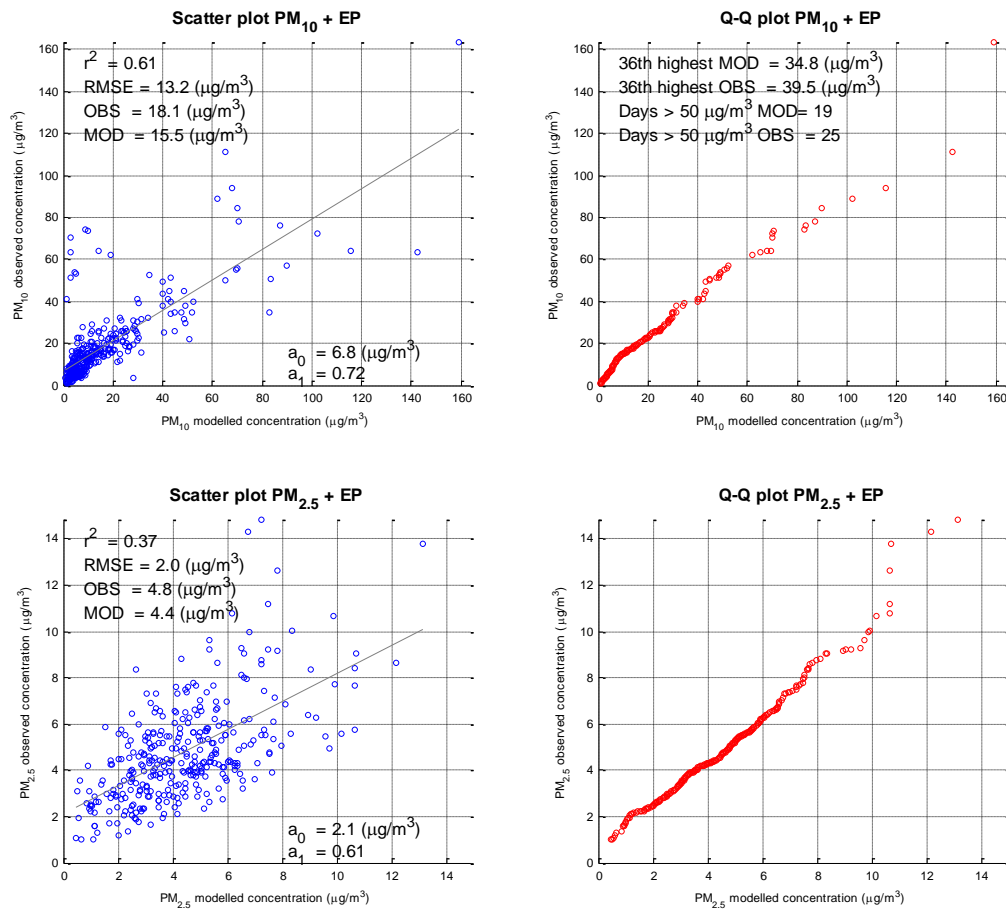


Figure E.8. Daily mean scatter and quantile-quantile plots of observed and modelled concentrations of PM_{10} , $PM_{2.5}$ for Hornsgatan 2010-2011.

| | | | |
|--|---|--|--------------------|
| REPORT SERIES SCIENTIFIC REPORT | REPORT NO. OR 23/2012 | ISBN: 978-82-425-2536-9 (print) 978-82-425-2537-6 (electronic) ISSN: 0807-7207 | |
| DATE 20.11.12012 | SIGN. For/ Kari Nygaard <i>Eva B. Andersen</i> | NO. OF PAGES 128 | PRICE NOK 150.- |
| TITLE NORTRIP model development and documentation: NO _N -exhaust Road TRaffic Induced Particle emission modelling | | PROJECT LEADER Bruce Rolstad Denby | |
| | | NILU PROJECT NO. O-110053 | |
| AUTHOR(S) Bruce Rolstad Denby and Ingrid Sundvor | | CLASSIFICATION * A | |
| | | CONTRACT REF. | |
| QUALITY CONTROLLER: Li Liu | | | |
| REPORT PREPARED FOR NILU, Nordic Council of Ministers and the Norwegian Climate and Pollution Agency | | | |
| <p>ABSTRACT</p> <p>The NORTRIP model is the result of research efforts carried out by a number of Nordic institutes to improve our understanding and ability to model non-exhaust traffic emissions and has been developed through the Nordic Council of Ministers project NORTRIP (NO_N-exhaust Road Traffic Induced Particle emissions). The NORTRIP model is a process based non-exhaust emission model that is intended for application without site specific empirical factors. It takes into account direct wear emissions, the build up of mass on the road surface, the suspension of this mass, as well as the application and suspension of salt and sand. It combines a road dust sub-model with a road moisture sub-model in order to properly describe the retention of dust on the road surface. The model can be applied for assessment purposes and for the management and evaluation of abatement strategies regarding road wear, salting and sanding. The model development and its documentation, along with its application to a large number of Nordic datasets, is described in detail in this report.</p> | | | |
| <p>NORWEGIAN TITLE</p> <p>NORTRIP modellutvikling og beskrivelse</p> | | | |
| KEYWORDS Non-exhaust emission modelling | Suspension | Road dust | |
| ABSTRACT (in Norwegian) | | | |

* Classification A Unclassified (can be ordered from NILU)
 B Restricted distribution
 C Classified (not to be distributed)

REFERENCE: O-110053
DATE: NOVEMBER 2012
ISBN: 978-82-425-2536-9 (print)
978-82-425-2537-6 (electronic)

NILU is an independent, nonprofit institution established in 1969. Through its research NILU increases the understanding of climate change, of the composition of the atmosphere, of air quality and of hazardous substances. Based on its research, NILU markets integrated services and products within analyzing, monitoring and consulting. NILU is concerned with increasing public awareness about climate change and environmental pollution.